

**Protection against Oxidative Glutamate Toxicity mediated by the mouse (*Mus musculus*)**

**Orphan Receptor GPR39**

**Dissertation**

**zur Erlangung des Doktorgrades**

**des Fachbereichs Biologie**

**der Universität Hamburg**

**vorgelegt von Mert Sahin**

**aus Ankara**

**Hamburg 2005**

<b>1</b>	<b>AIM OF THIS STUDY.....</b>	<b>4</b>
<b>2</b>	<b>INTRODUCTION.....</b>	<b>5</b>
2.1	G-PROTEIN COUPLED RECEPTORS .....	5
2.1.1	<i>Orphan G-Protein Coupled Receptors .....</i>	7
2.2	OXIDATIVE STRESS .....	7
2.2.1	<i>Oxygen and sources of reactive oxygen species .....</i>	7
2.2.2	<i>Oxidative stress and neurological diseases .....</i>	9
2.2.3	<i>Oxidative glutamate toxicity as a model for neuronal death due to oxidative stress.....</i>	11
2.2.4	<i>Oxidative glutamate toxicity and G-protein coupled signaling.....</i>	12
<b>3</b>	<b>MATERIALS AND METHODS .....</b>	<b>14</b>
3.1	BUFFERS .....	14
3.2	MOLECULAR BIOLOGY METHODS.....	14
3.2.1	<i>Cloning of GPR15, GPR39, VPAC2.....</i>	14
3.2.2	<i>Polymerase Chain Reaction .....</i>	16
3.2.3	<i>Protein Preparation and Western Blotting.....</i>	16
3.2.4	<i>In situ Hybridization .....</i>	17
3.3	CELL BIOLOGY METHODS.....	18
3.3.1	<i>Cell culture and viability assays.....</i>	18
3.3.2	<i>Transfection of DNA into mammalian cells.....</i>	18
3.3.2.1	Transfection by electroporation .....	18
3.3.2.2	Transfection by Calcium Phosphate.....	19
3.3.3	<i>Stable Cell Line Production.....</i>	19
3.3.4	<i>Flow Cytometry .....</i>	20
3.3.4.1	Measurement of ROS levels .....	20
3.3.4.2	Measurement of mGPR39 and HA expression .....	20
3.3.5	<i>Measurement of total GSH .....</i>	21
3.4	PREPARATION OF RNA .....	21
3.4.1	<i>Cell cultivation for RNA preparation .....</i>	21
3.4.2	<i>Isolation of total RNA.....</i>	21
3.4.3	<i>Qualitative analysis of total RNA by agarose electrophoresis .....</i>	22
3.4.4	<i>Quantification of RNA by absorption spectroscopy.....</i>	22
3.5	QUANTITATIVE PCR.....	22
<b>4</b>	<b>RESULTS .....</b>	<b>25</b>
4.1	OXIDATIVE GLUTAMATE TOXICITY .....	25
4.1.1	<i>HT22 cells die from oxidative glutamate toxicity upon exposure to glutamate.....</i>	25
4.1.2	<i>Susceptibility to glutamate is influenced by cell culture conditions .....</i>	26
4.1.3	<i>Oxidative glutamate toxicity depletes the glutathione levels within the cells .....</i>	29
4.1.4	<i>Glutamate resistant HT22 cells are also resistant to different kinds of cell death inducers.....</i>	30
4.1.5	<i>Resistance to glutamate can be induced by medium conditioned by HT22CR cells.....</i>	34
4.1.6	<i>Glutamate-resistant cells show an activation of CRE-dependent pathways.....</i>	36
4.1.7	<i>Resistant HT22 cells differ from the parental cell line in the expression of GPCRs .....</i>	37
4.1.8	<i>Activation of VIP receptors leads to a HT22CR like phosphorylation scheme.....</i>	39
4.1.9	<i>VIP and glutamate synergistically induce Bcl-2.....</i>	40
4.2	ORPHAN RECEPTORS.....	42
4.2.1	<i>Mouse GPR15.....</i>	44
4.2.1.1	Chromosomal Localization and Sequence Analysis .....	44
4.2.1.2	Phylogenetic Analysis.....	46
4.2.2	<i>Mouse GPR39.....</i>	46
4.2.2.1	Chromosomal Localization and Sequence Analysis .....	46
4.2.2.2	Phylogenetic Analysis.....	48
4.2.3	<i>Resistance to glutamate and hydrogen peroxide can be induced by orphan GPCRs .....</i>	49
4.2.4	<i>Mechanism of protection in HT22 cells.....</i>	51
4.2.5	<i>Expression of mGPR39 throughout the development .....</i>	53
4.2.6	<i>Stable HT22 cell lines.....</i>	55
4.2.6.1	Verification of the Stable Cell Lines.....	56

4.2.6.2	HT22 cells stably overexpressing mGPR39 show resistance to stress inducers.....	58
4.2.7	<i>Implications for mGPR39 to take a role in other diseases</i> .....	61
<b>5</b>	<b>DISCUSSION</b> .....	<b>63</b>
5.1	HT22 CELLS DIE FROM OXIDATIVE GLUTAMATE TOXICITY UPON EXPOSURE TO GLUTAMATE .....	63
5.2	GLUTAMATE SUSCEPTIBILITY OF HT22 CELLS IS MODULATED BY CELL CULTURE CONDITIONS .....	63
5.3	RESISTANT HT22 CELLS DIFFER FROM THE PARENTAL CELL LINE IN THEIR GPCR PATTERN .....	65
5.4	VPAC <sub>2</sub> – A MODEL NEUROPROTECTIVE RECEPTOR.....	66
5.5	RESISTANCE CONFERRED BY THE UPREGULATED ORPHAN RECEPTORS.....	68
5.6	STABLE HT22 CELLS OVEREXPRESSING MGPR39.....	69
5.7	IMPLICATIONS FOR A ROLE IN DISEASES .....	70
<b>6</b>	<b>SUMMARY</b> .....	<b>71</b>
<b>7</b>	<b>LITERATURE</b> .....	<b>73</b>
<b>8</b>	<b>ABBREVIATIONS</b> .....	<b>84</b>

## 1 Aim of this Study

Oxidative stress is involved in neurological diseases like Alzheimer's dementia, and Parkinson's disease. Oxidative stress can lead to the induction of programmed cell death and subsequent neuronal loss. Oxidative glutamate toxicity is an *in vitro* model for neuronal death due to oxidative stress in which glutamate induces glutathione depletion and subsequent oxidative stress. The aim of this study was to demonstrate protection against oxidative glutamate toxicity by G-protein coupled receptors, and to characterize the mechanism of protection mediated by the mouse orphan GPCR mGPR39.

As a first step, the influence of cell culture conditions on glutamate-induced death had to be characterized. Furthermore, the difference between a glutamate-sensitive and resistant cell line was used to analyse the role of G-protein coupled signaling pathways in this paradigm. The experiments led to the investigation of orphan receptors, identifying new receptors possibly involved in glutamate-induced oxidative toxicity.

These receptors were further tested and the most protecting receptor, mGPR39, was chosen. In order to understand its role in development, *in situ* hybridizations were carried out. To understand its role in glutamate toxicity, stable cells overexpressing the receptor were generated and analysed. Moreover, a possible role for mGPR39 in other diseases was investigated.

## 2 Introduction

### 2.1 G-Protein Coupled Receptors

G-protein-coupled receptors (GPCRs) are the largest family of cell-surface receptors, and transduce signals elicited by a diverse range of signaling molecules, including ions, biogenic amines, peptides and lipids, as well as photons, leading to alterations of cellular function (Bockaert, Claeysen et al. 2002). These receptors share a common general structure, which consists of an extracellular amino terminus, an intracellular carboxyl tail, and seven transmembrane helices connected by three extracellular and three intracellular loops. GPCRs can exist in an active or inactive form. The inactive conformation is favored in most cases, although some GPCRs exhibit constitutive activity under normal circumstances, that is, in the absence of respective activating ligands (Parnot, Miserey-Lenkei et al. 2002; Holst and Schwartz 2003).

Upon activation by a ligand, GPCRs associate with distinct classes of heterotrimeric G proteins composed of three subunits: the  $\alpha$ -subunit that has the guanine-nucleotide binding site and GTPase activity, and the  $\beta$ - and  $\gamma$ - subunits that form a tightly bound dimer. The subunits of G proteins show a wide range of heterogeneity. There are more than 20 different mammalian  $G\alpha$  subunits and 5  $\beta$  and 14  $\gamma$  subtypes currently known, which are found in nature in many possible combinations (Radhika and Dhanasekaran 2001).

The specific combination of  $\alpha$ ,  $\beta$ , and  $\gamma$  subunits, in combination with other regulatory and scaffolding proteins, connects a particular receptor to a specific effector pathway. The variety of  $G\beta\gamma$  dimers that can be formed adds to the large diversity among G proteins and thus presents another mechanism regulating receptor-G protein specificity (Neves, Ram et al. 2002). G-protein classes are defined according to the primary sequences of the  $\alpha$  subunits, resulting in four main families:  $G\alpha i/o$ ,  $G\alpha s$ ,  $G\alpha q/11$ , and  $G\alpha 12/13$ .

Although the classification is rather arbitrary, there is a general mechanism among the members of the subfamily. Stimulation of the  $G_s$  subfamily activates adenylyl cyclase whereas stimulation of the  $G_i$  subfamily leads to its inhibition. Stimulation of the  $G_q$  subfamily activates phospholipase C (PLC), and the  $G_{12}$  family is implicated in the regulation of small GTP binding proteins.

In many cases, these G proteins can couple to more than one receptor subtype, with differing affinities. GPCRs act as GEFs (guanine nucleotide exchange factors) for their cognate  $G\alpha$  subunits.  $G\alpha$  subunits bound to activated receptors undergo a conformational

change, resulting in the release of guanosine diphosphate (GDP), which is the rate-limiting step in G protein activation. The transient high-affinity empty state is followed by binding of GTP to  $G\alpha$  and its dissociation from  $G\beta\gamma$  and receptors. The GTP-bound  $G\alpha$  subunit and dissociated  $G\beta\gamma$  dimer can then interact with multiple downstream effectors, such as adenylyl cyclase, PLC $\beta$ , inward rectifier G protein-gated potassium channels, voltage-sensitive calcium channels, PI3 kinase, and molecules in the MAPK pathway (Garcia, Li et al. 1998; Maudsley, Martin et al. 2005). In the absence of other regulatory factors, the intrinsic guanosine triphosphatase (GTPase) activity of the  $G\alpha$  subunit dephosphorylates GTP to GDP, thereby returning to the inactive state, which allows reassociation of  $G\alpha$  and  $G\beta\gamma$  (Figure 1.1).

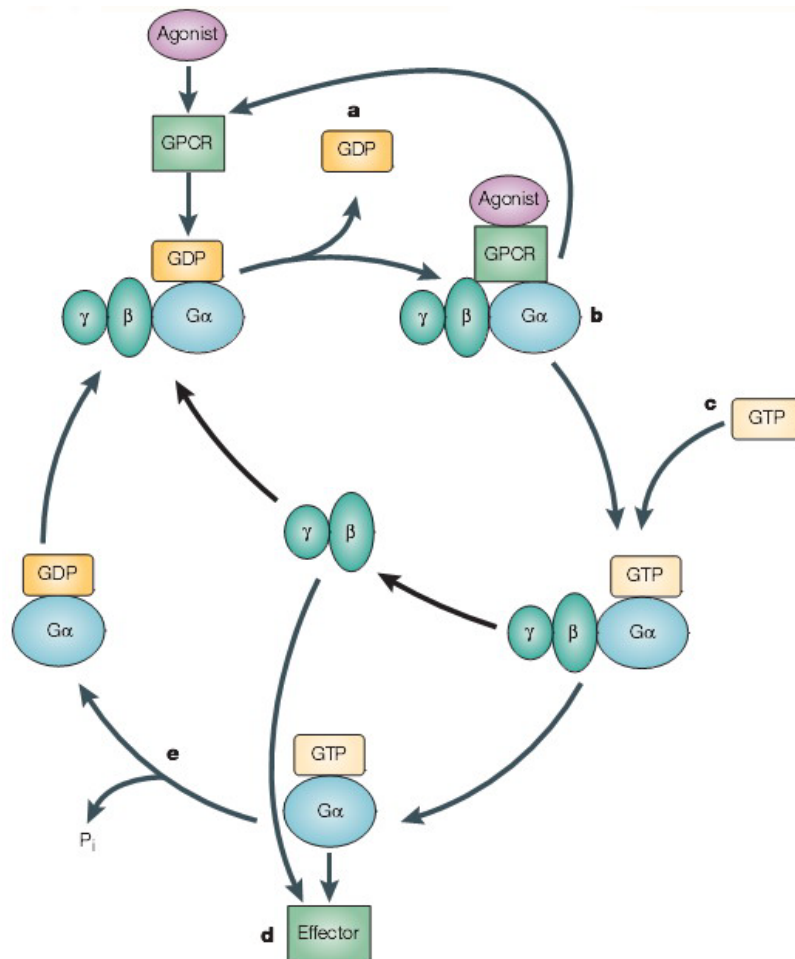


**Figure 1.1: G-protein cycling.** Rate-limiting receptor-promoted GDP dissociation (a) is followed by ternary complex formation (b). The GPCR then catalyzes the binding of GTP to  $G\alpha$  (c), which disrupts the ternary complex, causing dissociation of the G-protein heterotrimer into  $G\alpha$  and  $G\beta\gamma$ . Both entities regulate the activity of effector systems (d). G-protein activation is terminated by hydrolysis of the  $G\alpha$ -bound GTP to GDP and P (e).

GPCRs can be divided into 5 different families based on their structural and genetic characteristics: Family 1 consists of receptors related to Rhodopsin and the adrenergic receptor, family 2 of the receptors related to the calcitonin and PTH receptors. Family 3 consists of receptors related to the metabotropic receptors; family 4 is made up mainly of pheromone-related receptors, while family 5 is formed by cAMP receptors. Sequences within each family generally share over 25% sequence identity in the transmembrane core region, and a distinctive set of highly conserved regions and motifs. Among these families, little similarity is evident beyond the predicted seven-transmembrane architecture (7TM).

### **2.1.1 Orphan G-Protein Coupled Receptors**

At present, many open reading frames encoding putative members of the GPCR family have been identified, for which the ligands are not known. These receptors, commonly known as orphan receptors, are of interest for the pharmaceutical industry as drug targets, because it has been estimated that over 50% of all modern drugs modulate GPCR activity (Wilson and Bergsma 2000; Howard, McAllister et al. 2001). The human genome sequencing project has identified around 800 genes that belong to the GPCR superfamily (Lander, Linton et al. 2001; Venter, Adams et al. 2001). Half of these genes are thought to encode sensory receptors, and of the remaining 360 receptors, the natural ligands for approximately 210 have been identified. This leaves around 150 orphan GPCRs that have no known ligand or function (Wise, Jupe et al. 2004).

The first stage of any orphan GPCR screening experiment is to express the cloned receptor in a recombinant expression system that can provide the necessary transmission and G protein signaling machinery to enable the successful identification of an activating ligand. Irrespective of the expression system, the success of a ligand screening experiment depends entirely upon the receptor being expressed at the cell surface and the ability to couple to the signal transduction machinery of that cell to generate a detectable signal in the desired assay (Lewerenz, Letz et al. 2003; Civelli 2005).

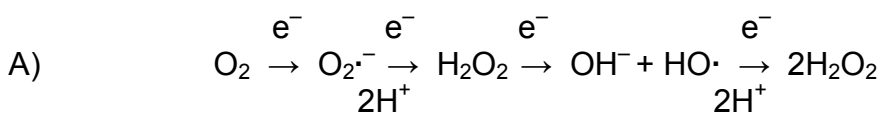
## **2.2 Oxidative Stress**

### **2.2.1 Oxygen and sources of reactive oxygen species**

The survival of aerobic organisms critically depends on the availability of oxygen (O<sub>2</sub>). O<sub>2</sub> acts as the final acceptor of electrons which, by moving through the electron transport

chain of the inner mitochondrial membrane, build up a proton gradient that serves as an energy source for the generation of adenosine triphosphate (ATP), a process by which  $O_2$  is reduced to two  $H_2O$  (Slater 1977). The energy stored in the terminal phosphoanhydride bond is used for the synthesis of biomolecules, transporting molecules against concentration gradients, for movement, establishing electric potentials across membranes or generating heat.

On the other hand, oxygen can induce tissue injury (Capellier, Maupoil et al. 1999). The toxicity of  $O_2$  arises from its structure (Fridovich 1998): The paramagnetism in its ground state indicates that it contains two unpaired electrons with parallel spin. Because the electron pairs of any other stable organic molecule have antiparallel spins they are preferentially transferred to  $O_2$  one at a time. Thus, for the complete reduction of  $O_2$  to two  $H_2O$  by four electrons and four protons generates intermediates like superoxide ( $O_2^{\bullet-}$ ), hydrogen peroxide ( $H_2O_2$ ) and the hydroxyl radical ( $HO^{\bullet}$ ).



These reactive oxygen species (ROS) are believed to be responsible for oxygen toxicity (Fridovich 1978; Davies 1995; Mates and Sanchez-Jimenez 2000).

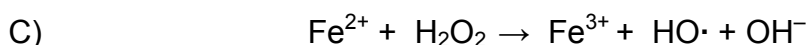
The discovery of superoxide dismutases (SODs), which are  $O_2^{\bullet-}$  scavenging enzymes, led to the proposal that  $O_2^{\bullet-}$  is the major component of oxygen toxicity (Fridovich 1989; Fridovich 1998)  $O_2^{\bullet-}$  is constantly produced by the electron transport chain of the mitochondria (Turrens and Boveris 1980). Here, a direct leakage of  $O_2^{\bullet-}$  occurs during the stepwise reduction of  $O_2$  to  $H_2O$  which is probably <5% but increases at higher  $O_2$  concentrations (Fridovich 1989; Fridovich 1998). The mechanisms by which  $O_2^{\bullet-}$  exerts its toxic effects were proposed to be mediated by direct oxidation and inactivation of enzymes that contain [4Fe-4S] clusters and by the reaction with nitric oxide (NO), with which the powerful oxidant peroxynitrite ( $ONOO^-$ ) is formed (Fridovich 1999). SOD's remove  $O_2^{\bullet-}$  by converting it to  $H_2O_2$ .



Though overexpression of several SOD isoforms has been observed to protect from certain oxidative stressors (Brockhaus and Brune 1999; Ilizarov, Koo et al. 2001; Wheeler, Nakagami et al. 2001), deleterious effects can develop under normal conditions mediated

by the subsequently increased production of H<sub>2</sub>O<sub>2</sub> (Fullerton, Ditelberg et al. 1998; Midorikawa and Kawanishi 2001).

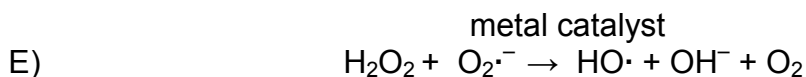
H<sub>2</sub>O<sub>2</sub> is known to be toxic in many systems, but it does not qualify as a radical itself because it has no unpaired electrons and is a poorly reactive oxidizing agent (Halliwell 1992). Instead, it mainly acts as the precursor of the highly reactive hydroxyl radical (HO·) formed by the Fenton reaction:



Copper ions also react with H<sub>2</sub>O<sub>2</sub> to form HO· (Halliwell and Gutteridge 1990). The Fe<sup>3+</sup> or Cu<sup>2+</sup> generated by this reaction can be reduced by O<sub>2</sub><sup>·-</sup>:



Combining equations C) and D) leads to the metal ion catalysed Haber-Weiss reaction:



This implies that much of the toxicity of O<sub>2</sub><sup>·-</sup> and H<sub>2</sub>O<sub>2</sub> is mediated by the production of HO·. This assumption is substantiated by the efficient mechanisms that have evolved to limit this reaction. One mechanism uses enzymes, like the catalases and selenium-dependent glutathione peroxidases (GPx), which metabolize H<sub>2</sub>O<sub>2</sub> (Hayes and McLellan 1999). On the other hand, the labile iron pool is kept under control by special iron binding proteins: excess iron is bound to either the storage protein ferritin or to transferrin (Crichton and Charlotiaux-Wauters 1987).

HO· generated by the Fenton or Haber-Weiss reaction reacts with great speed with almost every molecule found in living cells including DNA, causing chemical alteration and strand breakage (Halliwell and Aruoma 1991).

### 2.2.2 Oxidative stress and neurological diseases

The brain is particularly vulnerable to oxidative processes for several reasons (Behl, 1999): First, the brain has high-energy consumption and almost completely depends on the oxidative phosphorylation reaction to generate ATP, what leads to a high production of ROS by the mitochondria. Second, the brain contains a high concentration of polyunsaturated fatty acids, which are potential substrates for peroxidation. Third, it

contains relatively high amounts of iron and copper. Thus, it is not surprising that oxidative stress is assumed to play a role in neuronal diseases like Alzheimer's dementia, Parkinson's disease, and ischemic stroke.

Alzheimer's dementia is a chronic neurodegenerative disease which is neuropathologically characterized by extracellular senile plaques mainly loaded with amyloid  $\beta$  protein ( $A\beta$ ), intracellular neurofibrillary tangles, and degeneration of neurones (Glennner and Wong 1984; Braak and Braak 1991). The discovery that defects of the gene coding for the  $A\beta$  precursor protein (APP) can cause hereditary form of this disease substantiated the opinion that  $A\beta$  plays a causative role in the neurodegenerative process (St George-Hyslop 1995; Tanzi, Kovacs et al. 1996). Furthermore, the  $A\beta$  peptides which are generated by protease cleavage of APP are toxic to nerve cells in vitro and in vivo (Yankner, Dawes et al. 1989; Kowall, McKee et al. 1992). The observation that antioxidants can inhibit  $A\beta$  induced cell death in vitro (Behl, Davis et al. 1992; Behl, Davis et al. 1994) and nerve cell lines selected for the resistance to  $A\beta$  express increased amounts of antioxidant enzymes (Sagara, Dargusch et al. 1996) led to the opinion that  $A\beta$  somehow induces oxidative stress. How this is accomplished is not known, but the mechanism includes an induction of a superoxide generating enzyme system, sensitive to inhibitors of flavin-containing oxidases (Behl, Davis et al. 1994; Schubert, Behl et al. 1995).

In Parkinson's disease the loss of the dopaminergic neurones in the substantia nigra pars compacta leads to a movement disorder characterized by tremor and the difficulty to initiate movements (Hornykiewicz and Kish 1987). The pathological hallmark of this disease is the intraneuronal accumulation of  $\alpha$ -synuclein in Lewy bodies (Spillantini, Schmidt et al. 1997; Olanow and Tatton 1999).

The assumption that oxidative stress is involved in the pathophysiology of Parkinson's disease is based on several observations. First, it was recognised early that the metabolism of dopamine involves the generation of ROS either by production of  $H_2O_2$  by monoamino oxidases (Maker, Weiss et al. 1981) or by oxidation of the catechol ring to form dopamine quinines, semiquinones and ROS such as  $H_2O_2$  and  $O_2^-$  (Graham 1978; Hastings 1995). The quinones and semiquinones can react with glutathione (GSH) causing its depletion and the formation of glutathionyl conjugates (Spencer, Jenner et al. 1998; Spencer, Whiteman et al. 2002). In vitro dopamine was found to be neurotoxic, inducing oxidative stress (Basma, Morris et al. 1995; Si, Ross et al. 1998; Jones, Gunasekar et al. 2000). Recently, the observation that overexpression of either wild type or mutant  $\alpha$ -synuclein induces cell death due to oxidative stress selectively in dopaminergic neurones with a dependence on

dopamine synthesis provided the missing link between  $\alpha$ -synuclein dysregulation, oxidative stress, and selective degeneration of dopaminergic neurones (Xu, Kao et al. 2002).

### **2.2.3 Oxidative glutamate toxicity as a model for neuronal death due to oxidative stress**

Several in vitro models have been employed to investigate the steps leading to oxidative stress after specific insults imitating neurological diseases, i.e. Alzheimer's dementia and ischemic stroke, to cell death due to oxidative stress, and protective interventions using either primary neuronal cultures or neuronal cell lines and stressors like A $\beta$ , hydrogen peroxide, glutamate and others. Oxidative glutamate toxicity is an in vitro-model for studying neuronal death due to oxidative stress (Tan, Schubert et al. 2001).

After the initial description in a neuroblastoma-primary retina hybridoma cell line (N18-RE-105) (Murphy et al., 1989), it was observed in other neuronal cell lines (Schubert, Kimura et al. 1992; Davis and Maher 1994; Maher and Davis 1996; Froissard, Monroq et al. 1997), immature primary neurons which do not express ionotropic glutamate receptors (Murphy, Schnaar et al. 1990; Davis and Maher 1994; Ratan, Murphy et al. 1994), oligodendroglia (Oka, Belliveau et al. 1993) and astrocytes (Chen, Liao et al. 2000). Furthermore, part of the cell death observed after initial excitotoxic insult in mature neurones can be attributed to a secondary death of cells resistant to excitotoxicity but susceptible to oxidative glutamate toxicity induced by the high levels of glutamate released from neurones dying from excitotoxicity (Schubert and Piasecki, 2001).

Most studies which contributed to the characterization of the cell death program in oxidative glutamate toxicity were performed using the murine hippocampal cell line HT22 which was specifically selected for high sensitivity to oxidative glutamate toxicity (Davis and Maher 1994; Maher and Davis 1996; Li, Maher et al. 1997; Tan, Sagara et al. 1998; Tan, Wood et al. 1998; Ishige, Chen et al. 2001; Maher 2001). In comparison to glutamate excitotoxicity, oxidative glutamate toxicity is independent of ionotropic glutamate receptor activation (Murphy, Miyamoto et al. 1989; Schubert, Kimura et al. 1992).

In oxidative glutamate toxicity, elevated extracellular glutamate blocks the cystine import via the System X<sub>c</sub><sup>-</sup> glutamate/cystine antiporter (Murphy, Miyamoto et al. 1989; Tan, Schubert et al. 2001). The subsequent cystine depletion induces GSH depletion. Due to this impairment of the cells' antioxidant defence, ROS accumulate (Tan, Wood et al. 1998). Their sources are mainly the mitochondria (Maher and Davis 1996; Tan, Wood et al.

1998). The metabolism of catecholamines present in the cell culture medium further increases oxidative stress (Maher and Davis 1996). GSH depletion also activates 12-lipoxygenase which also contributes to ROS production (Li, Maher et al. 1997). The metabolites of the 12-lipoxygenase activate the soluble guanylate cyclase which induces an calcium influx via cGMP operated channels, which further increases the production of ROS (Li, Maher et al. 1997; Tan, Schubert et al. 2001). This leads to a form of programmed cell death, which morphologically shares some characteristics with apoptosis as well as necrosis (Tan, Sagara et al. 1998; Tan, Wood et al. 1998). However, hallmarks of classical apoptosis like nuclear fragmentation and DNA-laddering do not occur in this type and caspase-3 activation plays no significant role in the cell death execution, this form of cell death is critically dependent on gene transcription and translation and is blocked by inhibitors of caspases other than caspase-3 and serine proteases.

#### **2.2.4 Oxidative glutamate toxicity and G-protein coupled signaling**

Activation of G protein-coupled receptors (GPCRs) protects in diverse models of neurodegeneration (Yasui and Kawasaki 1995; Bond, O'Neill et al. 1998; O'Neill, Hicks et al. 1998; Takei, Skoglosa et al. 1998; Jolkkonen, Puurunen et al. 1999; Pizzi, Boroni et al. 1999); activation of others exacerbates neuronal cell death (Campbell 2001; Kimura, Mizukami et al. 2001). These differences might be explained by the capability of GPCRs to couple to different heterotrimeric G proteins. Receptor coupling to Gi/o seems to be detrimental as a result of oxidative stress, while Gs-coupling, at least in part, results in protection of neuronal cells (Lewerenz, Letz et al. 2003).

Pharmacologically distinct pathways, by which some GPCRs or GPCR-regulated kinases protect from oxidative glutamate toxicity in HT22 cells and immature primary neurones have been described (Ikeda, Ma et al. 1994; Papadopoulos, Koumenis et al. 1997; Sagara and Schubert 1998; Dargusch and Schubert 2002). G protein-coupled receptors that confer protection include the metabotropic glutamate receptors 1 and 5, which couple to Gq and block GSH depletion (Sagara and Schubert 1998), and the dopamine D4 receptor which block the cGMP-operated calcium channel (Ishige, Chen et al. 2001). Metabotropic glutamate receptors (mGluR) play roles in synaptic plasticity (Bashir, Bortolotto et al. 1993; Manzoni, Weisskopf et al. 1994; Riedel and Reymann 1996), seizure activity (Thomsen, Klitgaard et al. 1994), and excitotoxicity (Bruno, Battaglia et al. 1995; Bruno, Copani et al. 1995). Furthermore, a role for mGluRs in oxidative glutamate toxicity has also been described (Sagara and Schubert 1998).

GPCR mediated regulations consist mainly of the activation of protein kinase C (PKC) by phorbol esters, which protect by activation of the extracellular signal-regulated kinase (ERK) without modifying glutathione depletion or ROS accumulation. ERK, in turn, activates c-Jun NH<sub>2</sub>-terminal kinase (JNK) and blocks p38 mitogen-activated protein kinase (p38 MAPK) (Davis and Maher 1994; Maher 2001). Analysis of HT22 cells selected for resistance to glutamate revealed the upregulation of enzymes of the GSH-metabolism, catalase, and enzymes involved in the synthesis of the antioxidant bilirubin (Sagara and Schubert 1998). A detailed investigation of cross-resistances of either glutamate-resistant HT22 cells or PC 12 rat pheochromocytoma cells selected for resistance against A $\beta$  revealed a high cross-resistance between A $\beta$  and glutamate and related insults like cystine depletion and H<sub>2</sub>O<sub>2</sub> (Sagara and Schubert 1998). Thus, these cells employ mechanisms of general importance in the defence against oxidative stress.

## 3 Materials and Methods

### 3.1 Buffers

#### 10xMOPS running buffer

0.4 M MOPS, pH7.0

0.1 M sodium acetate

0.01 M EDTA

#### PBS

137 mM NaCl

2.7 mM KCl

7.4 mM Na<sub>2</sub>HPO<sub>4</sub>

1.5 mM KH<sub>2</sub>PO<sub>4</sub>

#### 50xTAE

1 M Tris base

5.71% (v/v) acetic acid

50 mM EDTA

Cell biology

### 3.2 Molecular Biology Methods

#### 3.2.1 Cloning of GPR15, GPR39, VPAC2

Full-length cDNAs of mGPR15, mGPR39 and hVPAC2 cloned in frame with a signal peptide and a hemagglutinin tag at the amino terminus were already cloned into pDNR *loxP* SP HA (modified from original Clontech vector) by Anna Pantlen.

For transient transfections, the sequences were cloned into pcDNA5 FRT/TO *loxP* expression vectors (Invitrogen), using the *loxP* site present in both vectors (Figure 3.1). This system is based on Cre Recombinase, a Type I topoisomerase from bacteriophage P1 that catalyzes the site-specific recombination of DNA between *loxP* sites (Abremski, Hoess et al. 1983). The enzyme requires no energy cofactors and Cre-mediated recombination quickly reaches equilibrium between substrate and reaction products. The

*loxP* recognition element is a 34 base pair (bp) sequence comprised of two 13 bp inverted repeats flanking an 8 bp spacer region which confers directionality (Metzger and Feil 1999).

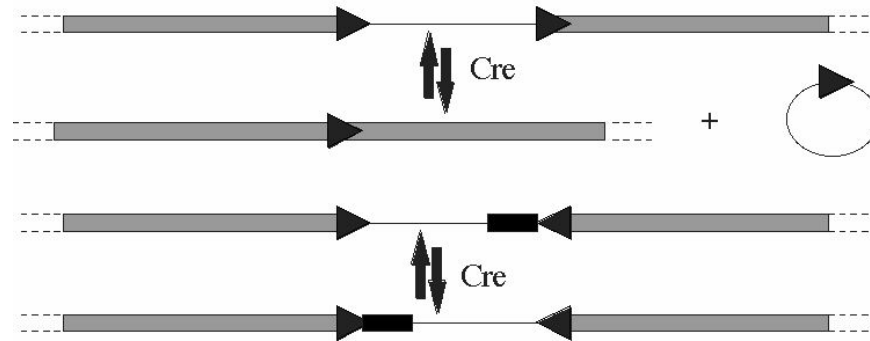


**Figure 3.1: The *loxP* system.** The system is based on a 34 bp sequence and a topoisomerase (Cre Recombinase). Sequences between two *loxP* sites facing the same direction are excised and the rest is ligated together by the enzyme, leaving a single *loxP* site. Sequences between two *loxP* sites facing towards each other are reversed.

For stable transfections, pDNR SP HA mGPR39 was used as a template for PCR. The product was cloned into pGEM-T Easy vector (Promega) and then digested using AgeI / BamHI sites (Figure 3.2). The digested fragment was then ligated with the pQCXIP vector (BD Biosciences), to get pQCXIP SP HA mGPR39. All constructs were verified by DNA sequencing.

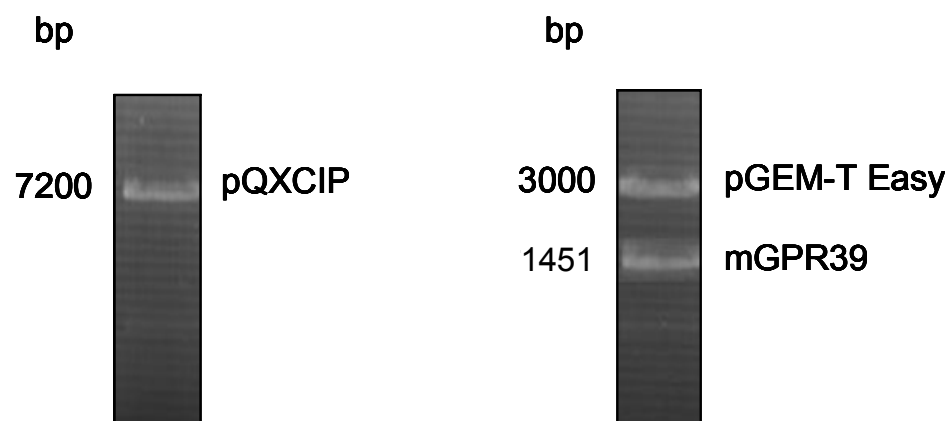


**Figure 3.2: Cloning of pQCXIP SP HA mGPR39.** Agarose gel showing both pQCXIP and pGEM-T Easy SP HA mGPR39, digested with the restriction enzymes AgeI / BamHI. The bands were at expected sizes.

### 3.2.2 Polymerase Chain Reaction

Full-length mGPR39 sequence was amplified from pDNR *loxP* SP HA mGPR39, together with Signal Peptide (SP) and Haemagglutinin tag (HA), using the following primers with AgeI (underlined) / BamHI (underlined) digestion sites:

forward 5'- ACCGGTCCACCATGAAGACGATCATCG - 3'

reverse 5'- GGATCCTCAAGATTCCTGCTCCTGTAA - 3'

For the reaction mixture, 1 µg template DNA, 5 µl 10xPCR Buffer (100 mM Tris-HCl, pH 8.4; 500 mM KCl; 0.8% NP-40), 1.5 µl MgCl<sub>2</sub> (50 mM), 1 µl of each primer (10 µM), 1 µl dNTP mixture (10mM), and 2.5 U Platinum Taq DNA Polymerase (Invitrogen) were combined in reaction tube and the total volume was brought to 50 µl with dH<sub>2</sub>O. Using the Biometra UNO II Thermocycler, PCR conditions were as follows: Denaturation at 94°C for 30 sec, annealing at 67°C for 30 sec, extension at 72°C for 30 sec and 25 cycles, followed by 10 minutes extension at 72°C.

### 3.2.3 Protein Preparation and Western Blotting

HT22 sensitive and resistant cells were harvested by treatment with 2 mM EDTA in PBS for 5 minutes, collected by centrifugation, and solved in Lysis Buffer (50 mM Tris-HCl pH 8.0, 150 mM NaCl, 1% SDS, 1% NP40, and 0.5% Sodium deoxycholate) containing a protease-inhibitor cocktail (complete-mini, Roche Molecular Biochemicals). Following incubation for 20 min at 4°C, the lysates were ultracentrifuged at 10.000 g for 10 min. The lysates were dissolved in SDS Sample Buffer (5 mM Na<sub>2</sub>HPO<sub>4</sub>, 2% SDS, 10 mM DTT, 5% β-mercaptoethanol, 10% glycerol, and bromphenolblue) and boiled at 95°C for 5 min. The resulting samples were subjected to denaturing 12% SDS polyacrylamide gel electrophoresis at 125 V. The electrophoretic transfer of the proteins onto nitrocellulose membrane was accomplished via semi-dry blotting at 125 mA for 50 min. After the transfer of the proteins, the nitrocellulose membrane was blocked in blocking solution (5% nonfat skim milk powder in TBS containing 0.1% TritonX100) overnight at 4°C. The following day, primary antibodies (rabbit polyclonal anti-GPR39 (Acris) or mouse monoclonal anti-Aktin (Covance)) were added to the blocking solution with a final dilution of 1:2000 and incubated at RT for 1 hour. After incubation the membrane was washed three times for 10 min in TBS containing 0.1% TritonX100, followed by an incubation of 1 h at RT with the second antibodies (goat anti-mouse or anti-rabbit IgG horse raddish peroxidase coupled antibody (Alexa)), diluted 1:125000. After another washing cycle (three times with TBS containing 0.1% TritonX100), the protein-antibody complex was

detected with the chemiluminescent reagent Lumi-Phos (Perbio Science). The Lumi-Phos reagent was evenly distributed onto the membrane and allowed to incubate for 5 min, before exposing the blot to X-ray film for the indicated times.

### 3.2.4 *In situ* Hybridization

For *in situ* hybridization, pDNR SP HA GPR39 was digested using EcoRI / PstI. The resulting 926 bp fragment was purified and inserted into pBluescript SK II + vector. The construct was verified by sequencing. After linearization with XhoI (sense) or NotI (antisense), the DNA was purified by phenol/chloroform extraction. The radioactively labelled RNA was synthesized by PD Dr. Irm Hermans-Borgmeyer using the MAXIscript *in vitro* transcription kit (Ambion, Frankfurt, Germany) with [<sup>35</sup>S]-UTP, according to the manufacturer's instructions. The labelled RNA was purified with Sephadex-G50 quick spin columns (Boehringer, Mannheim, Germany) in order to separate the unincorporated radioactive nucleotides from the transcripts. The antisense direction comprised a large part of the open reading frame (nucleotides 1-926) activity of the labelled RNA probe was determined by taking a sample and measuring the counts per minute (cpm) using a scintillation counter (Beckmann). The probe was diluted to a concentration of 5000 cpm/μl in hybridization solution containing 50% formamide, 1x Denhardt's solution, 4x SSC, 5% dextran sulphate, 500 μg/ml herring sperm DNA, 250 μg/μl yeast tRNA, and 10mM DTT. A minimum of 2x10<sup>6</sup> cpm/ml hybridization solution were used. Cryosections of 10 μm were fixed in 4% paraformaldehyde in phosphate buffered saline, acetylated, dehydrated, and subjected to *in situ* hybridization at 55°C for 18 hours. The slides were washed with 4x SSC and subsequently treated with RNase buffer (10 mM Tris-HCl, pH 8.0, 500 mM NaCl, 1 mM EDTA, 20 μg/ml RNase) for 30 min at 37°C, to digest single stranded non-hybridized RNA. The slides were then washed at decreasing salt concentrations. A 30 min high-stringency wash was performed in 0.1x SSC at 55°C- Sections were dehydrated and exposed to high-resolution X-ray film (Kodak Biomay MR). Subsequently, the slides were dipped in Kodak NTB-2 nuclear track emulsion, developed after 3 weeks in Kodak Dektol, and stained with Giemsa (Sigma). Specificity of the signals was verified by comparing antisense with the sense controls.

### **3.3 Cell Biology Methods**

#### **3.3.1 Cell culture and viability assays**

HT22 cells were obtained from Prof. Paschen, Max-Planck-Institute for Neurological Research, Cologne, Germany. These cells represent a subclone of the murine hippocampal cell line HT4 immortalized by a temperature-sensitive SV-40 T antigen (Morimoto and Koshland, 1990) selected for high sensitivity to glutamate (Maher and Davis, 1996). Cells were cultivated at 37 °C in an 5% CO<sub>2</sub>-atmosphere and high glucose-Dulbecco's modified minimal essential medium (high glucose-DMEM, PAA Laboratories) containing 5% fetal calf serum (FCS, Gibco), 2 mM L-glutamine (Life Technologies), 100 IU/ml penicillin, and 100 µg/ml streptomycin (both from Life Technologies). Cells were passaged by dissociation with 0.5% trypsin and 0.2 % EDTA (Life Technologies) every other day. For viability assays 5 x 10<sup>3</sup> cells in 100 µl were seeded into 96-well microtiter plates (Falcon). L-Glutamic acid (Sigma) was solubilised in H<sub>2</sub>O at a concentration of 250 mM, adjusted to pH 7.4 with sodium hydroxide and stored at -20° C. It was added 24 hours later for 8 hours as indicated. Other experimental agents were also added after 24 hours, unless indicated. Cell survival was judged by phase contrast microscopy and assayed using the methylthiazoltetrazolium (MTT) method (Hansen et al., 1989). Briefly, MTT (Sigma) solubilised in phosphate buffered saline (PBS, 5 mg/ml) was added to the cells 24 hours after addition of glutamate to a final concentration of 1 mg/ml. Two hours later, cells were lysed by addition of 125 µl of lysis buffer containing 50 % dimethyl formamide, 20% sodium dodecyl sulfate, 2% acetic acid, adjusted to pH 4.7. Absorbance was measured after 24 hours at 550 nm using a microplate reader (SLT labinstruments, Crailsheim, Germany). Each experiment was done in quadruplicates as not otherwise mentioned and done at least three times. Using the GraphPadPrism<sup>TM</sup> software the mean optic density obtained in the control not treated with neither glutamate nor experimental agents tested was normalised to 100% and data of three experiments were pooled and subjected to statistical analysis done by unpaired student's *t* test.

#### **3.3.2 Transfection of DNA into mammalian cells**

##### **3.3.2.1 Transfection by electroporation**

Adherent HT22 cells were trypsinized in 1 ml Trypsin/EDTA for 2 min at RT, followed by resuspension in 4 ml serum-containing DMEM, and centrifuged for 4 min at 1000 rpm.

The cell pellet was resuspended in 5 ml PBS and re-centrifuged for 4 min at 1000 rpm. The cell pellet was resuspended in 500  $\mu$ l ice-cold PBS, and mixed with 10  $\mu$ g of the DNA of interest. The tube containing the cells and DNA was incubated on ice for 15 min. After incubation, the mixture was transferred into an electroporation cuvette (Invitrogen, 4  $\mu$ m) and placed in the holder of the electroporation apparatus at room temperature. A single puls shock with 250 mV and 960  $\mu$ F was applied. The time constant was kept between 16-22 msec for all the transfections. After the electroporation, the cells were taken in 10 ml of serum-containing DMEM and incubated for 24 hours at 37°C, before continuing with the experiments.

### **3.3.2.2 Transfection by Calcium Phosphate**

In order to transfect pQCXIP SP HA mGPR39 and pQCXIP EGFP into the Phoenix-Eco cells (Orbigen), the cells were grown to 60-70% confluency. About 5 minutes prior to transfection, cell media was replaced with 3 ml fresh media supplemented with 25  $\mu$ M chloroquine for each plate. The transfection reagent (10  $\mu$ g DNA, 438  $\mu$ l dH<sub>2</sub>O, 61  $\mu$ l 2M CaCl<sub>2</sub>) was prepared in a 15 ml Falcon tube. Before transfection, 0.5 ml 2xHBS Solution (50 mM HEPES, pH 7.05; 10 mM KCl, 12 mM Dextrose; 280 mM NaCl; 1.5 mM Na<sub>2</sub>HPO<sub>4</sub>) was added into the transfection reagent and combined by vigorously pipetting. The finished transfection reagent was quickly added dropwise onto the dishes containing Phoenix-eco cells, and the dishes were rocked gently to distribute DNA/CaPO<sub>4</sub> particles evenly. The dishes were then incubated at 37°C for 24 hours and then with fresh medium for another 24 hours.

### **3.3.3 Stable Cell Line Production**

For obtaining a stable HT22 cell line overexpressing mGPR39, the packaging cell line Phoenix-Eco (Orbigen Inc) was co-transfected with pQCXIP SP HA mGPR39 and pQCXIP EGFP, using the Calcium Phosphate Method. Following transfection, the cells were incubated for 48 hours before adding Puromycin (final concentration: 2.5  $\mu$ g/ml) to the medium. The cells were kept in this medium for 2 weeks, with changing the medium every 48 hours. After this time, all the cells in culture were expressing EGFP stably and had Puromycin resistance. These cells were passaged and incubated at 37°C until they reached 60-70% confluency. At this stage, the medium was removed and centrifuged at 2000xg for 5 min, to get rid of cell debris. In order to achieve viral transfection, the resulting medium was put onto 24-hour-old HT22 cells in culture. After waiting for 48

hours, Puromycin was added into the medium at a final concentration of 2.5 µg/ml. The cells were kept in this medium for 3 weeks, with fresh medium being added every other day. Cells building colonies were isolated using cloning cylinders (Sigma) and transferred into 96-well plates, where they were further propagated.

### **3.3.4 Flow Cytometry**

#### **3.3.4.1 Measurement of ROS levels**

For analysis by flow cytometry,  $1 \times 10^5$  cells were seeded in six-well plates (Falcon) and grown for 24 hours. The next day, the cells were collected using PBS/EDTA and centrifuged at 1000 rpm for 4 minutes. Then the cells were incubated with 20 µM DCFDA for 30 minutes at 37°C, protected from light. After incubation, the cells were washed once with PBS, and centrifuged at 1000 rpm for 4 minutes and the pellets were resuspended in PBS containing 1 µg/ml 7-amino-actinomycin D (7-AAD, Calbiochem-Novabiochem). Cells were stored on ice until measurement at 488 nm with an FACS Calibur flow cytometer (Becton Dickinson). Median fluorescence of viable cells was calculated by the Cell Star™ software for each substance and time point.

#### **3.3.4.2 Measurement of mGPR39 and HA expression**

For analysis by flow cytometry,  $1 \times 10^5$  cells were seeded in six-well plates (Falcon) and grown for 24 hours. The next day, the cells were collected using PBS/EDTA and centrifuged at 1000 rpm for 4 minutes. Then the cells were incubated with the specific antibodies (mouse monoclonal anti-HA or rabbit polyclonal anti-GPR39) in PBS containing 2% FCS for 20 minutes at 4°C. After 20 minutes, cells were washed twice with PBS + 2% FCS, and incubated with the secondary antibodies (Alexa Fluor anti-mouse or anti-rabbit) for further 20 minutes. Cells were washed once more by centrifugation at 1000 rpm for 4 minutes and the pellets were resuspended in PBS + 2% FCS containing 1 µg/ml 7-amino-actinomycin D (7-AAD, Calbiochem-Novabiochem). Cells were stored on ice until measurement at 488 nm with an FACS Calibur flow cytometer (Becton Dickinson). For CRE-mediated EGFP measurements, the cells were directly stained with 7-AAD and measured. Dead cells were identified by 7-AAD staining and excluded from the analysis. Median fluorescence of viable cells was calculated by the Cell Star™ software for each substance and time point.

### **3.3.5 Measurement of total GSH**

Five thousand HT22 and HT22R cells were plated in white, non-transparent 96 well-microtiter plates. After 24 hours of cultivation, cells were incubated with glutamate or vehicle for six hours or as indicated. Cells were then carefully washed twice with phenol red-free media and incubated with 20  $\mu$ M MCB for five minutes at 37° protected from light. MCB fluorescence was then measured by a SpectraMax Gemini (Molecular Devices, Ismaning, Germany) using the SoftmaxPro 3.1.1 software (Softmax, San Diego, USA). Excitation wavelength was 393 nm and emission wavelength was 485 nm. After measurement, one volume normal medium and MTT were added immediately and cell viability assessed as described above two hours later. Results indicate MCB fluorescence per well normalized to the corresponding viability as measured by the MTT-test.

## **3.4 Preparation of RNA**

### **3.4.1 Cell cultivation for RNA preparation**

$5 \times 10^5$  HT22 and HT22CR were seeded in 92 mm-cell culture dishes. HT22CR were cultivated in the presence of 10 mM glutamate. Cells were harvested after 24 hours of cultivation. Additionally, HT22 cells were treated with 10 mM glutamate after 24 hours and harvested six hours later. For harvesting, cells were washed once with PBS and detached by PBS with 2 mM EDTA. After centrifugation with 200 x g for four minutes cells were washed with PBS and again pelleted by centrifugation. Supernatant was removed, cells were shock-frozen in liquid nitrogen and stored at  $-70^{\circ}\text{C}$  until RNA-preparation.

### **3.4.2 Isolation of total RNA**

Total RNA was prepared by single step isolation using TRIzol™ Reagent (Life Technologies). The reagent is a mono-phasic solution of phenol and guanidine isothiocyanate and an improvement of the method originally described by Chomczynski and Sacchi (Chomczynski and Sacchi, 1987). Each cell pellet weighting ~200 mg was thawed and homogenised in 2 ml TRIzol under constant aspiration through a 20 gauge-needle. To permit the dissociation of the nucleoprotein complexes samples were incubated five minutes at room temperature. 0.4 ml of chloroform was added and tubes shaken vigorously for 15 seconds to mix the phases and then again incubated at room temperature

for three minutes. Aqueous and organic phase were separated by centrifugation at 12 000 x g for 15 minutes at 4°C. The upper aqueous phase that contains the RNA was carefully aspirated and transferred into a fresh tube. The total RNA in the aqueous phase was precipitated by mixing with 1 ml isopropyl alcohol. After mixing and incubation at room temperature for ten minutes the tubes were centrifuged at 12 000 x g at 4 °C for ten minutes. The supernatant was removed and the RNA pellet was washed once with 75% ethanol by short vortexing, followed by centrifugation at 7500 x g for five minutes at 4°C. The pellet was air dried at 37°C and redissolved in five to ten µl RNase-free H<sub>2</sub>O.

### **3.4.3 Qualitative analysis of total RNA by agarose electrophoresis**

To detect contamination with RNA-degrading enzymes each RNA-sample was mixed with ethidium bromide to a final concentration of 0.25 µg/ml and size fractionated using 1% Seakem LE<sup>TM</sup> agarose (BMA) in 1xTAE and 20 Volt/cm for 10 minutes in a ice-water bath. RNA samples with clearly visible non-degraded 18S and 28 S RNA and tRNA were pooled.

### **3.4.4 Quantification of RNA by absorption spectroscopy**

To determine RNA-concentration absorption after appropriate dilution of samples in H<sub>2</sub>O was measured by spectroscopy at 260 nm wavelength and contamination with proteins was judged by the 260/280 nm-ratio of absorption using a UV-160A spectrophotometer (Shimadzu). RNA-concentration (µg/ml) was calculated by division of the absorption at 260 nm by 0.025. This equation uses  $0.025 \text{ (g/ml)}^{-1}\text{cm}^{-1}$  as specific absorption coefficient of single-stranded RNA.

## **3.5 Quantitative PCR**

Templates for PCR were single stranded cDNA from glutamate sensitive and resistant HT22 cells. To determine the exponential phase of amplification, aliquots of the PCR-reaction were removed after 15, 20, 25, 30, 35 and 40 cycles and visualized on ethidium bromide stained agarose gels. Then, aliquots were removed every other cycle starting five cycles before the first appearance in ethidium bromide stained gels and dot blotted onto nylon membranes with a 96 well pin tool. Oligonucleotides specific for differentially expressed GPCRs, as judged by ethidium bromide stained gels, were end-labeled with 5 µCi ( $\gamma$ -<sup>32</sup>P) ATP using the Megaprime DNA labeling system (Amersham Pharmacia

Biotech, UK) and hybridized to the membranes overnight at 42°C. Specific activity was  $>10^7$  cpm/pmol oligonucleotide. Membranes were washed under high-stringency conditions, exposed to phosphoimaging plates and analysed with Tina Version 2.10h (Raytest). The density of each spot on the blot was plotted on a semi logarithmic scale against the cycle number for each reaction to estimate the PCR efficiency. Values were presumed to be valid if compared curves were parallel at a given cycle number, indicating both reactions being in the exponential phase of amplification. The difference in PCR cycles between glutamate sensitive and resistant HT22 cells was multiplied with the PCR efficiency to calculate the magnitude of regulation. This was then normalized to  $\beta$ -actin and gapdh expression.

All experiments showing no difference between glutamate sensitive and resistant HT22 cells were replicated once; differences were reproduced three times with two different mRNA preparations to calculate the mean of regulation  $\pm$  SEM.

Specific primers corresponding to the given part of the receptors were synthesized by MWG Biotech: VPAC<sub>1</sub> (accession number NM\_011703, forward primer (fp) 325-345 bp, reverse primer (rp) 438-457 bp, probe (p) 356-378 bp, T<sub>m</sub> 59°C), VPAC<sub>2</sub> (NM\_009511, fp 897-918, rp 1058-1076, p 985-1007, T<sub>m</sub> 59°C), PAC<sub>1</sub> (NM\_007407, fp 1004-1022, rp 1124-1144, p 1065-1086, T<sub>m</sub> 63°C) AT<sub>2</sub> (NM\_007429, fp 645-667, rp 781-803, p 697-717, T<sub>m</sub> 59°C), A1 (XM\_129465, fp 728-746, rp 865-886 T<sub>m</sub> 55°C), A2A (XM\_125720, fp 921-940, rp 1247-1267, p 961-980, T<sub>m</sub> 63°C), A2B (NM\_007413, fp 605-627, rp 743-762 T<sub>m</sub> 55°C), A3 (AF069778, fp 5036-5055, rp 5289-5311, T<sub>m</sub> 55°C), P2Y1 (NM\_008772, fp 481-500, rp 692-712, T<sub>m</sub> 55°C), P2Y2 (NM\_008773, fp 943-963, rp 1215-1233, p 1002-1019, T<sub>m</sub> 55°C), P2Y4 (NM\_020621, fp 771-791, rp 910-928, T<sub>m</sub> 55°C), P2Y6 (XM\_133678, fp 744-764, rp 927-945, p 858-879, T<sub>m</sub> 63°C), S1P1 (NM\_007901, fp 1117-1139, rp 1216-1233, p 1189-1208, T<sub>m</sub> 55°C), LPA1 (BC025425, fp 989-1009, rp 1121-1142, p1007-1023, T<sub>m</sub> 55°C), S1P3 (NM\_010101, fp 683-702, rp 810-831, p 736-755, T<sub>m</sub> 55°C), PAR1 (NM\_010169, fp 659-679, rp 1041-1057, p 989-1007, T<sub>m</sub> 55°C), PAR2 (NM\_007974, fp 463-482, rp 586-605, T<sub>m</sub> 55°C), PAR3 (BC037126, fp 1137-1154, rp 1241-1262, p 1181-1203, T<sub>m</sub> 55°C), mGlu<sub>1</sub> (AF320126, fp 1743-1764, rp 1826-1846, p 1784-1805, T<sub>m</sub> 55°C), mGlu<sub>5</sub> (U31444, fp 5083-5101, rp 5176-5199, T<sub>m</sub> 55°C), mGlu<sub>3</sub> (AF170699, fp 395-415, rp 522-541, p 415-437, T<sub>m</sub> 59°C), mGlu<sub>8</sub> (XM\_194317, fp 2910-2931, rp 2973-2993, p 2939-2957, T<sub>m</sub> 55°C), CB1 (NM\_007726, fp 1073-1091, rp 1276-1296, T<sub>m</sub> 55°C) CASR (AF128842, fp 2967-2988, rp 3118-3116,

Tm 55°C), GAPDH (XM\_122186, fp 1007-1026, rp 1204-1225, p 1110-1130, Tm 55°C),  
β-ACTIN (NM\_007393, fp 817-838, rp 946-967, p 863-884, Tm 59°C)

## 4 Results

### 4.1 Oxidative Glutamate Toxicity

#### 4.1.1 HT22 cells die from oxidative glutamate toxicity upon exposure to glutamate

In order to determine the dose- and time dependence of glutamate-induced cell death,  $5 \times 10^3$  HT22 cells per well were seeded in 96-well microtiter plates and treated with 2.5 mM, 5 mM, and 10 mM glutamate after 24 hours. Glutamate exposure was stopped by changing the medium and cell survival was measured by the MTT test, 24 hours after addition of glutamate (Figure 4.1).

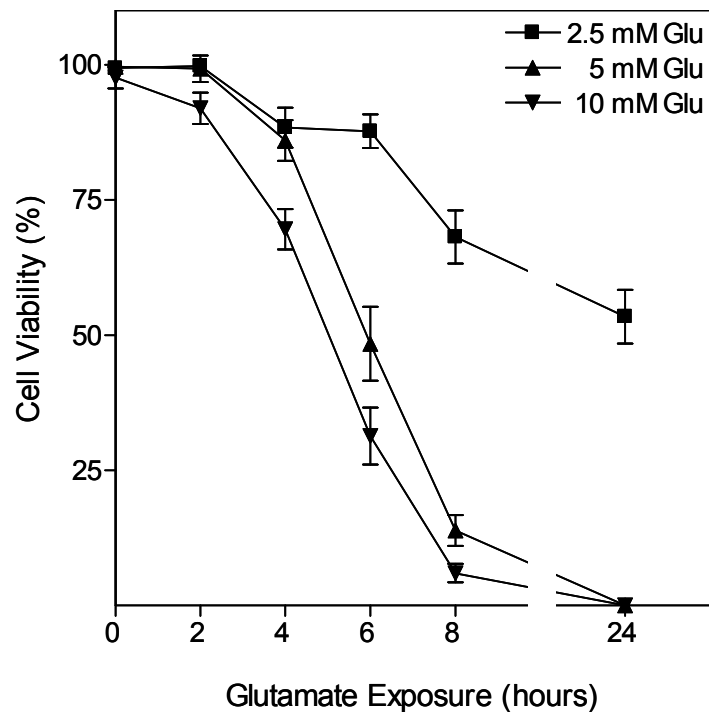


**Figure 4.1: Time and concentration dependence of glutamate-induced cell death.** HT22 cells were treated with the indicated concentrations of glutamate for the indicated times. Glutamate exposure was stopped by changing the medium, and cell survival was measured by MTT after the completion of 24 hours. Viability of untreated cells was normalized to 100%. The graph represents the data of the relative cell viability obtained from three independent experiments each done in quadruplicates as mean  $\pm$  SEM.

Two or four hours of glutamate treatment resulted only in limited cell death at all concentrations tested, whereas the next four hours led to a rapid decline in survival to ~14% and ~9% at 5 and 10 mM, respectively. Extending treatment to 24 hours completed

cell death in the presence of 10 mM glutamate, whereas only ~50% died at 2.5 mM glutamate.

In summary, HT22 are sensitive to glutamate under the chosen conditions and the induction of cell death by either 5 mM or 10 mM glutamate was nearly completed within the first eight hours of treatment.

#### 4.1.2 Susceptibility to glutamate is influenced by cell culture conditions

Next, it was investigated whether the susceptibility to glutamate was modulated by cell culture conditions. In order to answer this question, first the influence of cell density was investigated. HT22 cells were plated at different densities and treated with different concentrations of glutamate for 8 hours (Figure 4.2).

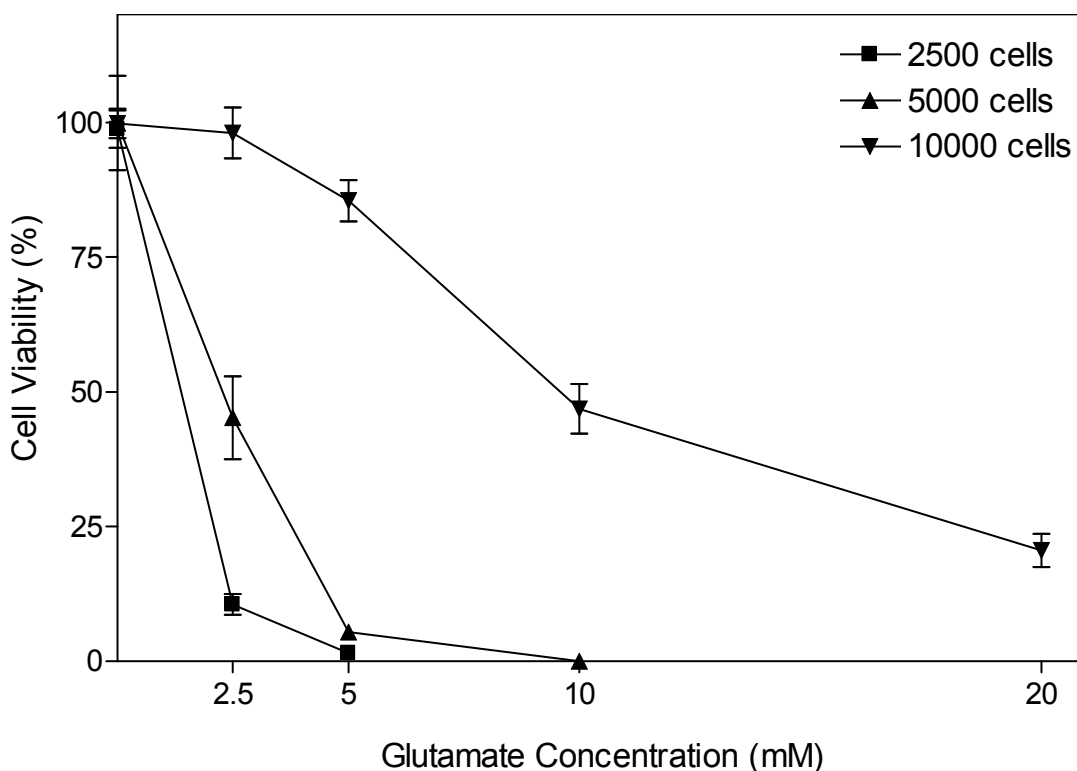


**Figure 4.2: Glutamate susceptibility depends on culture density.** HT22 cells were seeded with different densities and treated with the indicated concentrations of glutamate for 8 hours. Glutamate exposure was stopped by changing the medium, and cell survival was measured by MTT after the completion of 24 hours. Viability of untreated cells was normalized to 100%. The graph represents the data of the relative cell viability obtained from four independent experiments each done in quadruplicates as mean  $\pm$  SEM.

The LD<sub>50</sub> drastically increased from 2.41 mM (SEM 0.3559, n=16) glutamate for cells seeded at a density of  $5 \times 10^3$  per well to 9.786 mM (SEM 0.2015 n=16) when  $1 \times 10^4$  cells

were seeded, and dropped to 1.912 mM (SEM 0.0109 n=16) when  $2.5 \times 10^3$  cells were seeded.

We concluded that the observed modulation of glutamate toxicity by cell density might result from increased cell-cell interactions either in dense cultures or from pronounced modification of the growth medium by the increase in numbers of cells.

To characterize the influence of growth medium, normal growth medium was replaced with defined medium either with or without different concentrations of serum, simultaneous with glutamate treatment. In defined medium, limited cell death occurred during 8 hours of glutamate application. Cell death was prominently increased by the presence of 2.5% serum (Figure 4.3). The effect was further enhanced by increasing serum concentration to 5%. Under the latter conditions, a ~10-fold reduction of cell survival induced by 5 mM glutamate was observed compared to serum-free conditions. Therefore, we conclude that serum contains essential cofactors that modulate the susceptibility of HT22 cells to glutamate.

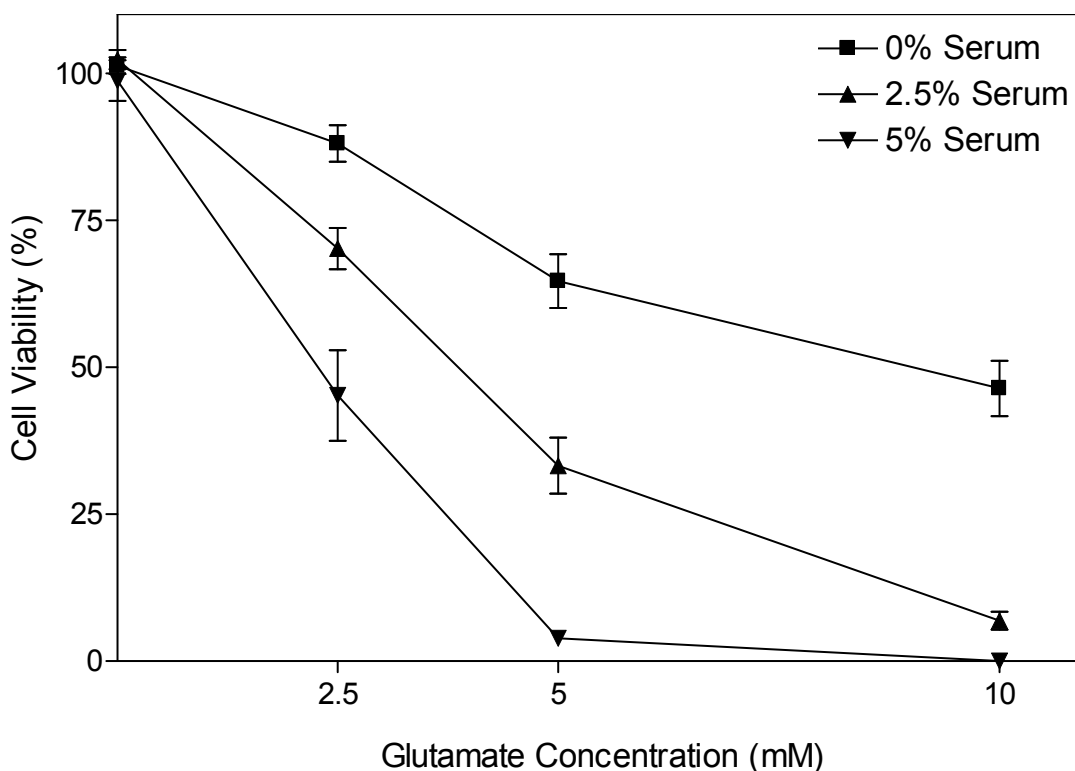


**Figure 4.3: The effect of serum concentration on glutamate susceptibility.** HT22 cells were seeded at  $5 \times 10^3$  cells per well with different serum and glutamate concentrations for 8 hours. Glutamate exposure was stopped by changing the medium, and cell survival was measured by MTT. Viability of untreated cells was normalized to 100%. The graph represents the data of the relative cell viability obtained from three independent experiments each done in quadruplicates as mean  $\pm$  SEM.

To answer this question, we tested if medium enriched with factors released by HT22 cells had protective properties. Normal growth medium was conditioned for 24 hours by confluent HT22 cultures. Twenty-four hours after plating  $5 \times 10^3$  HT22 cells per well, the conditioned medium was used for glutamate treatment and cell death compared to cultures with fresh medium and glutamate alone. Cells treated with glutamate for 8 hours, in the presence of HT22-conditioned medium did not die at 2.5 mM glutamate and survival after 10 mM glutamate was massively increased from ~5% to 50% (Figure 4.4).

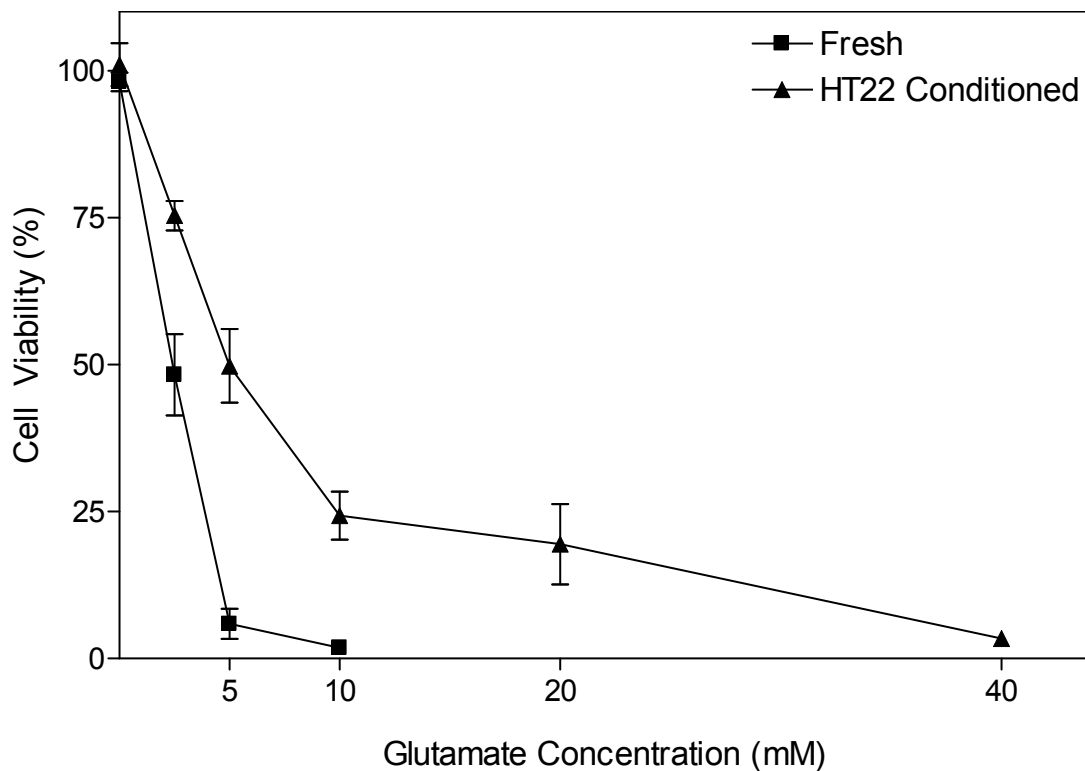


**Figure 4.4: Conditioned medium alters glutamate sensitivity.** HT22 cells were seeded at  $5 \times 10^3$  cells per well with different glutamate concentrations for 8 hours. Glutamate exposure was stopped by changing the medium with either fresh or conditioned medium from sub-confluent HT22 cultures, and cell survival was measured by MTT after the completion of 24 hours. Viability of untreated cells was normalized to 100%. The graph represents the data of the relative cell viability obtained from three independent experiments each done in quadruplicates as mean  $\pm$  SEM.

Thus, HT22 cells modify the growth medium in a manner that protects other cells in the vicinity from glutamate-induced cell death.

### 4.1.3 Oxidative glutamate toxicity depletes the glutathione levels within the cells

Oxidative glutamate toxicity, unlike glutamate excitotoxicity, is known to proceed through a mechanism independent of ionotropic glutamate-receptor activation (Murphy, Miyamoto et al. 1989). In oxidative glutamate toxicity, elevated extracellular glutamate blocks the cystine import *via* the System X<sub>c</sub><sup>-</sup> glutamate/cystine antiporter (Tan, Schubert et al. 2001). The subsequent decrease in cystine results in GSH depletion. Due to the subsequent impairment of the cells' antioxidant defence, ROS accumulate (Tan, Sagara et al. 1998).

To verify the depletion of GSH followed by ROS accumulation, the cells were treated with or without different concentrations of glutamate for 6 hours, and then incubated with the fluorescent probe Monochlorobimane (MCB). Following incubation, glutathione levels in the cells were measured in a GEMINI Fluorescence Plate Reader, using indicated wavelengths.

Unlike older methods utilizing 5,5'-dithiobis(2-nitrobenzoic acid) (DTNB or Ellman's reagent) in an oxidation or oxidation-reduction scheme, monochlorobimane allows intracellular glutathione S-transferase detection (Rice, Bump et al. 1986; Cook, Pass et al. 1989). This membrane-permeable reagent has been used to measure GSH in tissue homogenates (Kamencic, Lyon et al. 2000), in cultured neural cells (Devesa, O'Connor et al. 1993; Reichelt, Stabel-Burow et al. 1997) and also in HT22 cells (Tan, Sagara et al. 1998), using flow cytometry and other fluorometric systems. It has been found that monochlorobimane readily enters cells to form a fluorescent GSH–monochlorobimane adduct that can be measured fluorometrically and that this reaction is catalyzed by glutathione S-transferase.

For measuring ROS levels, the cells were incubated with another fluorescent probe, DCFDA. After incubation, the cells were incubated in 7-amino-actinomycin D (7-AAD). Reactive oxygen species levels were measured at 488 nm with a flow cytometer. DCFDA is both cell-permeable and non-fluorescent until oxidized in the cytoplasm of live cells. After entering live cells, the diacetate group is cleaved by intracellular esterases. Oxidation of the reduced dye can then occur in the presence of ROS, causing the dye to fluoresce (Zhu, Bannenberg et al. 1994).

Incubating the cells with 5 mM glutamate reduced the glutathione levels from 100% (SEM 12.244 n=12) to 10.8% (SEM 2.141 n=12), while increasing ROS levels by 108% (SEM 15.179 n=12) (Figure 4.5). In conclusion, glutamate alters the glutathione and ROS levels within the HT22 cells leading to cell death.

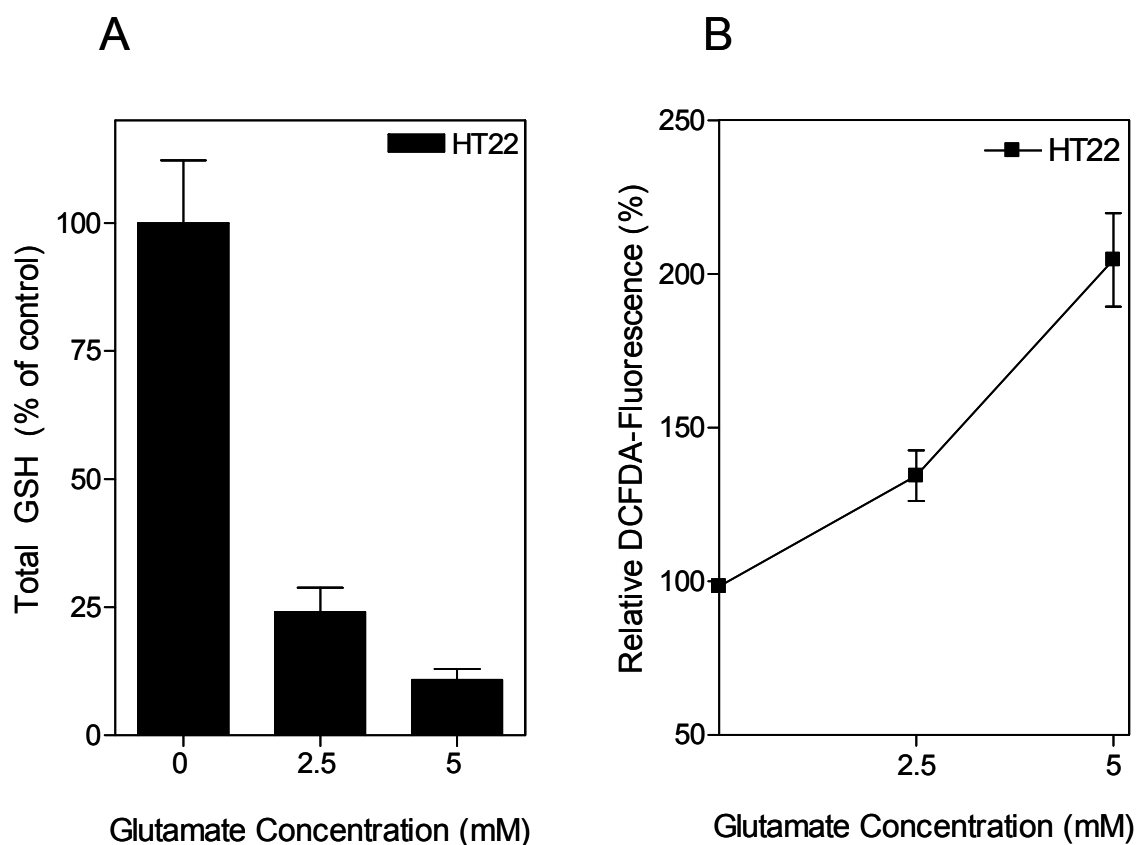


**Figure 4.5: Glutathione and ROS levels change under glutamate toxicity.** HT22 cells were seeded in 96-well or 6-well plates with different glutamate concentrations. **(A)** For GSH-measurements, the cells in 96-well plates were incubated with Monochlorobimane and then analysed using a GEMINI Fluorescence Plate Reader. Cell survival was measured by MTT directly after the measurements. **(B)** For ROS measurements, cells in 6-well plates were collected and incubated with DCFDA and 7-AAD, followed by FACS analysis at 488 nm. Starting levels of untreated cells were normalized to 100%. The graphs represent the data of the relative cell viabilities obtained from three independent experiments each done in quadruplicates as mean  $\pm$  SEM.

#### 4.1.4 Glutamate resistant HT22 cells are also resistant to different kinds of cell death inducers

Cell selection for resistance is widely used to identify mechanisms of resistance to toxic substances, e.g. to characterize resistance to anti-cancer drugs in neoplastic cell lines and the cellular defence against A $\beta$  toxicity and other forms of oxidative stress (Mulcahy et al., 1994; Sagara et al., 1998; Sagara et al., 1996).

Glutamate resistant cell lines were previously generated by Dr. Jan Lewerenz in our group. Briefly, HT22 cells that were to be selected for resistance against glutamate toxicity were repetitively exposed to glutamate for 24 hours. Between two treatments, the surviving cells

were expanded until they reached a reasonable number for the next selection. For the first round, the cells were treated with 10 mM glutamate, while the next three treatments were done with 20 mM glutamate. The last selection was expanded to 48 hours and those, which survived, were cultivated further in 10 mM glutamate. These cells were referred to as chronically resistant HT22 cells (HT22CR).

In contrast to wild type HT22 cells, HT22CR cells tolerate up to 20 mM glutamate without substantial reduction in viability (HT22 2.45% survival (SEM 0.243 n=52) vs. HT22CR 96.56% survival (SEM 4.282 n=52)) (Figure 4.6).

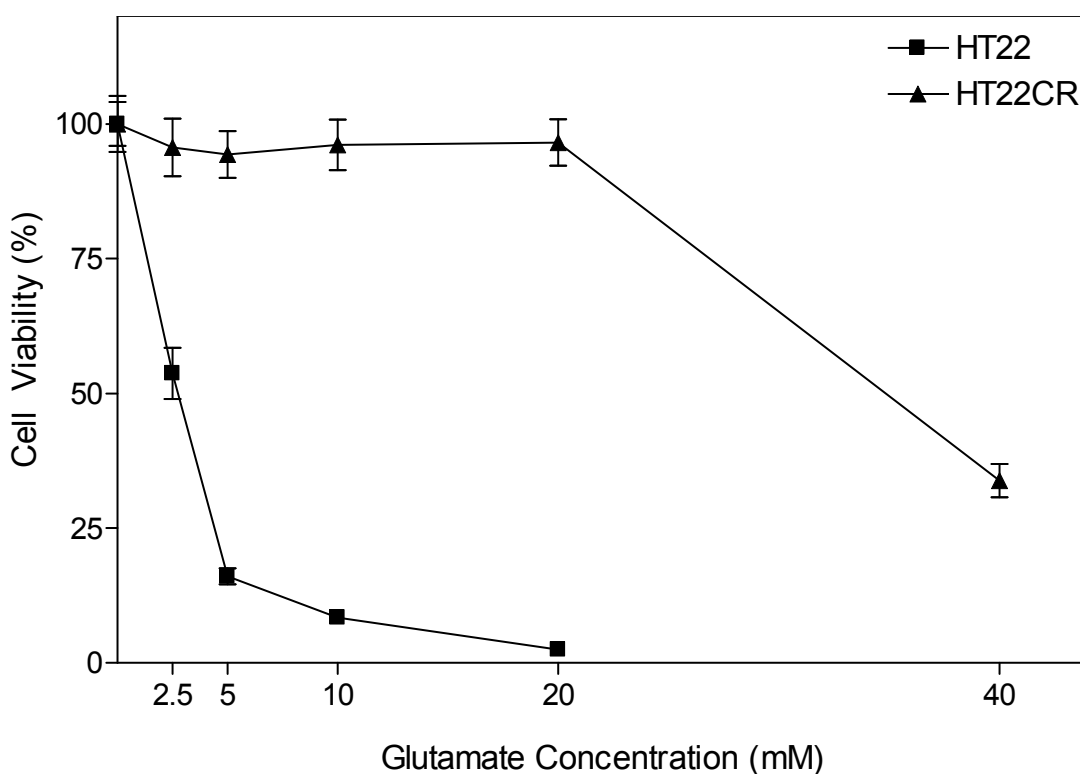


**Figure 4.6: Glutamate resistant and sensitive cells differ in viability under glutamate.** HT22 cells were seeded at  $5 \times 10^3$  cells per well with increasing glutamate concentrations for 8 hours. Glutamate exposure was stopped by changing the medium, and cell survival was measured by MTT. Viability of untreated cells was normalized to 100%. The graph represents the data of the relative cell viability obtained from thirteen independent experiments each done in quadruplicates as mean  $\pm$  SEM.

To test further resistance in HT22CR, the wild type and resistant cell lines were subjected to  $H_2O_2$  stress. Most of the HT22CR cells (62.5% (SEM 3.367 n=18)) survived a treatment with 750  $\mu M$   $H_2O_2$ , whereas only 23.4% of HT22 cells (SEM 6.091 n=18) survived at the same concentration (Figure 4.7). Consequently,  $LD_{50}$  increased from 564  $\mu M$  (SEM 3.58 n=18) in HT22, to 874  $\mu M$  (SEM 3.467 n=18) in HT22CR cells.

In order to test the capacity of resistance, HT22CR cells were subjected to other kinds of stress inducers that directly induce oxidative stress. The first stress-inducing agent was the pro-apoptotic signaling sphingolipid Ceramide, that is capable of modifying the activity of a number of proteins, including receptors, ion channels, and enzymes as well as intracellular Calcium levels (Colombaioni and Garcia-Gil 2004).

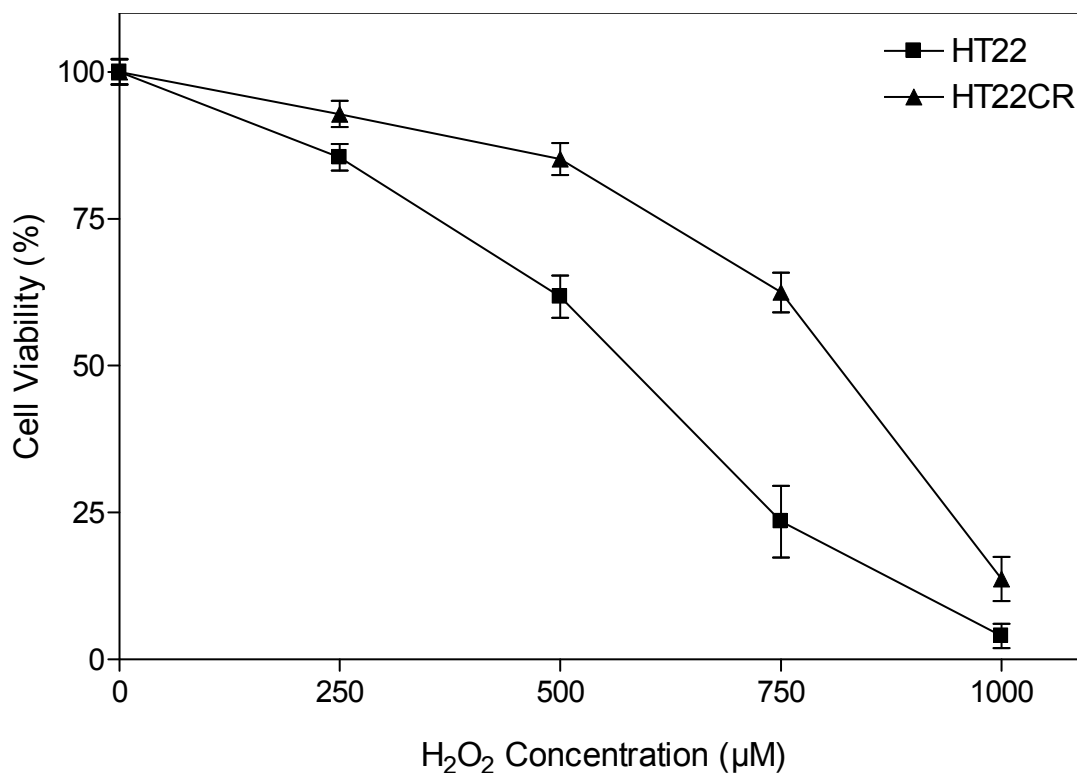


**Figure 4.7: Glutamate-resistant cells show also resistance against hydrogen peroxide.** HT22 cells were seeded at  $5 \times 10^3$  cells per well with different hydrogen peroxide (H<sub>2</sub>O<sub>2</sub>) concentrations for 24 hours. Cell survival was measured by MTT. Viability of untreated cells was normalized to 100%. The graph represents the data of the relative cell viability obtained from three independent experiments each done in quadruplicates as mean  $\pm$  SEM.

Ceramide has been known to act in different cellular processes leading to apoptosis, differentiation, or survival, depending on the amount that is used (Goodman and Mattson 1996; Irie and Hirabayashi 1998; Lu and Wong 2004). The apoptotic effect is mediated mainly by the activation of components of the family of MAPK (ERK, JNK and p38) and inhibition of the phosphatidylinositol-3-kinase/Akt pathway (Xia, Dickens et al. 1995; Verheij, Bose et al. 1996; Blazquez, Galve-Roperh et al. 2000; Salinas, Lopez-Valdaliso et al. 2000).

Various concentrations of Ceramide for 24 hours showed a clear protection in the HT22CR cell line (Figure 4.8). At 5  $\mu\text{M}$  only 27% (SEM 3.455 n=12) of the HT22 cells survived, while at the same concentration 74.2% (SEM 1.870 n=12) viability was observed in HT22CR cells. Moreover, LD<sub>50</sub> increased from 2.375  $\mu\text{M}$  (SEM 5.064 n=12) in HT22, to 10.23  $\mu\text{M}$  (SEM 2.143 n=12) in HT22CR cells.

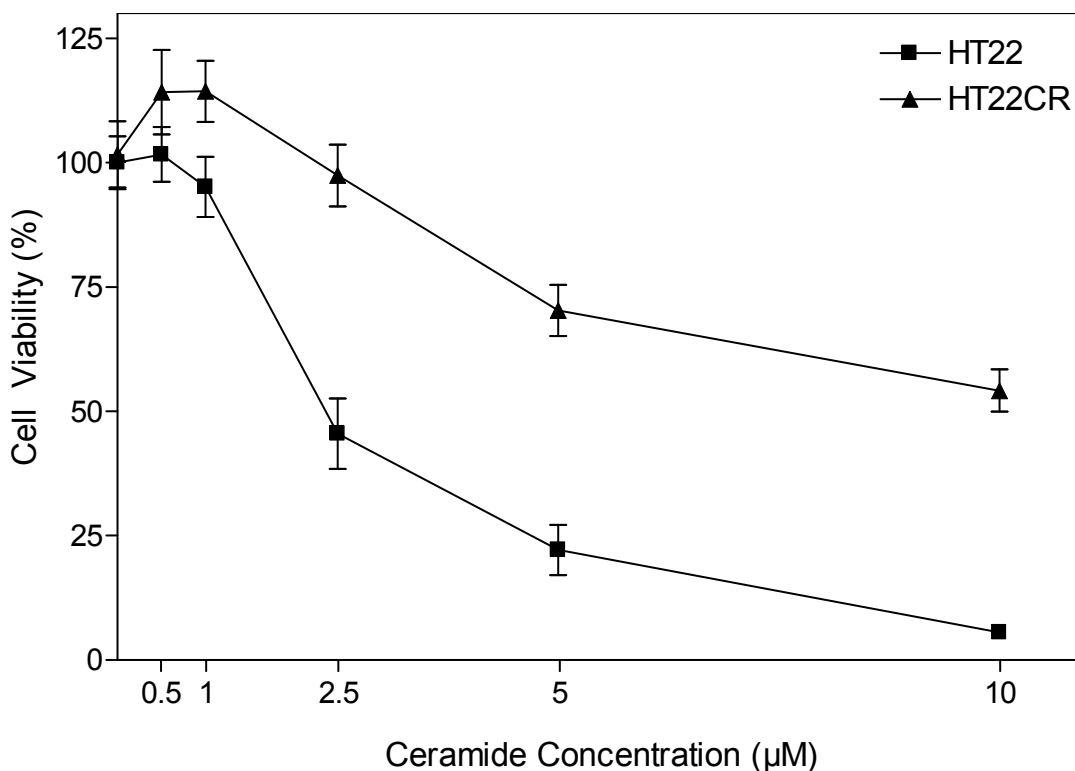


**Figure 4.8: Glutamate-resistant cells are also resistant against ceramide.** HT22 cells were seeded at  $5 \times 10^3$  cells per well with different ceramide concentrations for 24 hours. Cell survival was measured by MTT. Viability of untreated cells was normalized to 100%. The graph represents the data of the relative cell viability obtained from three independent experiments each done in quadruplicates as mean  $\pm$  SEM.

Another stress-inducing agent used in this study was Tunicamycin, an inhibitor of glycosylation of newly synthesized proteins in the ER, which causes the accumulation of unfolded proteins in the ER leading to ER Stress (Tordai, Brass et al. 1995). ER Stress triggers three compensatory responses: the unfolded protein response, which is mediated by increased expression of molecular chaperones, such as GRP94 and GRP78/Bip, promoting the proper folding of proteins (Mori 2000; Urano, Bertolotti et al. 2000); the generalized suppression of translation (Harding, Zhang et al. 1999); and ER-associated degradation (Ng, Spear et al. 2000). These three protective responses act transiently to control the accumulation of misfolded proteins within the ER, but sustained ER stress leads

to apoptosis, which in turn results in cell death (Annis, Zamzami et al. 2001; Wei, Zong et al. 2001).

Application of different concentrations of Tunicamycin for 24 hours was tested. High concentrations of Tunicamycine, like 25  $\mu\text{g}/\text{ml}$ , lead to almost complete cell death in HT22 cells (2.14% (SEM 0.691 n=12)), while reducing the viability of HT22CR cells by only 29% (SEM 3.311 n=12) (Figure 4.9).

Thus, HT22CR cells are not only resistant to oxidative glutamate toxicity, but are also also resistant to other forms of oxidative stress and apoptosis.

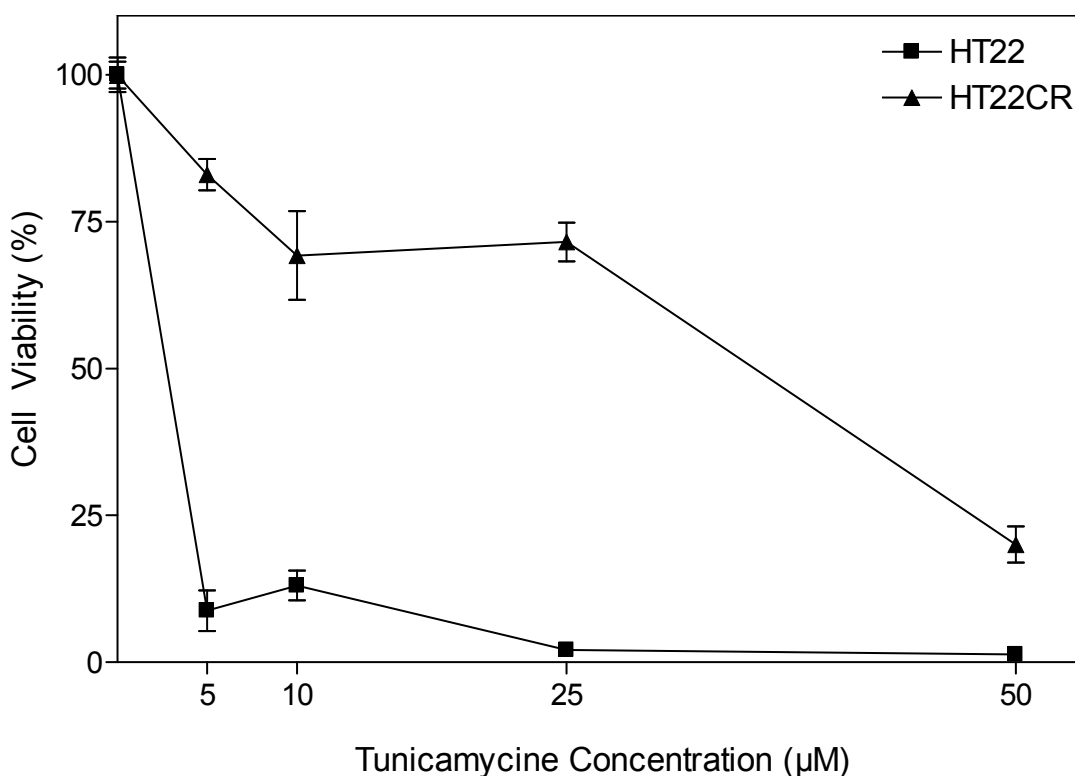


**Figure 4.9: Glutamate resistant cells show also Tunicamycine resistance.** HT22 cells were seeded at  $5 \times 10^3$  cells per well with increasing tunicamycine concentrations for 24 hours. Cell survival was measured by MTT. Viability of untreated cells was normalized to 100%. The graph represents the data of the relative cell viability obtained from three independent experiments each done in quadruplicates as mean  $\pm$  SEM.

#### 4.1.5 Resistance to glutamate can be induced by medium conditioned by HT22CR cells

After testing the capacity of resistance in HT22CR cells, we tested if medium enriched with factors released by these cells had protective properties, as in the case of HT22 cells. To achieve this, normal growth medium was conditioned for 24 hours by confluent HT22

and HT22CR cultures. Twenty-four hours after plating the HT22 cells, conditioned media were used for glutamate treatment and compared to cultures treated with glutamate in fresh medium alone. Interestingly, cells treated with conditioned medium from HT22CR had much higher tolerance against glutamate toxicity when compared to cells treated with conditioned medium from HT22 (Figure 4.10). Cells not only survived 2.5 mM glutamate without any loss in viability (96.08% survival (SEM 6.993 n=12)), but also the amount of glutamate tolerated increased to 40 mM (34.88% survival (SEM 12.165 n=12)). When exposed to 10 mM glutamate, a fatal concentration under normal circumstances, conditioned medium from resistant cells led to 81.95% survival (SEM 7.964 n=12).

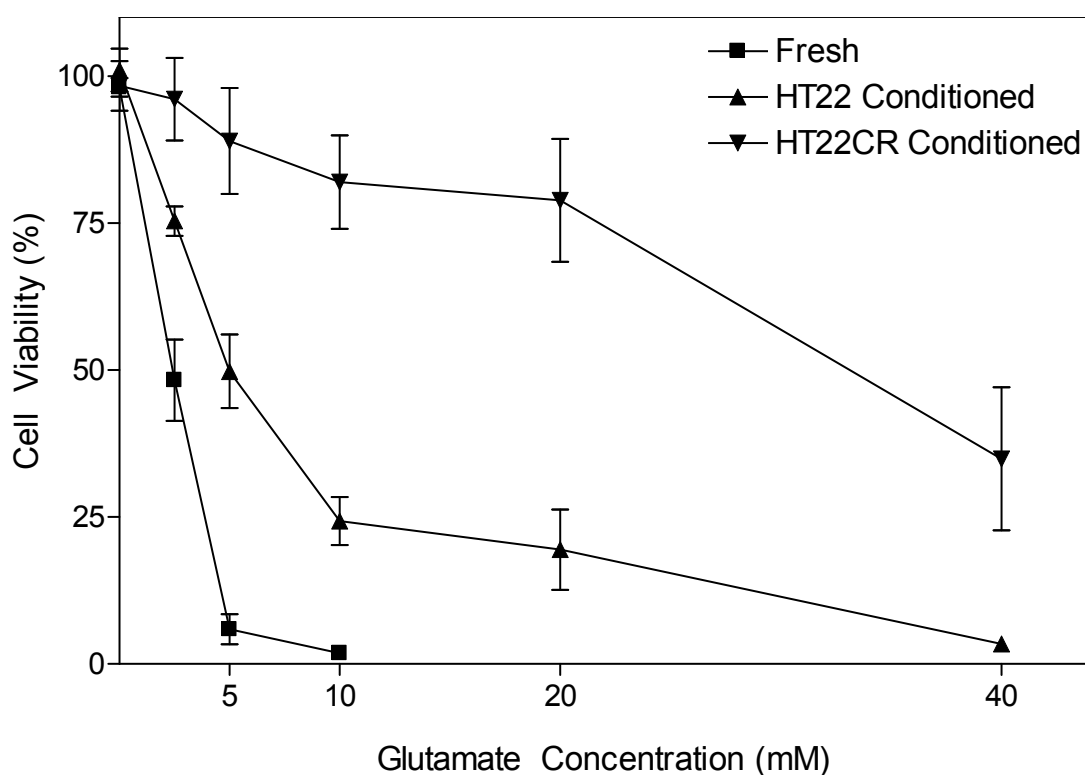


**Figure 4.10: Glutamate resistance can be induced by conditioning the medium.** HT22 cells were seeded at  $5 \times 10^3$  cells per well with increasing glutamate concentrations in either fresh or conditioned medium from sub-confluent HT22 or HT22CR cultures for 8 hours. Glutamate exposure was stopped by changing the medium and cell survival was measured by MTT. Viability of untreated cells was normalized to 100%. The graph represents the data of the relative cell viability obtained from three independent experiments each done in quadruplicates as mean  $\pm$  SEM.

According to these results, we hypothesized that HT22CR cells released protective substances into the medium, which in turn help the cells to survive.

#### 4.1.6 Glutamate-resistant cells show an activation of CRE-dependent pathways

Recent studies done (Davis and Maher 1994; Maher 2001; Lewerenz, Letz et al. 2003) suggested that these substances might protect by activating G-protein coupled membrane receptors. Therefore we compared the activation of signal transduction pathways involved in GPCR signaling in glutamate-sensitive and resistant cells with phosphorylation-specific antibodies and found more phosphorylated cAMP-response element binding protein (CREB) and decreased phosphorylation of extracellular-signal regulated protein kinases 1 and 2 (ERK1/2) in glutamate-resistant cells. The amount of phosphorylated c-Jun N-terminal kinases/stress-activated protein kinases, total protein, and total ERK, in contrast, remained unchanged (Figure 4.11). CREB is mainly phosphorylated in response to the activation of G<sub>s</sub>-coupled receptors; ERK1/2 phosphorylation can occur downstream of receptor tyrosine kinase activation, through G<sub>i</sub>-coupled mechanisms or via activation of protein kinase C (PKC) by G<sub>q</sub> coupled receptors (Gutkind 1998).

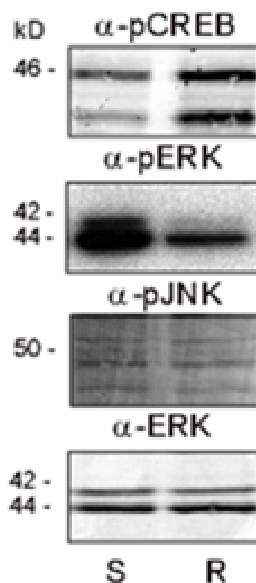


**Figure 4.11: Distinct signaling pathways are activated in resistant cells compared to sensitive cells.** HT22 and HT22CR cells were seeded at a density of  $5 \times 10^5$  cells in 92 mm cell culture dishes and grown for 24 hours. Whole cell extracts were made using boiling lysate buffer and analysed by western blotting. The primary antibodies used were monoclonal phospho-MAPK44/42 (1:2000), a polyclonal total MAPK44/42 (ERK1/2) (1:1000), and a monoclonal phospho-CREB (1:2000). Total ERK is shown as a loading control.

We next quantified the assumed increase in CRE activation in HT22CR cells using an independent method by transfection of a reporter vector containing a CRE element controlled EGFP (Roeder, Gorich et al. 2004) into HT22 and HT22CR cells. HT22CR cells exhibited a 55% increase in CRE activation as judged by mean CRE-EGFP dependent fluorescence (Figure 4.12). CMV-driven EGFP fluorescence was not different in HT22 and HT22CR cells (data not shown). Forskolin treatment served as positive control and induced CRE-EGFP to a similar extent in both cell lines.

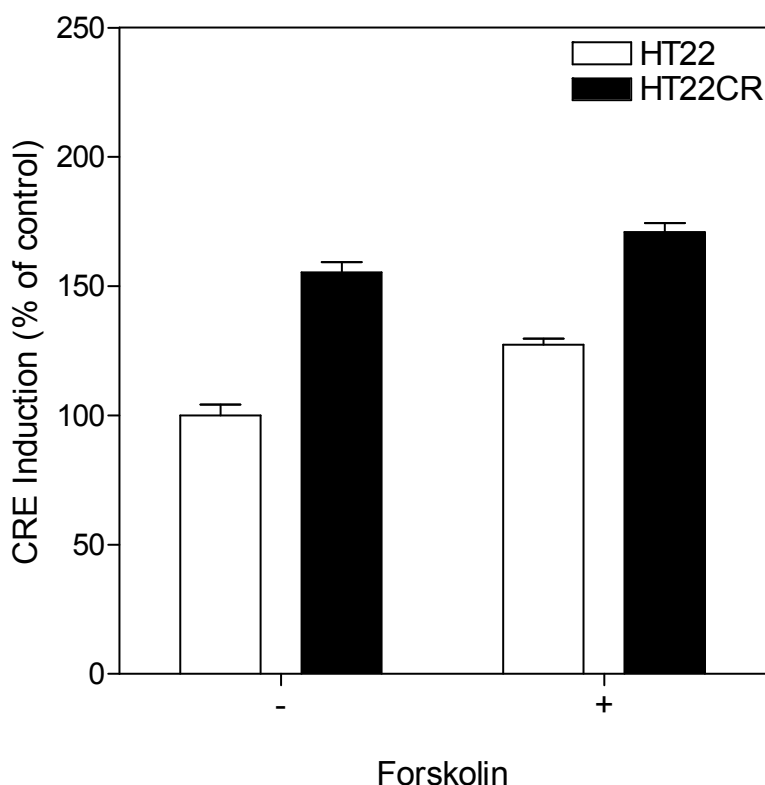


**Figure 4.12: Glutamate resistance functions over the CRE pathway.** HT22 and HT22CR cells were transfected with a CRE-EGFP construct and incubated. The next day they were seeded at a density of  $1 \times 10^4$  cells in 6-well plates and grown for another 24 hours. Cells were collected and incubated with either  $5 \mu\text{M}$  forskolin or PBS, followed by FACS analysis at 488 nm. The graph represents the data of the relative CRE induction obtained from three independent experiments each done in triplets as mean  $\pm$  SEM.

In summary, HT22CR cells demonstrate an activation of  $G_s$ -coupled signal transduction pathways, which could at least in part underlie the resistance to oxidative stress.

#### 4.1.7 Resistant HT22 cells differ from the parental cell line in the expression of GPCRs

The activation of  $G_s$ -coupled signal transduction pathways could theoretically occur via paracrine or autocrine activation of protective GPCRs by their cognate ligands or by an

increase in the amount of protective GPCRs as described for group I metabotropic glutamate receptors (Sagara and Schubert 1998). Therefore we quantified the relative mRNA expression of 24 candidate receptors in wild type and HT22R cells by real-time PCR.

The receptors chosen were previously reported to be involved in cell differentiation, survival, and apoptosis or, like the metabotropic glutamate receptors, because their ligand obviously plays a role in glutamate-mediated cell death. The vasoactive intestinal peptide (VIP) receptors VPAC<sub>1</sub> and VPAC<sub>2</sub> were chosen since the peptide itself was previously reported to be involved in fetal growth (Waschek 1995) and in the suppression of inflammation and immunomodulation (Delgado and Ganea 2001). Angiotensin receptor 2 (AG<sub>22</sub>) was taken, because it was reported to confer neuroprotection against  $\beta$ -Amyloid (1-42) induced stress (Shaw, Bencherif et al. 2002; Shaw, Bencherif et al. 2003), though angiotensin receptors have also been implicated in ROS production (Strawn 2002) and blocking the receptors resulted in cardiovascular protection (Ruilope, Rosei et al. 2005). The nucleotide receptor P2Y<sub>6</sub> was described in neuroprotection against tumor necrosis factor  $\alpha$ -induced apoptosis and shown to activate PKC (Kim, Gao et al. 2003; Kim, Soltysiak et al. 2003). The cannabinoid receptor, CB<sub>1</sub>, was chosen since it was described to decrease glutamatergic and GABAergic synaptic transmissions resulting in protection against excitotoxicity in hippocampal neurons (Marsicano, Moosmann et al. 2002; Azad, Eder et al. 2003; Marsicano, Goodenough et al. 2003).

We observed that three out of the 24 receptors were reproducibly regulated differently in HT22 and HT22CR cells. The receptors for the vasoactive intestinal peptide (VIP), VPAC<sub>2</sub> (12.6-fold, SEM 1.8), and the metabotropic glutamate receptor mGlu<sub>1</sub> (5.3-fold, SEM 0.11) were found more prominently expressed in resistant cells, and the angiotensin receptor AG<sub>22</sub> (6-fold, SEM 1.23) in sensitive cells.

Four receptors were upregulated less than five-, but more than two-fold. Two of these, VPAC<sub>1</sub> (3.6-fold, SEM 0.59) and PAC<sub>1</sub> receptor (2.7-fold, SEM 0.85) are activated by VIP too. The nucleotide receptor P2Y<sub>6</sub> (3.9-fold, SEM 0.86) was also found to be upregulated while the adenosine receptor A<sub>2A</sub> (2.2-fold, SEM 0.66) was downregulated in resistant cells. The nucleotide receptor P2Y<sub>4</sub>, the metabotropic glutamate receptor mGlu<sub>5</sub> and the cannabinoid receptor CB<sub>1</sub> were found to be expressed scarcely in resistant cells. No receptor was found to be expressed only in sensitive or resistant cells (Figure 4.13).

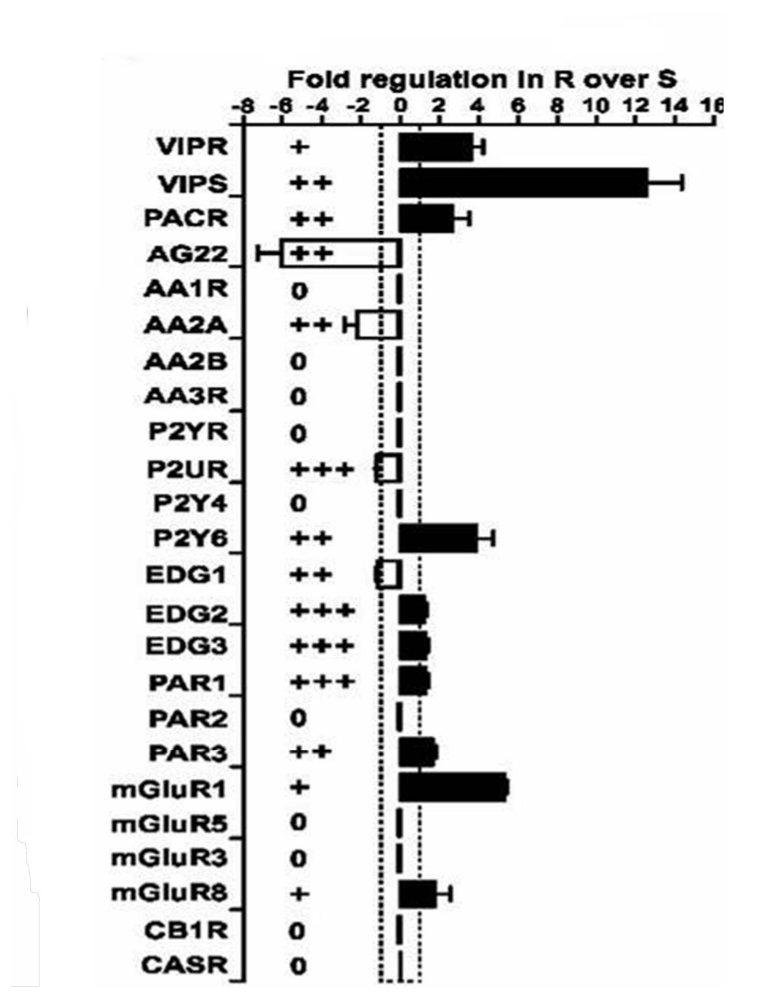


**Figure 4.13: GPCR regulation in resistant cells.** Regulation was calculated by  $\Delta\text{CT}$  R and S normalized to *gapdh* and  $\beta$ -actin expression. The dashed line indicates equal expression in both cell lines. Relative expression level is depicted to the left as: 0 for no expression; + for first detection at 40 cycles PCR; ++ for detection at 35 cycles; +++ for detection at 30 cycles. The graph represents the data of three independent quantitative PCR experiments with two different mRNA preparations as mean  $\pm$  SEM.

In summary, the resistant cells clearly show a changed GPCR expression level.

#### 4.1.8 Activation of VIP receptors leads to a HT22CR like phosphorylation scheme

We next examined the effect of the natural ligands of the most prominently regulated receptors on CREB and ERK phosphorylation to assess their role in the constitutive activation or inhibition observed in glutamate-resistant cells. The effect of VIP on sensitive HT22 cells was studied under serum-free conditions to exclude the influence of VIP contained in the serum. Western blot analyses of HT22 cells treated with VIP showed increased CREB and decreased ERK1/2 phosphorylation (Figure 4.14). Treating the cells

with glutamate for 20 minutes had the same effect, probably mediated by metabotropic glutamate receptors, as these cells do not express ionotropic glutamate receptors.

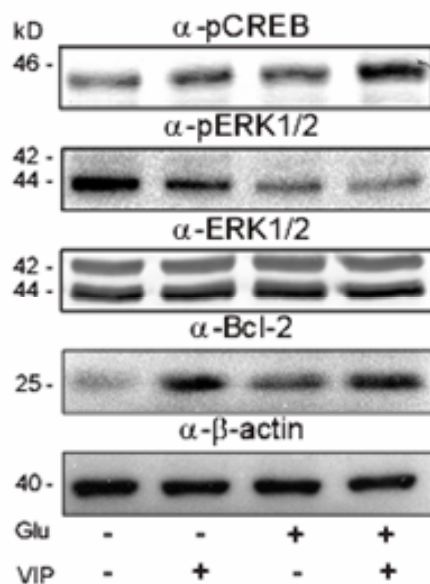


**Figure 4.14: VIP and glutamate act synergistically and induce Bcl-2.** HT22 cells were seeded at a density of  $5 \times 10^5$  cells in 92 mm cell culture dishes and treated with VIP ( $10^{-8}$  M), glutamate (2.5 mM) or both for 20 minutes. Whole cell extracts were made using boiling lysate buffer and analysed by western blotting. The primary antibodies used were monoclonal phospho-MAPK44/42 (1:2000), a polyclonal total MAPK44/42 (ERK1/2) (1:1000), a monoclonal phospho-CREB (1:2000), a monoclonal Bcl-2 clone 100 (1:2000), and a monoclonal  $\beta$ -actin (1:5000). Total ERK and  $\beta$ -actin are shown as loading control.

Taken together, these receptors and their ligands result in the same phosphorylation pattern that is constitutively active in glutamate-resistant HT22 cells.

#### 4.1.9 VIP and glutamate synergistically induce Bcl-2

The antiapoptotic protein Bcl-2 is upregulated in a cAMP-dependent manner (Hui, Nourparvar et al. 2003) and is capable of suppressing the formation of ROS (Kane, Sarafian et al. 1993; Ellerby, Ellerby et al. 1996). It could thus represent a suitable downstream mediator of GPCR signaling. We therefore studied the induction of Bcl-2 by VIP and glutamate (Figure 4.14). VIP increased the amount of Bcl-2 just like glutamate, although to a lesser extent. Again, Bcl-2 was clearly increased in resistant cells, whereas the amount of the housekeeping protein  $\beta$ -actin remained unchanged (Figure 4.14). We hypothesized therefore that VIP and glutamate signaling converge, at least in part, on an

induction of Bcl-2. To test if this induction confers resistance against glutamate, we transiently overexpressed Bcl-2 in glutamate-sensitive HT22 cells (Figure 4.15). We observed an explicit increase in viability up to fivefold in cells treated with 40 mM glutamate (mock 3.79% survival (SEM 0.89, n=12) vs. Bcl-2 19.15% (SEM 1.99, n=12)), which was different from VPAC<sub>2</sub> overexpression (data not shown).

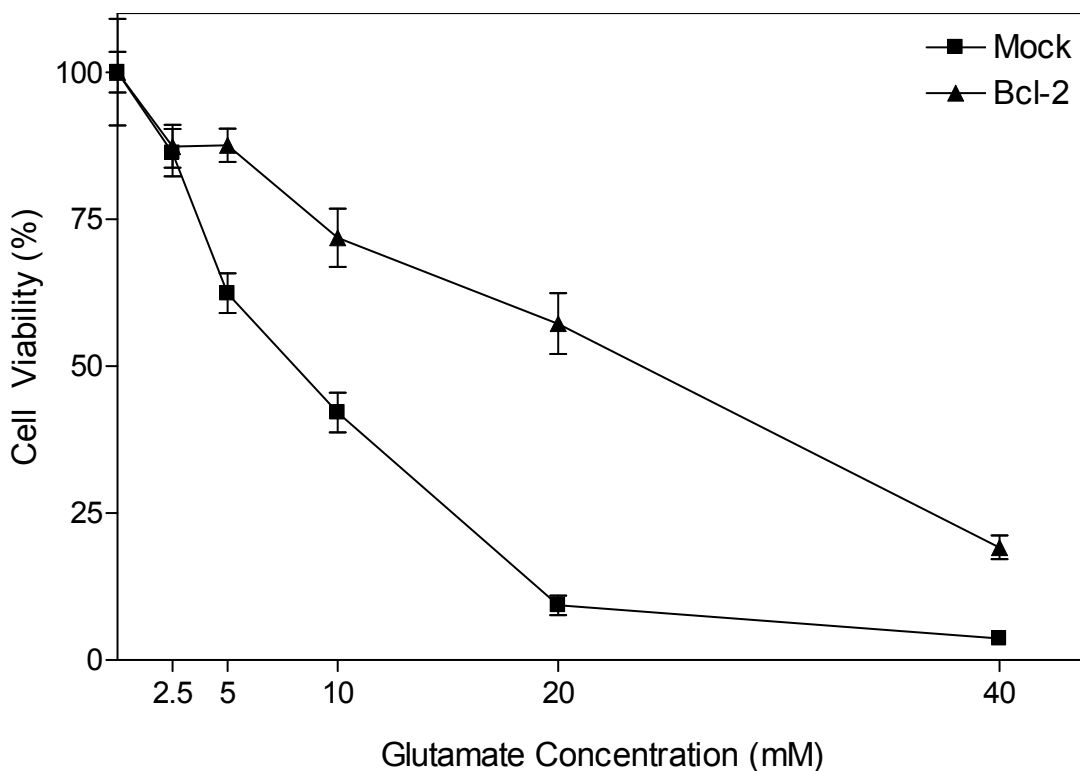


**Figure 4.15: Bcl-2 transfected cells show resistance against glutamate.** HT22 cells were transfected with bcl-2 or empty vector (mock) and seeded at a density of  $5 \times 10^3$  cells. The next day they were exposed to the indicated amounts of glutamate for 8 hours. Glutamate exposure was stopped by changing the medium, and cell survival was measured by MTT. Viability of untreated cells was normalized to 100%. The graph represents the data of the relative cell viability obtained from three independent experiments each done in quadruplicates as mean  $\pm$  SEM.

This protection was accompanied and probably caused by a significant increase in intracellular glutathione content as measured by monochlorobimane fluorescence in increasing amounts of glutamate (Figure 4.16).

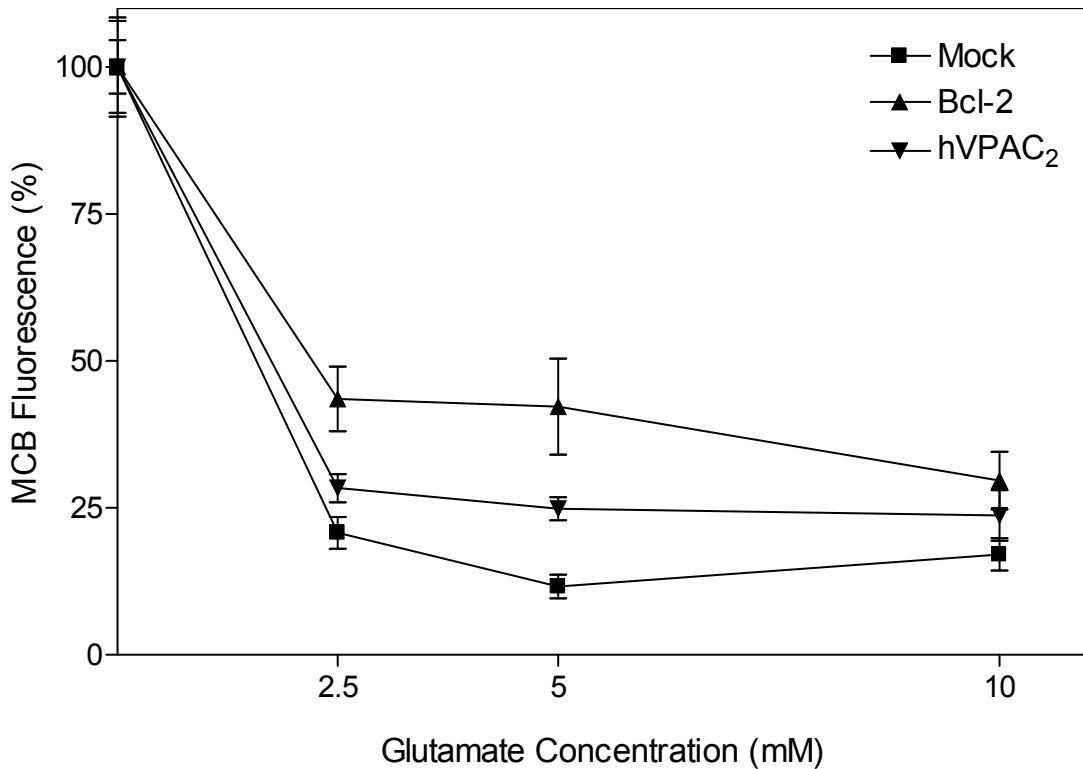


**Figure 4.16: Glutathione levels are higher in Bcl-2 and hVPAC<sub>2</sub> transfected cells.** HT22 cells were transfected with bcl-2, hVPAC<sub>2</sub> or empty vector (mock) and seeded at a density of  $5 \times 10^3$  cells. The next day they were exposed to the indicated amounts of glutamate and incubated with Monochlorobimane (MCB) before analysis using a GEMINI Fluorescence Plate Reader. Cell survival for 96-well plates was measured by MTT directly after the measurements. Starting levels of untreated cells were normalized to 100%. The graph represents the data of MCB Fluorescence obtained from three independent experiments each done in quadruplicates as mean  $\pm$  SEM.

## 4.2 Orphan Receptors

After identifying differing GPCR concentrations in the sensitive and resistant HT22 cell lines, we wanted to quantify the relative mRNA expression of 82 mouse orphan receptors by real-time PCR (Table 4.1). Orphan receptors are proteins that share GPCR structural motifs, but lack a defined ligand and function.

<b>Not Detected</b>	BAI3, Emr1, ETBR-LP, GPR102, GPR17, GPR20, GPR25, GPR26, GPR27, GPR30, GPR40, GPR41, GPR42, GPR43, GPR44, GPR49, GPR50, GPR55, GPR57, GPR58, GPR6, GPR62, GPR7, GPR72, GPR80, GPR81, GPR86, GPR88, GPR90, GPR91, GPR92, GPRC5C, GPRC5D, H963, HM74, LGR7, P2Y10, PNR, PSP24, SALPR, SREB3		
	<b>Detected</b>	<b>Not regulated</b>	A-2, BAI1, BAI2, CML1, EBI2, GPR#, GPR1, GPR103, GPR18, GPR19, GPR21, GPR22, GPR3, GPR34, GPR35, GPR48, GPR52, GPR56, GPR61, GPR63, GPR73, GPR75, GPR82, GPR84, GPR85, GPR87, GPRC5B, LGR6, P2Y5, RAI3, RDC1, RE2, RRH, TM7SF3, TPRA40
<b>Regulated</b>			<b>Not Reproduced</b>
<b>Regulated</b>		<b>Reproduced</b>	P2Y9, GPR15, GPR39

**Table 4.1: Orphan GPCR regulation in resistant cells.** Orphan GPCRs that were not detected were marked as not detected, while receptors that were detected were grouped according to their regulation. Regulation was calculated by the difference in cycle thresholds ( $\Delta CT$ ) of HT22CR and HT22, normalized to gapdh and  $\beta$ -actin expression. The table represents the data of three independent quantitative PCR experiments with two different mRNA preparations.

Most had been identified by methods like degenerate PCR, exploiting conserved amino acid residues (Methner, Hermey et al. 1997; Hermey, Methner et al. 1999). Two receptors, namely GPR39 and GPR15, were found to be upregulated 4-fold, while another receptor, P2Y9, was upregulated 2.5-fold (Figure 4.17).

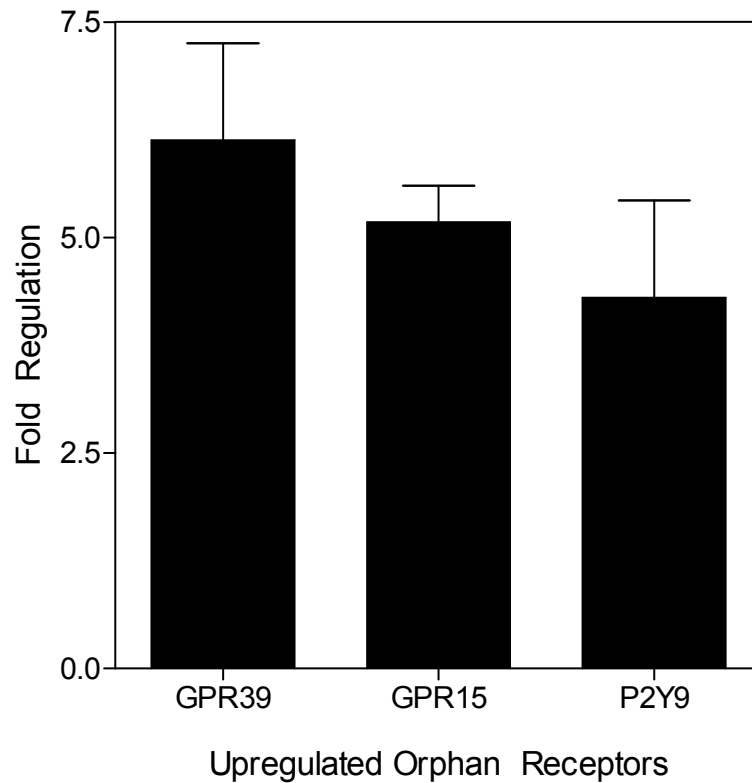


**Figure 4.17: Fold regulation in resistant cells over sensitive cells.** Regulation of orphan receptors was calculated by the difference in cycle thresholds ( $\Delta$ CT) of HT22CR and HT22, normalized to gapdh and  $\beta$ -actin expression. The graph represents the data of three independent quantitative PCR experiments with two different mRNA preparations.

The P2Y9 receptor was recently characterized by another group as the lysophosphatidic acid receptor 4 (LPA4) (Noguchi, Ishii et al. 2003). Therefore, the two-upregulated orphan receptors were used for further studies.

#### 4.2.1 Mouse GPR15

##### 4.2.1.1 Chromosomal Localization and Sequence Analysis

The gene for mouse GPR15 (mGPR15) codes for 1080 basepairs and is localized on Chromosome 16 (ENSMUST00000023425). The deduced protein is 360 amino acids long with a calculated MW of 40541.22 Daltons. GPR15 is an orphan receptor that belongs structurally to the Family 1 GPCRs, i.e. the rhodopsin and angiotensin receptors (Joost and Methner 2002). Following its identification (Heiber, Marchese et al. 1996), it was isolated under the name of BOB (also known as GPRF), a co-receptor for SIV, HIV-1, and HIV-2 (Deng, Unutmaz et al. 1997). Both Human Immunodeficiency Virus (HIV) and Simian Immunodeficiency Virus (SIV) infect the cells through their interaction with the CD4

Receptors and several other co-receptors, mainly chemokine receptors. CCR5 and CXCR4 are the first chemokine receptors identified, with a function as co-receptors for HIV- and SIV-infection (Davis, Dikic et al. 1997).

Although showing structural differences (Farzan, Choe et al. 1997), GPR15 has a similar function to the chemokine receptors as a co-receptor for HIV-infection (Deng, Unutmaz et al. 1997). Recently, it was described to be one of the major co-receptors in HIV-1 and HIV-2, together with CCR5 and CXCR6 (Blaak, Boers et al. 2005). The mouse sequence shows 81% identity to the human sequence (Figure 4.18).

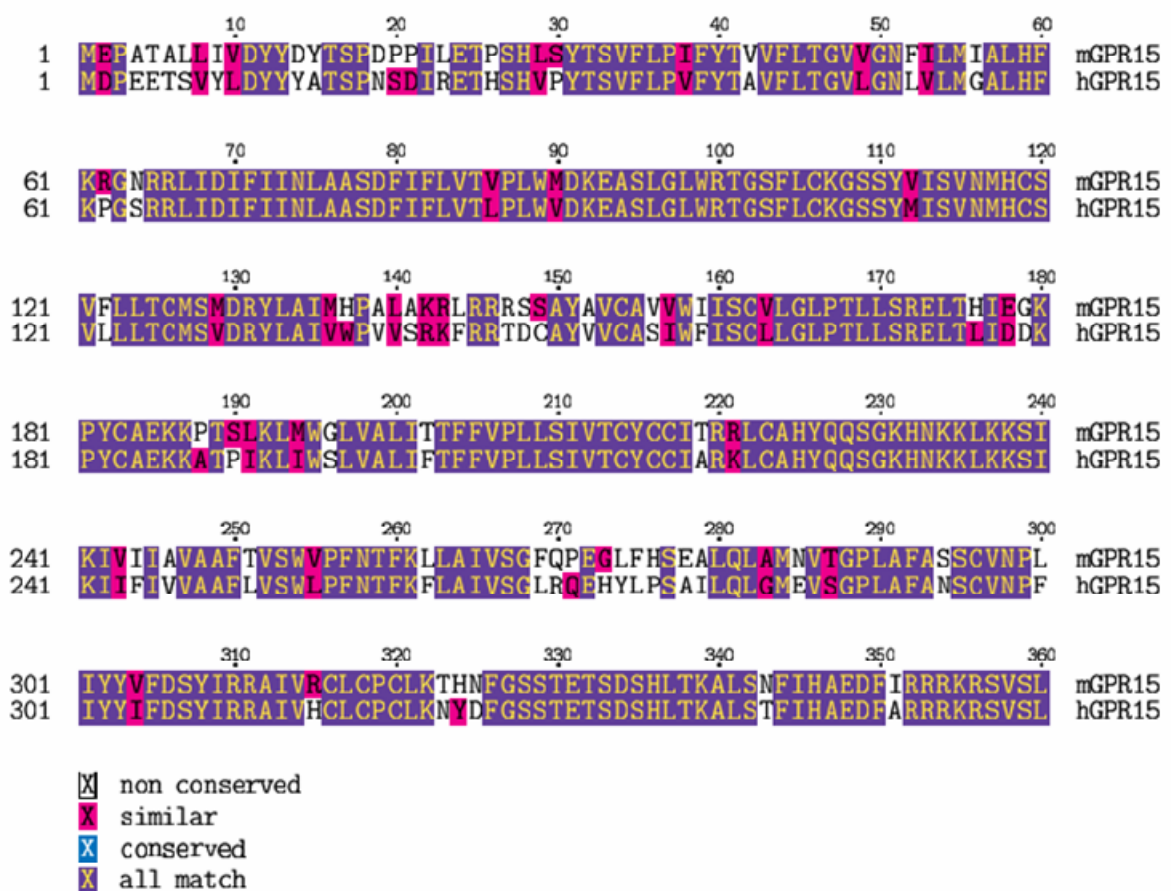


**Figure 4.18: Alignment of mouse and human GPR15 sequences.** Identical residues are presented in purple, similar residues in red, and non-conserved residues are not shaded. Amino acid sequences were aligned with ClustalW within Workbench (<http://wokbench.sdsc.edu>)

The mouse sequence was identified and subcloned in our group by Anna Pantlen.

#### 4.2.1.2 Phylogenetic Analysis

Despite its known function, GPR15 still lacks a ligand. A ligand could possibly be found using the similarities with other receptors within its family, for instance the Apelin, Angiotensin, and Bradykinin Receptors (Figure 4.19). As all the receptors within the family are peptide receptors, one can deduce from this that mGPR15 might bind a peptide ligand (Joost and Methner 2002).

The expression of human GPR15 has only been described in the immune system, like the CD4-T-Lymphocytes, macrophages, leukocytes, as well as liver, prostate and the intestine (Deng, Unutmaz et al. 1997; Farzan, Choe et al. 1997). Anna Pantlen, in our group, found in qPCR analysis that in contrast with its human homologue, mouse GPR15 was predominantly expressed in the brain.

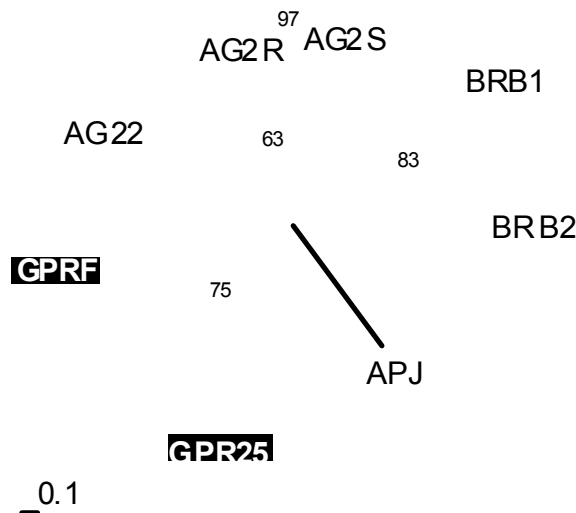


**Figure 4.19: Phylogenetic tree of GPR15 (GPRF).** AG2R: Type-1A Angiotensin II Receptor, AG2S: Type-1B Angiotensin II Receptor, BRB1: B1 Bradykinin Receptor, BRB2: B2 Bradykinin Receptor, APJ: Apelin Receptor, AG22: Type-2 Angiotensin II Receptor, GPR25: G Protein-Coupled Receptor 25, GPRF: G Protein-Coupled Receptor 15. Adapted from (Joost and Methner 2002).

#### 4.2.2 Mouse GPR39

##### 4.2.2.1 Chromosomal Localization and Sequence Analysis

The gene for mGPR39 (ENSMUSG00000026343) codes for 1660 basepairs and is localized in Chromosome 1. The resulting protein is 456 amino acids long with a calculated MW of 51584.32 Daltons. GPR39 is an orphan receptor that belongs to the

Family 1 GPCRs, a family consisting of rhodopsin and angiotensin receptors (Joost and Methner 2002).

Analysis of the gene shows several sites for N-myristoylation, N-glycosylation, and phosphorylation sites for Protein kinase C (PKC), Casein kinase II (CK2), and cAMP- and cGMP-dependent protein kinase (CAMP).

Phosphorylation occurs through the serine-, threonine- or tyrosine-residues, and is mainly responsible for the internalization of GPCRs (Hanyaloglu, Vrecl et al. 2001; Dale, Babwah et al. 2002). Arrestin binds to the phosphorylated receptors (Krupnick and Benovic 1998) and prevents them from binding to G-proteins and other effectors, attenuating signaling (Pippig, Andexinger et al. 1993; Metaye, Gibelin et al. 2005). Through this binding GPCRs are targeted into clathrin-coated vesicles for their internalization into endosomes (Goodman, Krupnick et al. 1996).

Myristoylation is the covalent addition of myristate (a C14-saturated fatty acid) to an N-terminal Glycine *via* an amide linkage (Towler, Gordon et al. 1988) that alters the interaction between a protein and the cell membrane (Resh 2004). N-glycosylation is one of the major post-translational modifications that occur in GPCRs and is carried out by the glycosylation of Asparagine residues in the consensus sequence Asn-X-Ser/Thr, where X is any amino acid other than Proline (Gavel and von Heijne 1990). Glycosylation plays not only an important role in the cell surface expression of the receptors (Duvernay, Filipeanu et al. 2005), but might also be crucial as in the case of AT1 receptors (Deslauriers, Ponce et al. 1999). Moreover, glycosylation at the second extracellular loop seems to be required for the proper folding of all GPCRs, including the AT1 receptors (Lanctot, Leclerc et al. 2005). mGPR39 has three of its five glycosylation sites at its second extracellular loop.

Thus, it can be concluded that mGPR39 has all the characteristic modification sites that are present in GPCRs.

The mouse sequence shows 83% identity to the human sequence (Figure 4.20). The mouse sequence was identified and subcloned in our group by Anna Pantlen.

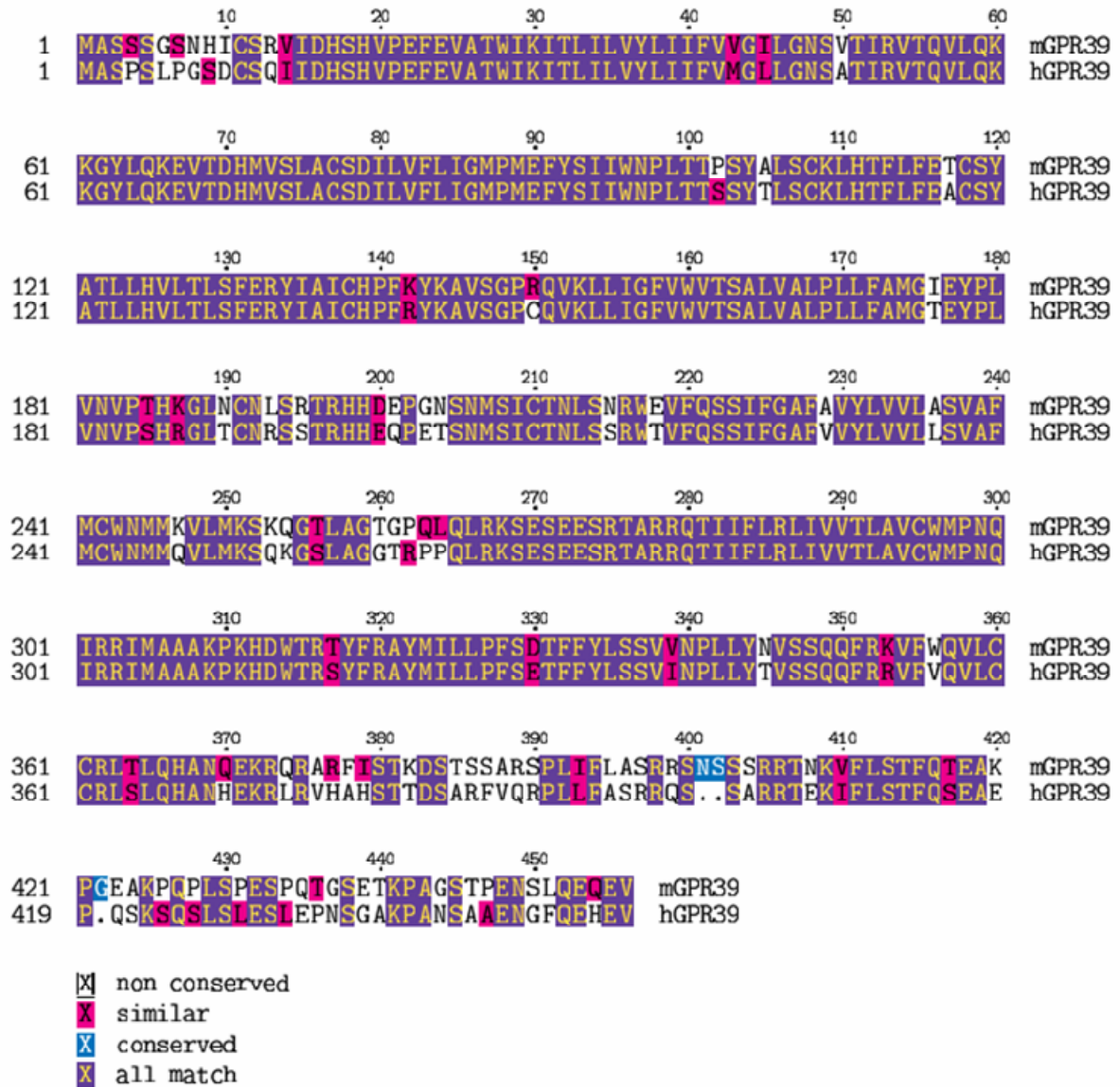


**Figure 4.20: Alignment of mouse and human GPR39 sequences.** Identical residues are presented in purple, similar residues in red, and non-conserved residues are not shaded. Amino acid sequences were aligned with ClustalW within Workbench (<http://wokbench.sdsc.edu>)

#### 4.2.2.2 Phylogenetic Analysis

GPR39 was first identified through the growth hormone secretagogue receptor (GHSR), and placed in the group of peptide receptors using nucleotide sequence comparisons (McKee, Tan et al. 1997). After the identification of Ghrelin, a GHSR-binding peptide (Kojima, Hosoda et al. 1999), a phylogenetic analysis characterized the Ghrelin Receptor, Neurotensin Receptors 1 and 2, as well as Neuromedin U Receptors 1 and 2 to be further group members of the human GPR39 receptor (Holst, Holliday et al. 2004). The same

results had already been obtained in a phylogenetic analysis carried out in our group (Joost and Methner 2002) (Figure 4.21).

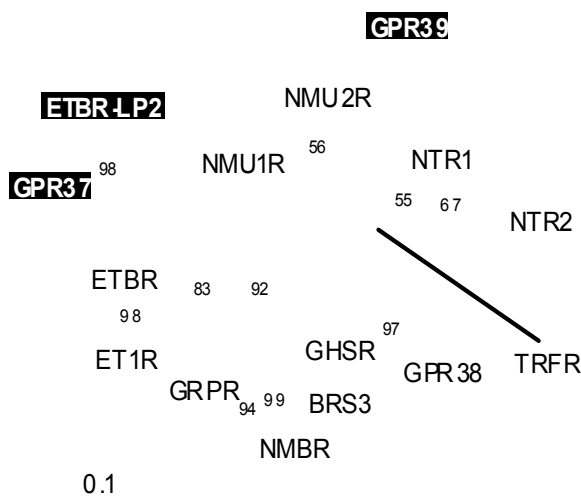


**Figure 4.21: Phylogenetic Analysis of GPR39.** NMU2R: Neuromedin U Receptor 2, NMU1R: Neuromedin U Receptor 1, NTR1: Neurotensin Receptor Type 1, NTR2: Neurotensin Receptor Type 2, TRFR: Thyrotropin-Releasing Hormone Receptor, GHSR: Growth Hormone Secretagogue Receptor Type 1, BRS: Bombesin Receptor Subtype-3, NMBR: Neuromedin-B Receptor, GRPR: Gastrin-Releasing Peptide Receptor, ETBR: Endothelin B Receptor, ET1R: Endothelin-1 Receptor, ETBR-LT2: Endothelin B Receptor-Like Protein-2, GPR37: G Protein-Coupled Receptor 37, GPR39: G Protein-Coupled Receptor Gpr39. Adapted from (Joost and Methner 2002)

### 4.2.3 Resistance to glutamate and hydrogen peroxide can be induced by orphan GPCRs

In order to test whether the cloned GPCRs had an effect on cell survival under oxidative stress, HT22 cells were transiently transfected by electroporation. For transfection, pcDNA5 FRT/TO loxP SPHA mGPR15, pcDNA5 FRT/TO loxP SPHA mGPR39, pcDNA5 FRT/TO loxP SPHA hVPAC<sub>2</sub> and pcDNA5 FRT/TO loxP SPHA (mock) were used.

Cells transfected with mGPR39 had the highest amount of cell survival, similar to resistant HT22 cells, while mGPR15 had almost no effect at all (Figure 4.22). At 20 mM glutamate, 40% survival (SEM 2.264 n=12) was observed in mGPR39 transfected cells, where only 2% (SEM 0.683 n=12) of mGPR15 transfected cells could survive. The human vasointestinal peptide receptor, hVPAC<sub>2</sub>, was used as a control and showed similar protection (27% survival at 20 mM (SEM 3.190 n=12)) against glutamate-induced oxidative toxicity as mGPR39.

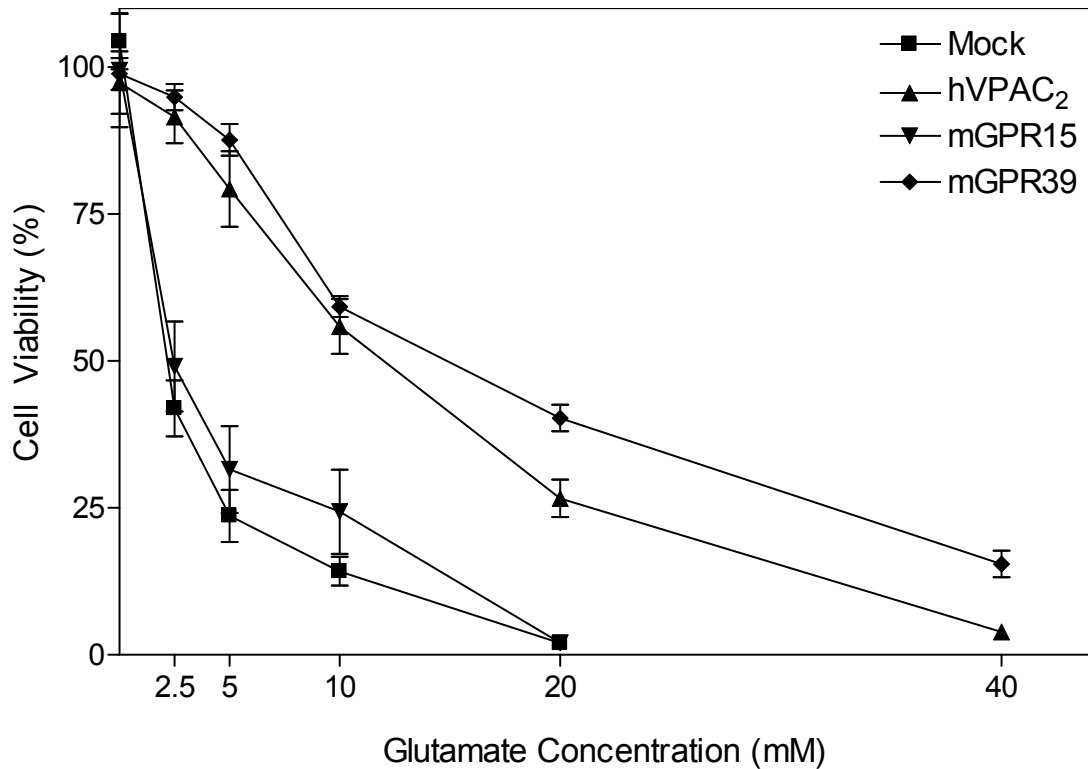


**Figure 4.22: Transient GPCR transfection confers resistance against glutamate.** HT22 cells were transfected with hVPAC<sub>2</sub>, mGPR15, mGPR39, or empty vector (mock) and seeded at a density of  $5 \times 10^3$  cells. The next day they were exposed to the indicated amounts of glutamate for 8 hours. Glutamate exposure was stopped by changing the medium, and cell survival was measured by MTT. Viability of untreated cells was normalized to 100%. The graph represents the data of the relative cell viability obtained from three independent experiments each done in quadruplicates as mean  $\pm$  SEM.

Moreover, mGPR39 and hVPAC<sub>2</sub> protected the cells against hydrogen peroxide (H<sub>2</sub>O<sub>2</sub>), even at higher concentrations (Figure 4.23). At 934  $\mu$ M, mGPR39 conferred a 2-fold protection compared to mock transfected cells (mGPR39 66.6% survival (SEM 5.445 n=12) vs. mock 34.8% survival (SEM 3.288 n=12)). As mGPR15 did not confer any resistance in our hands, we focused on mGPR39.

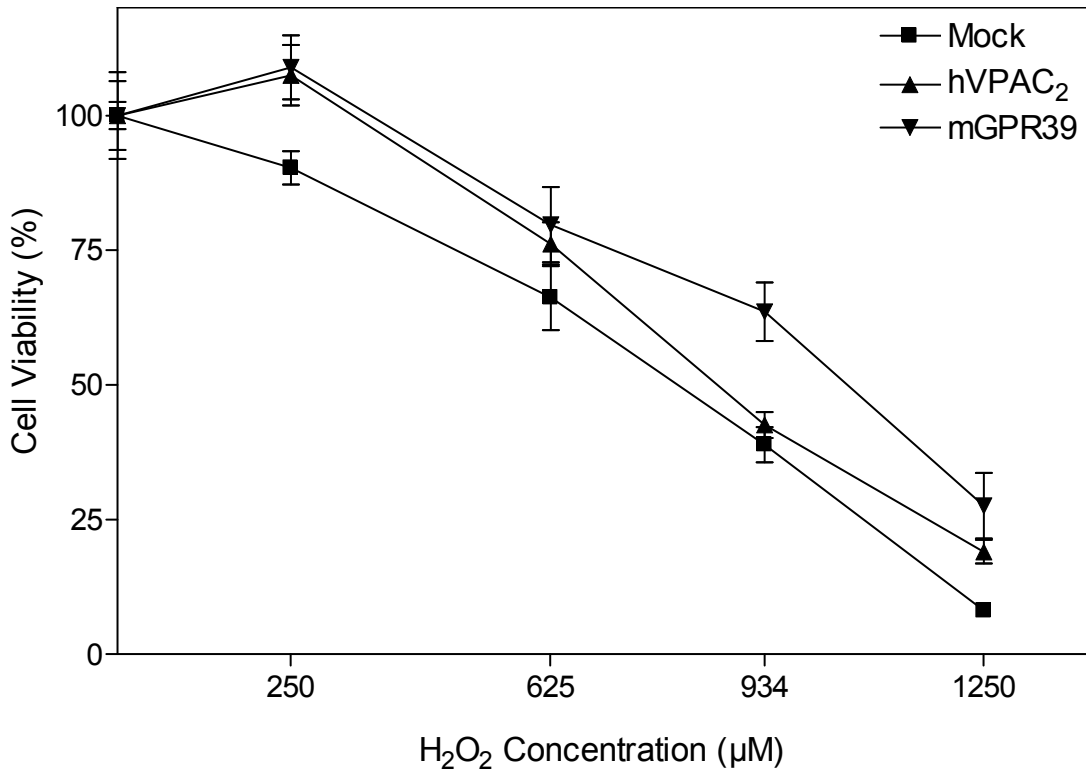


**Figure 4.23: Resistance against hydrogen peroxide induced by transient transfections.** HT22 cells were transfected with mGPR39, hVPAC<sub>2</sub>, or empty vector (mock) and seeded at a density of  $5 \times 10^3$  cells in 96-well plates. The next day they were exposed to the indicated amounts of hydrogen peroxide for 24 hours. Cell survival was measured by MTT. Viability of untreated cells was normalized to 100%. The graph represents the data of the relative cell viability obtained from three independent experiments each done in quadruplicates as mean  $\pm$  SEM.

In conclusion, we hypothesized that the resistance against oxidative glutamate toxicity, and hydrogen peroxide to some extent, could be induced by activating or overexpressing GPCRs.

#### 4.2.4 Mechanism of protection in HT22 cells

To elucidate the mechanisms involved at the cellular level for the protection observed by mGPR39, we transiently transfected HT22 cells with hVPAC<sub>2</sub>, Bcl-2, mGPR39, and empty vector. The cells were transfected and 24 hours later seeded into 96-well plates and incubated for another 24 hours. Two days after electroporation, the cells were incubated with fluorescent dyes and increasing amounts of glutamate. The dyes used were monochlorobimane (MCB) for determining the intracellular glutathione levels or DCFDA for determining intracellular ROS levels. At the end of incubation, the signals were measured using a Gemini Plate Reader. Glutathione levels in mGPR39 and hVPAC<sub>2</sub> were

higher than in mock transfected HT22 cells as expected, and Bcl-2 transfected cells had higher glutathione levels than the rest (Figure 4.24). At 2.5 mM glutamate, Bcl-2 transfected cells had 40% more glutathione than mGPR39 or hVPAC<sub>2</sub> transfected cells (Bcl-2 71.70% (SEM 8.909 n=24) vs. mGPR39 49.56% (SEM 4.720 n=24) and hVPAC<sub>2</sub> 33.67% (SEM 2.767 n=24)).

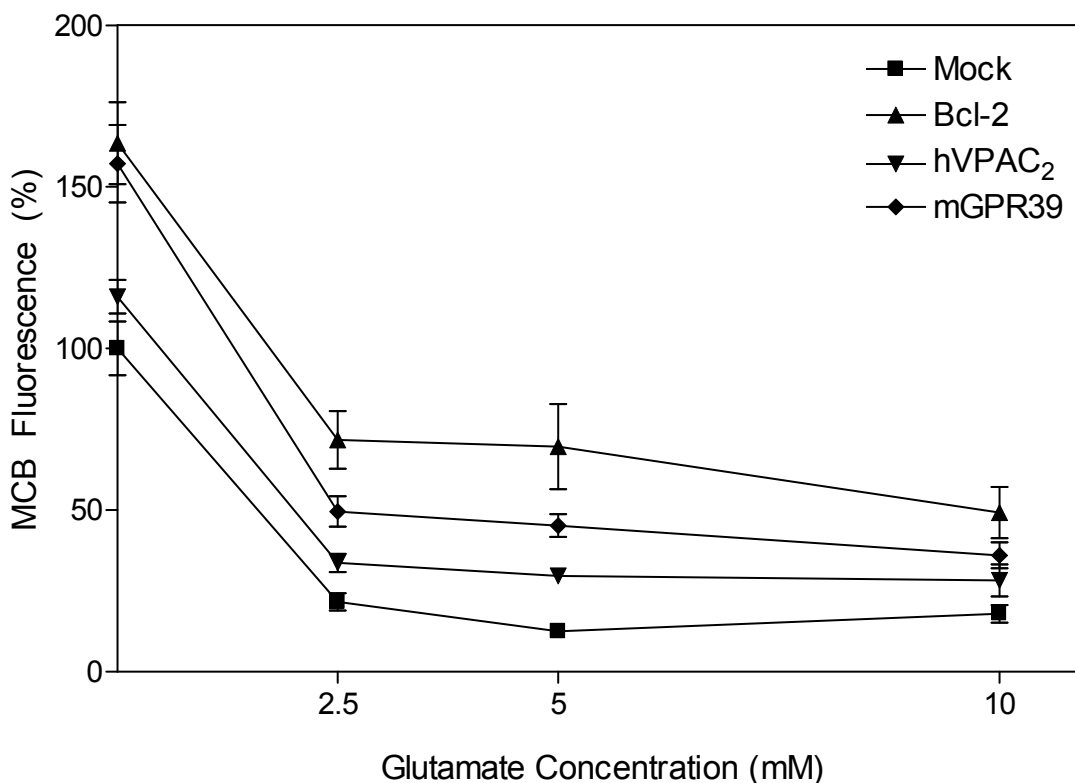


**Figure 4.24: Glutathione levels are higher in mGPR39 transfected cells.** HT22 cells were transfected with bcl-2, mGPR39, hVPAC<sub>2</sub> or empty vector (mock) and seeded at a density of  $5 \times 10^3$  cells. The next day they were exposed to the indicated amounts of glutamate and incubated with Monochlorobimane before analysis using a GEMINI Fluorescence Plate Reader. Cell survival was determined by MTT directly after the measurements. The graph represents the data of the relative MCB fluorescence obtained from six independent experiments each done in quadruplicates as mean  $\pm$  SEM.

Moreover, mGPR39 transfected cells had less intracellular ROS than mock-transfected cells (mock 242.7% (SEM 13,332 n=12) vs. mGPR39 183.8% (SEM 8.319 n=12)), and the rest of the transfected cells (Bcl-2 213.6% (SEM 22.916 n=10) and hVPAC<sub>2</sub> 225% (SEM 9.703 n=10)) (Figure 4.25).

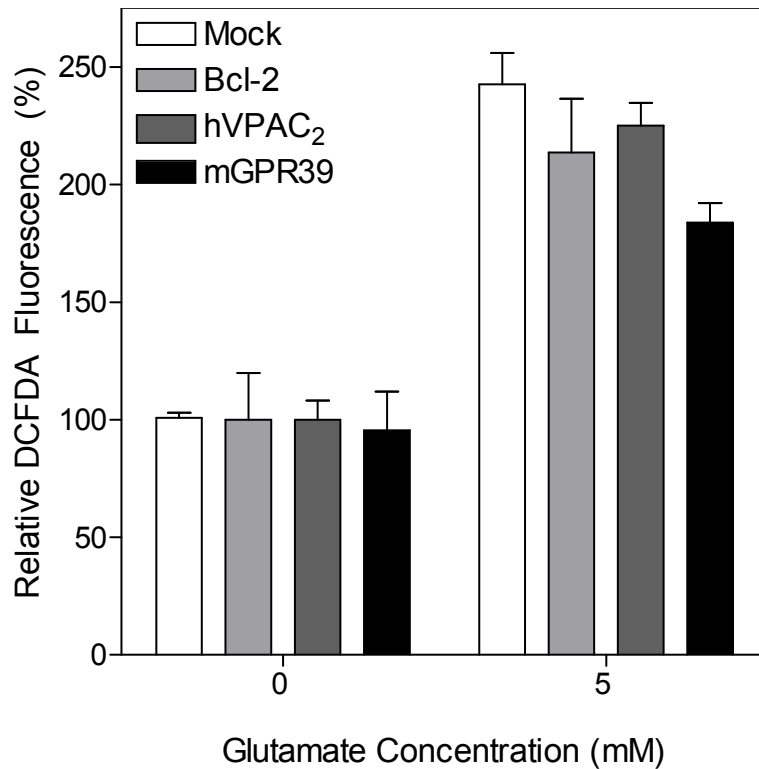


**Figure 4.25: mGPR39 protects cells against glutamate by increasing the glutathione content.** HT22 cells were seeded in 6-well plates with indicated glutamate concentrations, collected, and incubated with DCFDA and 7-AAD, followed by FACS analysis at 488 nm. Starting levels of untreated cells were normalized to 100%. The graph represents the data of the relative DCFDA fluorescence obtained from three independent experiments each done in quadruplicates as mean  $\pm$  SEM.

As a result, mGPR39 protected the cells as well as Bcl-2 by increasing the glutathione content and reducing ROS levels within the cells.

#### 4.2.5 Expression of mGPR39 throughout the development

mGPR39 was detected in the mouse hippocampal cell line HT22 and HT22CR, and cloned by Anna Pantlen. To get insight into a possible role in development, *in situ* hybridizations on sections of mouse embryos were performed. Starting from E12.5, mGPR39 mRNA was detected in both central and peripheral nervous systems, and epithelial tissues (Figure 4.26).

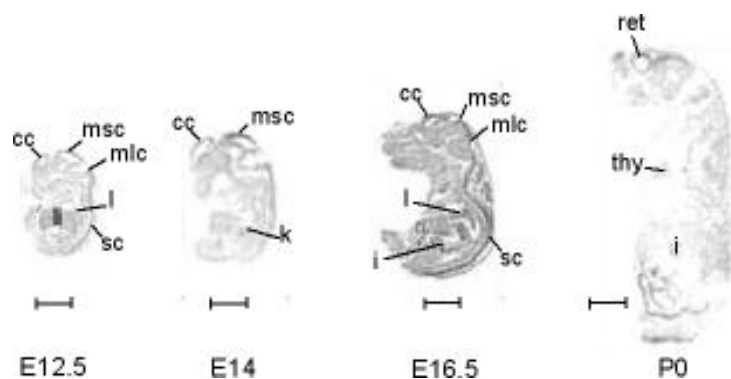


**Figure 4.26: Expression of mGPR39 during mouse embryogenesis.** Autoradiograms of parasagittal sections through mouse embryos are shown at the stages indicated (E12.5, E14, E16.5, P0). Abbreviations: *cc*, cerebral cortex; *i*, intestine; *k*, kidney; *l*, lung; *li*, liver; *mlc*, metencephalon; *msc*, mesencephalon; *ret*, retina; *sc*, spinal cord; *thy*, thymus. Scale bar is 2 mm.

The cerebral cortex and midbrain showed more intense labeling than other brain areas. Starting at E12.5 the hybridization intensity of mGPR39 in the cerebral cortex and midbrain regions increased at each stage. The most intense labeling was observed in epithelial tissues (liver, kidney, stomach, intestine) and declined at further stages. Further signals were detected in trigeminal ganglion, spinal cord, olfactory bulb, tongue epithel.

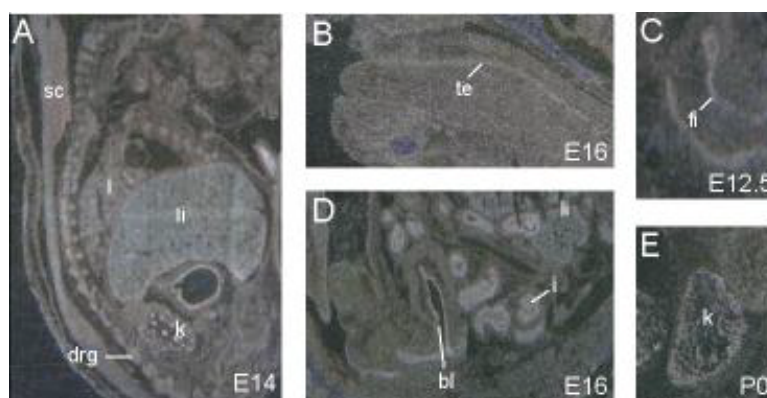


**Figure 4.27: Photoemulsion-dipped sagittal sections of mouse embryos.** Expression of mGPR39 in distinct epithelial tissues throughout the development is shown in sagittal sections. Abbreviations: *bl*, bladder; *drg*, dorsal root ganglion; *fi*, future intestine; *i*, intestine; *k*, kidney; *l*, lung; *li*, liver; *sc*, spinal cord; *te*, tongue epithelial cell layer.

Analysis of emulsion-dipped sections revealed strong signals in dorsal root ganglia, spinal cord, kidneys, lung, liver, intestine, and bladder (Figure 4.27A-E). Analysis of the brain and central nervous system revealed signals in the retina and retinal pigment epithelium (RPE)

(Figure 4.28D), and cerebral cortex, hippocampus, amygdala, piriform cortex, Purkinje and Granular cell layers, as well as dentate gyrus (Figure 4.28A-C).

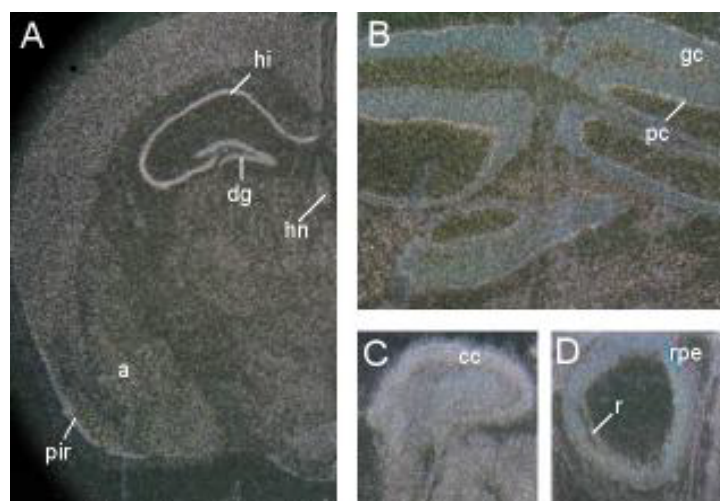


**Figure 4.28: Photoemulsion-dipped sections through mouse brain.** Dark-field photomicrographs of photoemulsion-dipped sections through adult and developing (C) mouse brains are shown. Abbreviations: *a*, amygdala; *cc*, cerebral cortex; *dg*, dentate gyrus; *gc*, Granular cell layer; *hi*, hippocampus; *hn*, medial habenular thalamic nuclei; *pc*, Purkinje cell layer; *pir*, piriform cortex; *r*, retina; *rpe*, retinal pigment epithelium.

#### 4.2.6 Stable HT22 cell lines

After observing the induced protection and the expression pattern through different developmental stages, we decided to create an HT22 cell line overexpressing mGPR39. For this purpose, we used the Retroviral Gene Transfer and Expression System (BD Biosciences) vector pQCXIP and the Phoenix Retroviral Expression System (Orbigen Inc). Both systems consist of a HEK-293-based packaging cell line that stably expresses the viral *gag*, *pol*, and envelope genes. To produce infectious virus, a retroviral expression vector has to be transfected into this cell line, using the viral envelopes' ability to infect other cells. The retroviral expression vector, pQCXIP, contains the extended retroviral packaging signal, which promotes high-titer virus production. The vector itself is a self-inactivating bicistronic expression vector that is driven by a CMV promoter and has an internal ribosome entry site (IRES) followed by the Puromycin gene for conferring antibiotic resistance. The viruses produced possess an ecotropic envelope (*gap70*), and thus can infect only mouse and rat cells.

In our case, the packaging cell line Phoenix-Eco (Orbigen Inc) was transfected with pQCXIP SP HA mGPR39, using the Calcium Phosphate Method. An EGFP vector was used to test the transfection efficiency and to assure the expression of mGPR39. Phoenix-Eco cells stably overexpressing EGFP, as a control, were also created. Following transfection, the cells were incubated in puromycin containing medium, until all the cells in culture were expressing EGFP stably and had Puromycin resistance. These cells were then used for the transfection of HT22 cell line. In order to achieve viral transfection, the resulting medium was put onto sub-confluent HT22 cells in culture followed by puromycin selection. In total, 55 colonies were removed from the transfected HT22 cells that survived puromycin stress. These colonies were further propagated until they reached confluency and then transferred into 24-well plates and from there to 6-well plates. In the end, there were 37 surviving colonies, and these were propagated until they could be tested for mGPR39 expression.

#### **4.2.6.1 Verification of the Stable Cell Lines**

To verify the stable integration of SP HA mGPR39 into the HT22 cells, FACS analysis was performed. HT22 clones that were kept constantly under Puromycin stress were analysed by FACS for surface expression, using a monoclonal mouse antibody against the haemagglutinin (HA) tag (Covance) and Alexa Fluor anti-mouse secondary antibody (data not shown).

Among the 37 clones, HA surface expression differed drastically from 5-62%. Out of these clones, six clones were picked for glutamate toxicity experiments: Clones 1 and 34 for low-level expression, clones 7 and 26 for mid-level expression, and clones 17 and 18 for high-level expression. Of the six clones, the least and most HA expressing clones turned out to confer the lowest and highest level of protection against glutamate toxicity, respectively (Figure 4.29). Clone 1 had a viability of 52.62% (SEM 4.061 n=16) under 40 mM glutamate, while clone 17 had a viability of 72.46% (SEM 3.940 n=16). Clones 26 and 34 had almost the same viabilities (clone 26 60.65% (SEM 5.088 n=16) and clone 34 58.87% (SEM 3.065 n=16)).

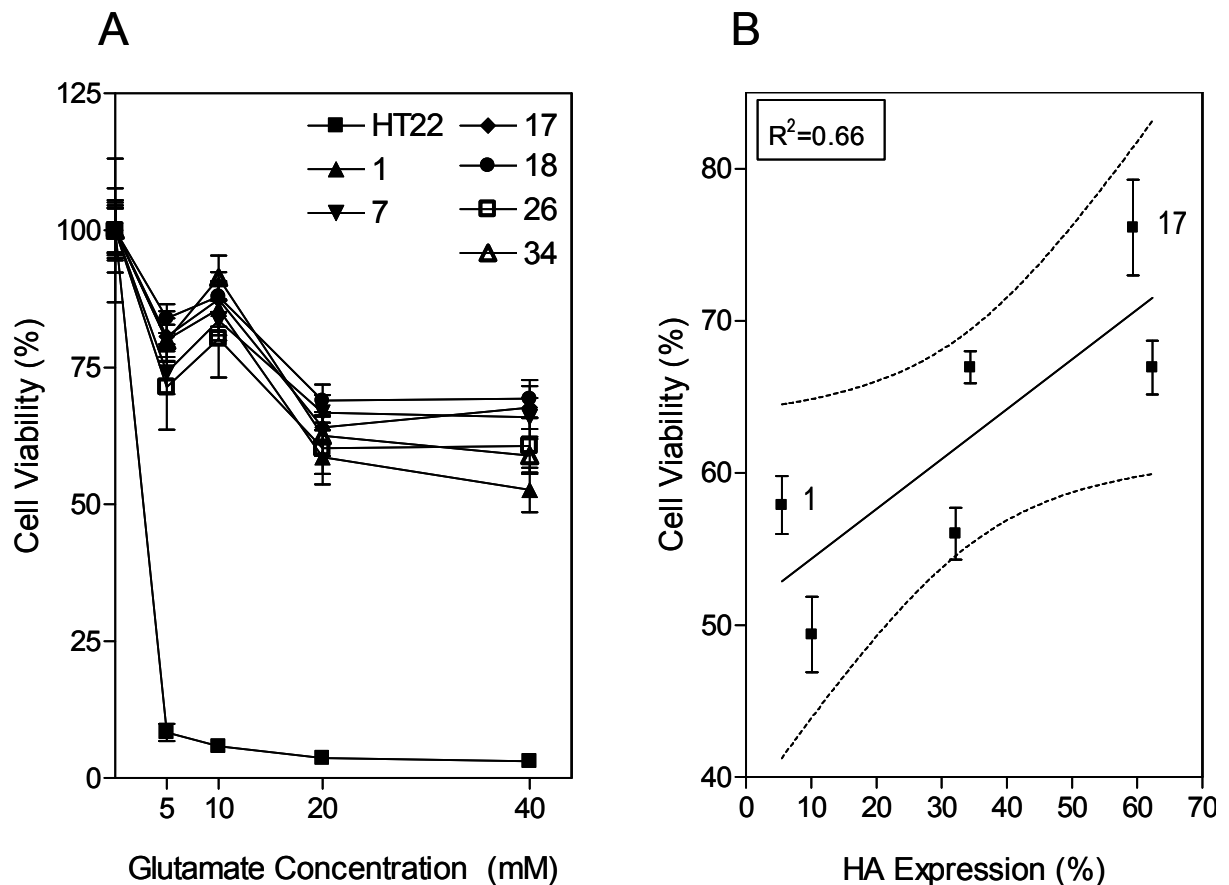


**Figure 4.29: Glutamate resistance in HT22 cells stably overexpressing mGPR39.** (A) Six of the clones (1, 7, 17, 18, 26, 34) selected by their HA surface expression were seeded at a density of  $5 \times 10^3$  cells. The next day they were exposed to the indicated amounts of glutamate for 8 hours. Glutamate exposure was stopped by changing the medium, and cell survival was measured by MTT. Viability of untreated cells was normalized to 100%. (B) According to the viability results, a correlation graph was generated. The graphs represent the data of the relative cell viabilities obtained from four independent experiments each done in quadruplicates as mean  $\pm$  SEM.

The two clones that conferred the most and least protection were then analysed by FACS, using a polyclonal rabbit anti-GPR39 antibody (Acris Antibodies). Clone 1 showed an upregulation of 243-fold, while clone 17 showed an upregulation of 345-fold (Figure 4.30). In contrast, HT22CR cells had a 1.8-fold upregulation in mGPR39 expression over HT22 cells.

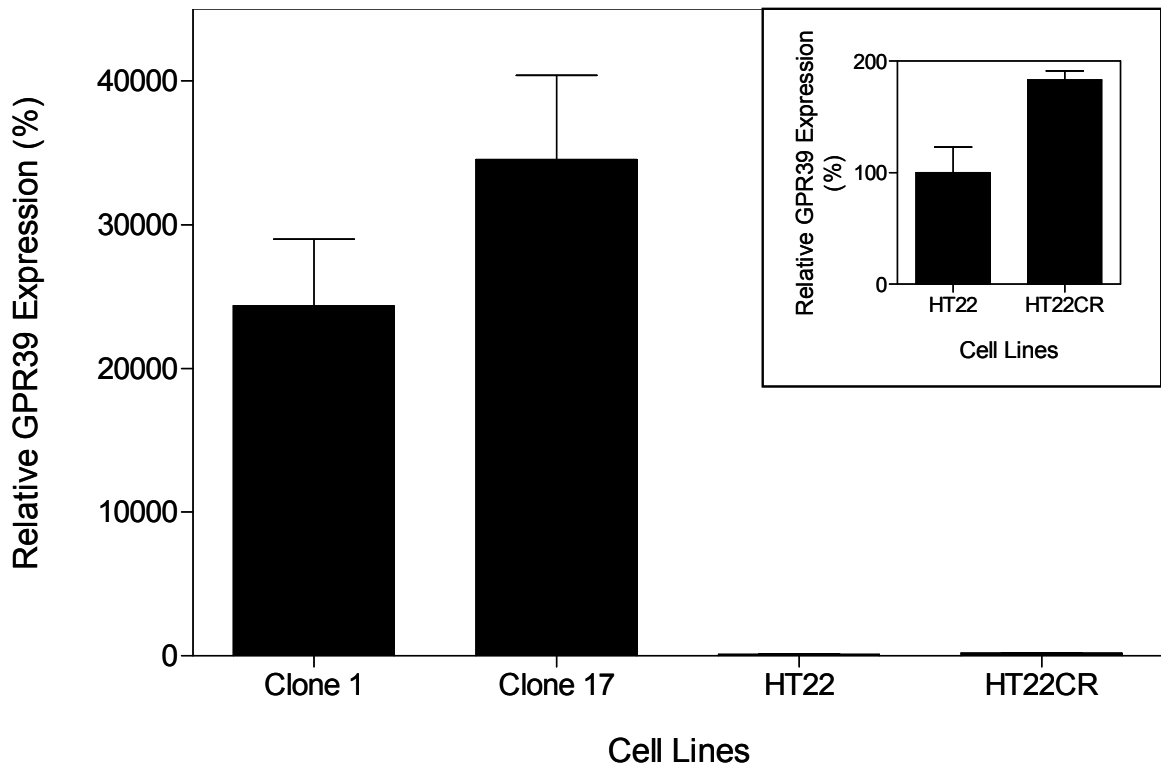


**Figure 4.30: mGPR39 upregulation in stable HT22 cells.** The most and the least HA-overexpressing clones were selected and seeded in 6-well plates at a density of  $1 \times 10^4$  cells. The next day they were incubated with a polyclonal anti-GPR39 antibody (1:1000) and analysed by FACS at 488 nm. The graph represents the data of the relative GPR39 expression obtained from three independent experiments each done in quadruplicates as mean  $\pm$  SEM.

#### 4.2.6.2 HT22 cells stably overexpressing mGPR39 show resistance to stress inducers

In order to test the capacity of resistance in the newly created stable cell lines, these were subjected to different kinds of stress inducers. The first one to be tested was oxidative glutamate toxicity, the classical paradigm where mGPR39 was identified. Both clones conferred resistance even under 40 mM glutamate after 8 hours, while HT22 cells could not survive 20 mM glutamate for the same duration (Figure 4.31). Clone 1 had a viability of 51.83% (SEM 2.453 n=12), while clone 17 yielded a 66.71% survival (SEM 4.317 n=12) under 40 mM glutamate.

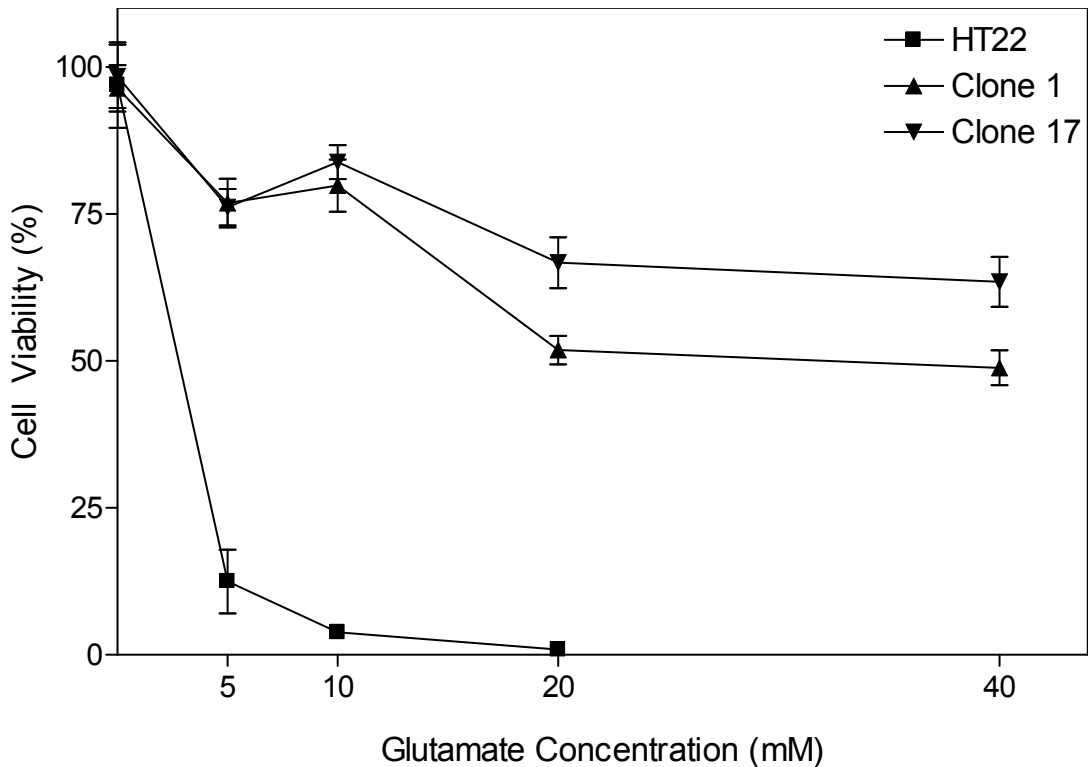


**Figure 4.31: Glutamate resistance in selected clones.** HT22 clones overexpressing mGPR39 stably were seeded at a density of  $5 \times 10^3$  cells in 96-well plates. The next day they were exposed to the indicated amounts of glutamate for 8 hours. Glutamate exposure was stopped by changing the medium and cell survival was measured by MTT. Viability of untreated cells was normalized to 100%. The graph represents the data of the relative cell viability obtained from three independent experiments each done in quadruplicates as mean  $\pm$  SEM.

After testing the clones for glutamate, we were curious about the protection against hydrogen peroxide. As HT22CR conferred some resistance, it was asked whether the mGPR39 overexpressing clones could protect the cells similarly. Although both clones protected the cells from hydrogen peroxide, the protection was less than expected (Figure 4.32). After 24 hours of 1mM hydrogen peroxide treatment, 9.85% (SEM 1.542 n=12) of the cells in clone 1 and 16.54% (SEM 2.646 n=12) of the cells in clone 17 could survive. Clone 1 showed under hydrogen peroxide the same results as before, protecting the cells with less efficiency than clone 17.

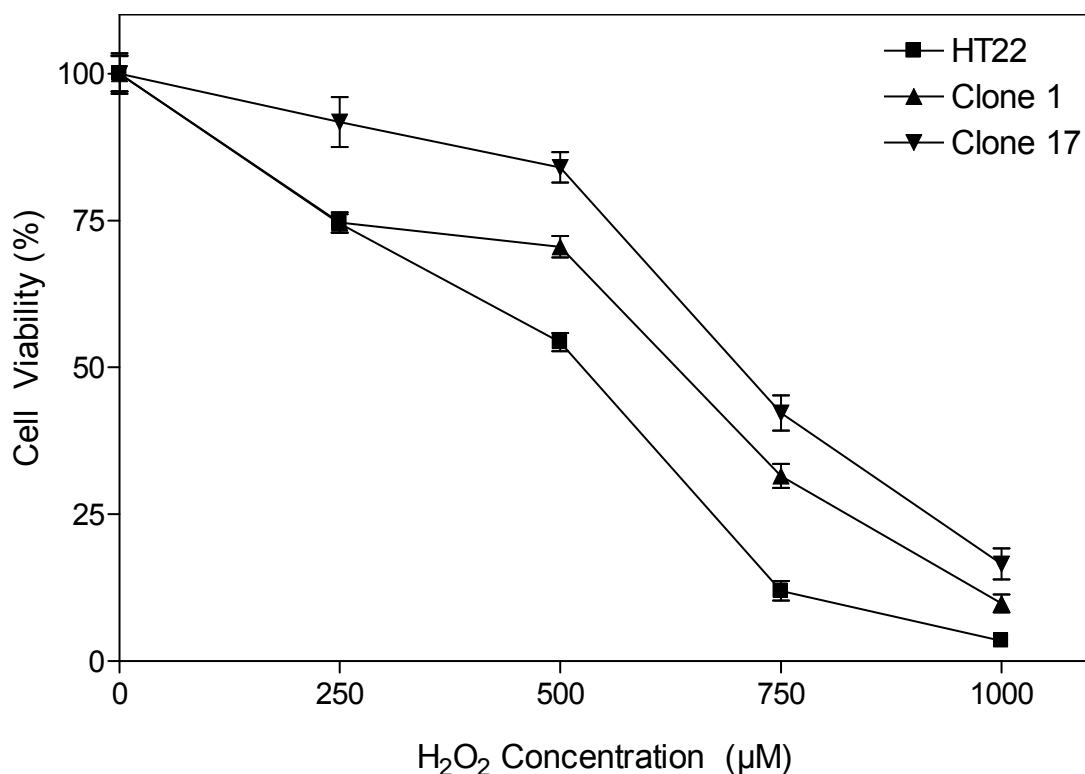


**Figure 4.32: Overexpression of mGPR39 resulted in hydrogen peroxide resistance.** HT22 clones 1 and 17 were seeded at a density of  $5 \times 10^3$  cells in 96-well plates. The next day they were exposed to the indicated amounts of hydrogen peroxide for 24 hours. Cell survival was measured by MTT. Viability of untreated cells was normalized to 100%. The graph represents the data of the relative cell viability obtained from three independent experiments each done in quadruplicates as mean  $\pm$  SEM.

Ceramide and tunicamycin toxicities did not change the protection observed in the clones. Both clones were protected against high doses of ceramide and tunicamycin (Figure 4.33). Interestingly, ceramide stress had no effect on all the cells until a concentration of 2.5  $\mu$ M, and even at this concentration clones 1 and 17 showed very little loss in viability (Clone 1 82.92% (SEM 8.115 n=12) vs. clone 17 88.40% (SEM 9.624 n=12)). Increasing the concentration to 5  $\mu$ M decreased the viability of the clones 1 and 17 to 32.64% (SEM 1.859 n=12) and 37.15% (SEM 6.893 n=12), respectively.

Tunicamycin decreased the viability of HT22 cells abruptly to 12.85% (SEM 4.603 n=12), starting at a concentration of 5  $\mu$ M, while clone 1 had a viability of 73.53% (SEM 1.963 n=12) and clone 17 a viability of 76.01% (SEM 2.641 n=12). Both of the clones could protect the cells over 50% until a concentration of 50  $\mu$ M, where the viabilities decreased to 6.54% (SEM 1.577 n=12) and 11.47% (SEM 1.022 n=12).

In conclusion, stable transfections of mGPR39 conferred protection against different kinds of cell death inducers, as observed by the resistant cell line.

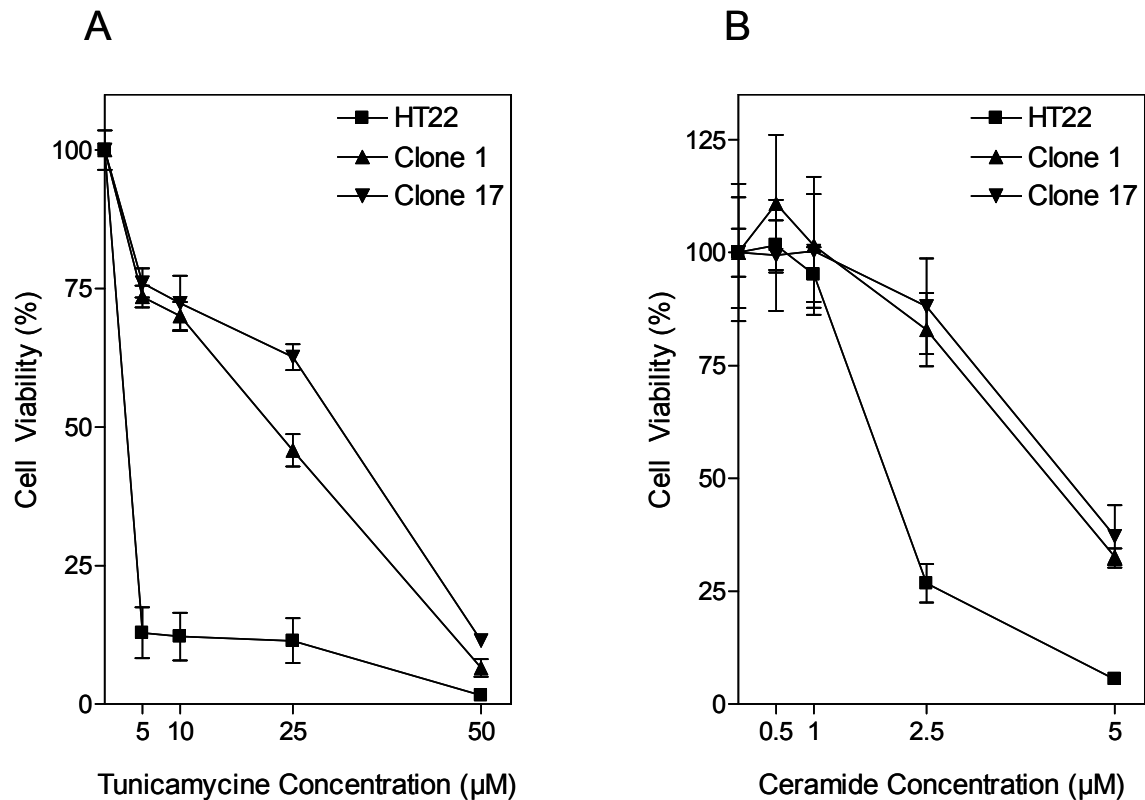


**Figure 4.33: Tunicamycine and ceramide toxicities in stable cell lines.** HT22 clones 1 and 17 were seeded at a density of  $5 \times 10^3$  cells in 96-well plates. The next day they were exposed to the indicated amounts of (A) tunicamycine or (B) ceramide for 24 hours. Cell survival was measured by MTT. Viability of untreated cells was normalized to 100%. The graphs represent the data of the relative cell viabilities obtained from five independent experiments each done in quadruplicates as mean  $\pm$  SEM.

#### 4.2.7 Implications for mGPR39 to take a role in other diseases

Since mGPR39 was expressed abundantly on epithelial tissues and the retina during development (Figure 4.28D), tests were carried out whether mGPR39 was expressed in the adult retinal pigment epithelium. The retinal pigment epithelium (RPE) is a monolayer of pigmented cells forming a part of the blood/retina barrier (Strauss 2005). The apical membrane of the RPE faces the photoreceptor outer segments. Long apical microvilli surround the light-sensitive outer segments establishing a complex of close structural interaction.

As a layer of pigmented cells, the RPE absorbs the light energy focused by the lens on the retina (Boulton and Dayhaw-Barker 2001). It also transports ions, water, and metabolic products from the subretinal space to the blood (Marmor 1999; Hamann 2002). Most importantly, retinal is constantly exchanged between photoreceptors and the RPE (Baehr,

Wu et al. 2003). As there is plenty amount of oxygen and light energy, the RPE is also one of the main oxidative stress production sites. An increase in oxidative stress due to a reduction in protective mechanisms or an increase in number and concentration of active photo-oxidative reaction species can contribute to a disease called age-related macular degeneration (AMD), the most common cause for blindness in industrialized countries (Beatty, Koh et al. 2000; Ambati, Ambati et al. 2003). The disease starts mostly with the accumulation of lipofuscin in the RPE, and develops by a chain of events that alter the RPE in an age-dependent manner (Delori, Goger et al. 2001; Hageman, Luthert et al. 2001). These events include, but are not limited to, reduction in cell density due to apoptosis (Delori, Goger et al. 2001) and change in pigmentation (Feeney-Burns, Hilderbrand et al. 1984), resulting in RPE and photoreceptor loss over large areas. To show the presence of mGPR39 in the RPE, cDNA from RPE cells with specific GPR39 primers was used in PCR amplification. In order to verify the results, FACS-Analysis using a GPR39-specific antibody was carried out (Figure 4.34). RPE cells, containing vast amounts of pigments, are dark in colour and able to fluoresce. An increase in fluorescence could be observed when the specific antibody was added, indicating for the presence of mGPR39 in the RPE.

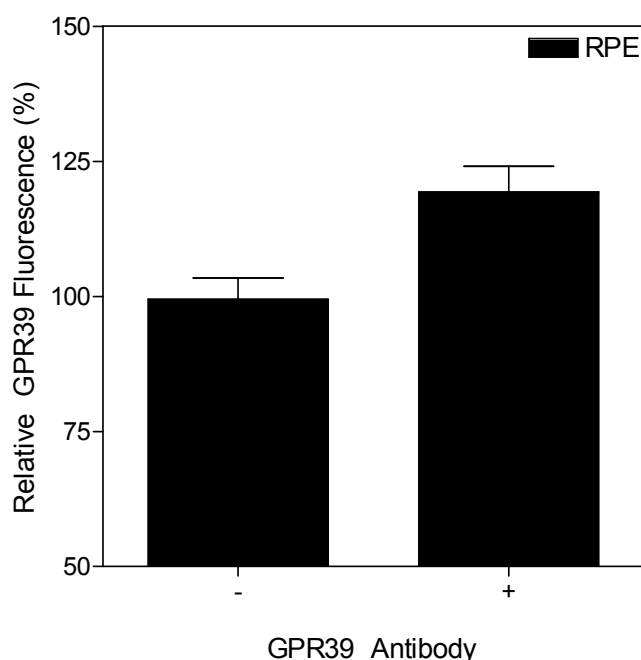


**Figure 4.34: mGPR39 is present in the RPE.** RPE cells were freshly prepared and incubated with a polyclonal GPR39 antibody followed by FACS analysis at 488 nm. The graph represents the data of the relative GPR39 fluorescence obtained from three independent experiments each done in triplets as mean  $\pm$  SEM.

## **5 Discussion**

### **5.1 HT22 cells die from oxidative glutamate toxicity upon exposure to glutamate**

Glutamate can induce cell death in neuronal cells either via excitotoxicity or oxidative glutamate toxicity (Choi 1988; Murphy, Miyamoto et al. 1989; Murphy, Schnaar et al. 1990; Coyle and Puttfarcken 1993). Both ways differ in the concentration of glutamate and the duration of exposure needed to induce cell death.

Mature cortical neurones that are susceptible to excitotoxic glutamate toxicity face a rapid cell death, prominent within the first hour after glutamate exposure, at micromolar concentrations of glutamate with an exposure of only a few minutes *via* activation of ionotropic glutamate receptors (Schubert and Piasecki 2001).

HT22 cells express neither an ionotropic glutamate receptor nor die in response to agonists of ionotropic glutamate receptors (Maher and Davis 1996). The glutamate-induced cell death observed in HT22 cells has been shown to occur *via* oxidative glutamate toxicity (Tan, Somia et al. 2001). The glutamate concentration and duration of treatment sufficient to induce a cell death program in HT22 cells by oxidative glutamate toxicity were reported to be 5 mM glutamate for seven hours (Davis and Maher 1994; Tan, Schubert et al. 2001). In our hands, 10 mM and eight hours of glutamate treatment were sufficient to exert almost maximal cell death (Figure 4.1). This increase in tolerance can be attributed to different kinds and concentrations of serum used (Figure 4.3).

Analyses using fluorescent dyes (DCFDA and MCB) in flow cytometry and fluorescence plate readers confirmed the decrease of glutathione and ROS accumulation after glutamate challenge in HT22 cells (Figure 4.5). Thus, the glutamate-induced cell death under the conditions used in this work is in line with the work done by other groups and is mediated by the oxidative pathway.

### **5.2 Glutamate susceptibility of HT22 cells is modulated by cell culture conditions**

Many neuronal cells are dependent on secreted survival signals that counteract otherwise detrimental effects resulting in programmed cell death (Raff, Barres et al. 1993). Furthermore, factors promoting survival were described to act in autocrine and paracrine

manners (Desire, Courtois et al. 2000; Krieglstein, Strelau et al. 2002). On the other hand, decreased cell density can trigger apoptosis by soluble factors or may induce an increased susceptibility to apoptosis-inducing agents in non-neuronal cells (Saeki, Yuo et al. 1997; Washo-Stultz, Crowley et al. 2000). In retinal epithelial cells, programmed cell death due to oxidative stress was reduced in denser cultures and accompanied by an increased synthesis of FGF2, which acts as a survival-promoting factor for these cells (Bryckaert, Guillonneau et al. 1999; Wada, Gelfman et al. 2001).

Thus, the attenuation of glutamate-induced cell death by a higher cell density (Figure 4.2), might be explained through the release of survival promoting factors by the HT22 cells in an auto- and paracrine fashion. This hypothesis could be further substantiated by the protective effect of medium conditioned by confluent cultures (Figure 4.4 and 4.10). Alternatively, HT22 cells might remove substances from the growth medium that otherwise promote programmed cell death.

Studying the impact of serum concentration on glutamate-induced cell death, it was clearly shown that major cofactors for the initiation of glutamate-induced cell death originating from fetal calf serum are present in the growth medium (Figure 4.3). Although the identity of these substances is not known, catecholamines may represent, at least partially, these death-promoting cofactors: They are present in serum and, their metabolism with monoamine oxidases produces  $H_2O_2$  (Weyler, Hsu et al. 1990; Singer and Ramsay 1995). In addition, the inhibition of catecholamine transporters in HT22 cells was reported to protect these from oxidative glutamate toxicity (Maher and Davis, 1996).

Moreover, serum may contain growth factors that were shown to intensify glutamate-toxicity (Schubert, Kimura et al. 1992). Serum and growth factors are potent inducers of the transcription factor AP-1. AP-1 was recognized as one of the key regulators of life and death in a cell. It was reported to induce the transcription of both pro- and antiapoptotic gene products whose final balance was context-dependent (Shaulian and Karin 2002). This is supported by the observation that growth factors mediating survival in serum deprivation can also induce cell death in models of ischemic stroke and excitotoxicity (Koh, Gwag et al. 1995). The context-dependence of the biological action of some factors can be further exemplified by nitric oxide. Nitric oxide was reported to switch from a protective agent to a death promoter in GSH depleted mid brain cultures (Canals, Casarejos et al. 2001; Canals, Casarejos et al. 2001).

Glutathione was shown to be depleted in oxidative glutamate toxicity, previously (Tan, Schubert et al. 2001). Elevated extracellular glutamate blocks the cystine import *via* the

System  $X_c^-$  glutamate/cystine antiporter and the subsequent decrease in cystine results in GSH depletion. The same results were obtained in our hands (Figure 4.5), leading to ROS accumulation in the cells, and inevitably to cell death.

Considering the similarities, signaling induced by serum-derived factors that support survival under normal circumstances might as well be interpreted as a death-promoting signal by the HT22 cells during oxidative glutamate toxicity.

### **5.3 Resistant HT22 cells differ from the parental cell line in their GPCR pattern**

Next to growth factor receptors, belonging to the family of receptor tyrosine kinases (Schlessinger and Ullrich 1992), GPCRs are a family of candidate receptors that may account for the modulation of susceptibility in HT22 cells under cell culture conditions. Serum contains a vast amount of substances that are ligands of GPCRs and thus, activate G-protein dependent signaling cascades (Milligan 1987; Bogoyevitch, Clerk et al. 1995; Wenzel, Muller et al. 2005). Activation or inactivation of different types of GPCRs had been reported to protect the cells in different models of neurodegeneration (Bond, O'Neill et al. 1998; Jolkkonen, Puurunen et al. 1999; Kimura, Mizukami et al. 2001). In addition, the activation of metabotropic glutamate receptor 1 and 5 (Sagara and Schubert 1998), the dopamine D4 receptor (Ishige, Chen et al. 2001), and stimulation of the GPCR-activated protein kinase C (Davis and Maher 1994; Maher 2001) were reported to protect HT22 cells and immature neurones from oxidative glutamate toxicity.

To investigate the role of GPCRs in glutamate-induced oxidative toxicity, the glutamate resistant cell line HT22CR, created by Dr. Jan Lewerenz in our group, was used. Repetitive treatment with high doses of glutamate, followed by expansion of the surviving cells, led to the glutamate resistant cell line HT22CR. In line with previous results (Sagara and Schubert 1998), the evoked resistance was not specific to glutamate as the selected cells were also resistant to the induction of cell death by direct exposure to  $H_2O_2$  (Figure 4.7) or other stress inducing agents like ceramide and tunicamycine (Figure 4.8 and 4.9).

As an initial step, the activation of signal transduction pathways involved in GPCR signaling was compared, using phosphorylation-specific antibodies (Figure 4.11). An increase in phosphorylated cAMP-response element binding protein (CREB) levels hinted towards an activation of  $G_s$ -coupled receptors, which has been described to confer neuroprotection in other systems (Walton, Sirimanne et al. 1996; Lee, Butcher et al. 2005;

Papadia, Stevenson et al. 2005) and in HT22 cells (Lewerenz, Letz et al. 2003). A reduction in phosphorylation of extracellular-signal regulated protein kinases 1 and 2 (ERK1/2) confirmed this result, as ERK1/2 phosphorylation is known to occur downstream of receptor tyrosine kinase activation, through  $G_i$ -coupled mechanisms or via activation of protein kinase C (PKC) by the  $G_q$ -coupled receptors (Gutkind 1998). The exact mechanism is still not known, as several studies have showed the phosphorylation to occur through the  $\beta\gamma$ -subunits without PKC activation (Crespo, Xu et al. 1994; Koch, Hawes et al. 1994). Nevertheless, these results were in line with previous findings on glutamate-induced oxidative toxicity (Maher 2001; Lewerenz, Letz et al. 2003).

As the observed activation of  $G_s$ -coupled signal transduction pathways could occur through the activation of protective GPCRs by their cognate ligands or an increase in the expression of GPCRs, the relative mRNA expression of 24 candidate receptors was quantified (Figure 4.13). These receptors were chosen for their roles in cell differentiation, survival, and apoptosis. Out of the 24 receptors, the receptors for the vasoactive intestinal peptide (VIP), VPAC<sub>2</sub>, and the metabotropic glutamate receptor mGlu<sub>1</sub> were found to be upregulated in the resistant cells, while the angiotensin receptor AG<sub>22</sub> was expressed to a higher extent in sensitive cells.

From these results, it was hypothesized that in glutamate-resistant cells protective GPCRs are upregulated, while detrimental receptors are downregulated.

#### **5.4 VPAC<sub>2</sub> – a model neuroprotective receptor**

The vasoactive intestinal peptide (VIP) is a well-known neuropeptide that has a wide distribution in peripheral and central nervous systems and a large spectrum of biological actions in mammals. It has been described to have effects in the digestive tract, cardiovascular system, airways, reproductive system, immune system, endocrine glands and brain (Rayan, Said et al. 1991). Besides its short-term actions on exocrine secretions and hormone release, VIP has also been characterized as a growth regulator for fetuses (Gressens, Hill et al. 1993; Waschek 1995) and a regulator in the suppression of inflammation and immunomodulation (Delgado and Ganea 2001).

Following the cloning of the first VIP receptor (later termed VPAC<sub>1</sub>) from a rat cDNA (Ishihara, Shigemoto et al. 1992) other orthologues (Sreedharan, Patel et al. 1993; Couvineau, Rouyer-Fessard et al. 1994), and a second VIP receptor (later termed as VPAC<sub>2</sub>) were cloned (Lutz, Sheward et al. 1993). Both receptors bind to the neuropeptides vasoactive intestinal peptide (VIP) and pituitary adenylate cyclase-activating peptide

(PACAP) with similar affinities, VIP having a slightly higher affinity than PACAP (Vaudry, Gonzalez et al. 2000).

It was early identified that cellular action of VIP induces a robust increase in cyclic AMP production in target cells (Laburthe, Rousset et al. 1978) and, it still represents the signaling pathway for VIP through the VPAC receptors. This increase in cyclic AMP production was shown to activate adenylyl cyclase, which further activated protein kinase A (Shreeve, Sreedharan et al. 2000). Furthermore, it was clearly demonstrated that both of these receptors couple mainly to stimulatory type G-proteins (Gs) when transmitting a signal (Luo, Zeng et al. 1999; Shreeve, Sreedharan et al. 2000).

To demonstrate the action of VIP in glutamate-induced oxidative toxicity, cell extracts from glutamate-sensitive cells were analysed with or without the addition of VIP and glutamate (Figure 4.14). It was shown that by the addition of VIP and even glutamate, CREB phosphorylation could be increased while ERK1/2 phosphorylation was decreased. This was similar to the phosphorylation pattern observed in HT22CR cells. Interestingly, adding both VIP and glutamate substantiated this effect, suggesting a synergistic activity.

Because Bcl-2 expression is regulated by the transcription factor cyclic AMP response element-binding protein (CREB) (Pugazhenthii, Nesterova et al. 2000; Freeland, Boxer et al. 2001), Bcl-2 expression levels were also checked. As expected, the addition of VIP and/or glutamate increased Bcl-2 expression in HT22 cells, underlining the synergistic activity of glutamate and VIP. According to these results, it was hypothesized that VPAC<sub>2</sub> activation through VIP would lead to Bcl-2 activation, which in turn would result in a protective effect in glutamate-induced oxidative stress.

In order to test the hypothesis, HT22 cells were transfected with Bcl-2 or VPAC<sub>2</sub> (Figure 4.15 and 4.16). Bcl-2 transfection not only increased the viability of the cells under glutamate, but also resulted in higher glutathione levels in the cell. This result was in line with previous work done (Pugazhenthii, Nesterova et al. 2003). Furthermore, the same results, though in a lesser content, were observed in the VPAC<sub>2</sub> transfected cells. Although, an increase in glutathione levels through VIP had been described (Offen, Sherki et al. 2000), and protection mediated by VIP is a well-known phenomena (Brown 2000; Steingart, Solomon et al. 2000), the mechanism of protection was not characterized. Studies done on the VIP receptors and neuroprotection, suggested a protection through the VPAC<sub>1</sub> receptor, as in the case of serum-withdrawal (Gutierrez-Canas, Rodriguez-Henche et al. 2003), but not the VPAC<sub>2</sub> receptor.

In conclusion, it was clearly shown that VPAC<sub>2</sub> activation leads to neuroprotection and functions at least partially over the Bcl-2 pathway.

## 5.5 Resistance conferred by the Upregulated Orphan Receptors

The difference in GPCR patterns between glutamate-sensitive and resistant HT22 cells, led to the investigation of orphan receptors in mouse, with the aim of finding new receptors that could lead to neuroprotection. By using the same method, three receptors were found to be upregulated in glutamate-resistant HT22 cells: mGPR15, mGPR39, and mP2Y9 (Figure 4.17). P2Y9 receptor was later characterized by another group as the lysophosphatidic acid receptor 4 (LPA4), increasing the adenylate cyclase activity within the cell (Noguchi, Ishii et al. 2003). A neuroprotection mediated by the LPA4 receptor has not been reported yet. As P2Y9 (LPA4) was deorphanized, studies were concentrated on mGPR15 and mGPR39.

As a first step, cells transfected with mGPR15, mGPR39, and hVPAC<sub>2</sub> were subjected to different concentrations of glutamate. While mGPR39 protected the cells even under high concentrations, mGPR15 had almost no effect at all. The positive control, hVPAC<sub>2</sub>, had the same effect as mGPR39, though surprisingly to a lesser extent (Figure 4.22). This result remained the same under hydrogen peroxide toxicity, but this time the only difference between mGPR39 and hVPAC<sub>2</sub> was seen at 934  $\mu$ M (Figure 4.23).

After observing protection against both glutamate and hydrogen peroxide, the transfected cells were used to investigate two main oxidative stress indicators: glutathione and ROS. A difference in cellular glutathione levels had already been shown in cells transfected with hVPAC<sub>2</sub> and Bcl-2 (Figure 4.16). Cells transfected with Bcl-2 had the highest amount of cellular glutathione, followed by mGPR39- and hVPAC<sub>2</sub>-transfections with higher glutathione contents than mock-transfected cells (Figure 4.24). Interestingly, mGPR39 transfected cells had the lowest amount of ROS levels in the cells, while Bcl-2 and hVPAC<sub>2</sub> transfected cells had higher values.

These differences could be due to the expression and activation requirements of GPCRs, as they have to be transported to the cell surface to become fully activated while Bcl-2 becomes active once it is expressed within the cell. Next, once activated both of the GPCRs have to function over some G-proteins and effectors, which takes longer than the effect observed by Bcl-2. Furthermore, the presence of an endogenous ligand in the medium would result in direct activation of the receptors and once expressed, hGPR39 was shown to be constitutively active (Holst, Holliday et al. 2004).

As a next step, the expression of mGPR39 during mouse development was investigated. GPR39 was expressed predominantly in epithelial tissues, with a consistent intensity through different developmental stages (Figure 4.26). Starting as early as E12.5, the signals could be detected in tissues forming later the intestines, lungs, liver, kidneys, bladder, stomach, spinal cord, and the ribs. In the brain, cerebral cortex, hippocampus, cerebellum and amygdala were labelled at all stages of development. Later in development, signals could be detected in the trigeminal ganglion, cochlea and cochlear gang, as well as the olfactory bulb (not shown). Starting at E14, signals could also be detected in the retina and the epithelium surrounding the retina. These signals indicated a role for mGPR39 in various functions within the development, concentrating on the gastrointestinal tract.

While this work was in progress, mGPR39 was characterized as the receptor for obestatin (Zhang, Ren et al. 2005), a peptide opposing the effects of ghrelin, suppressing food intake, inhibiting jejunal contraction, and decreasing body-weight gain. This is in line with our findings, since mGPR39 is mainly expressed in the gastrointestinal tract in our studies. Furthermore, oxidative stress is known to take a role in intestinal ischemia (Aw 1999), radiation enteritis, sepsis (Sener, Arbak et al. 2005), inflammatory bowel disease and the promotion of gastric and colorectal cancer (Thomson, Hemphill et al. 1998; Zhou, Wang et al. 2005).

Because of these results and for further investigating the mechanisms at the cellular level, HT22 cells stably overexpressing mGPR39 were generated.

## **5.6 Stable HT22 cells overexpressing mGPR39**

HT22 cells overexpressing mGPR39 were generated using a retroviral expression system. The cells generated expressed not only mGPR39 but also EGFP, since a construct containing EGFP was co-transfected as a marker for positive transfection. Positive clones were investigated for surface HA expression using FACS-Analysis and the best six clones were selected for further investigations. These clones were selected according to their HA-expression levels, with two clones with low-, mid- and high-level expression.

The selected clones were first subjected to glutamate (Figure 4.29A) and then to hydrogen peroxide (not shown). Between these six clones, clones 1 and 17 showed the least and most protection, respectively. As this result was in line with surface HA-expression levels, these two clones were selected for further analyses. Before progressing with other experiments, these clones were tested for their surface mGPR39 expression levels using a GPR39-specific antibody, directed against the third extracellular loop by FACS analysis, that

became available recently (Figure 4.30). As expected and in line with HA-expression levels, clone 1 had less mGPR39 expressed on its surface when compared to clone 17, though both levels were much higher than in both HT22 and HT22CR. These clones showed also resistance against hydrogen peroxide (Figure 4.32), ceramide (Figure 4.33A) and tunicamycin (Figure 4.33B). Different from other stress inducers, ceramide did not affect cell survival in HT22 cells until a concentration of 2.5  $\mu\text{g/ml}$ , while it increased the viability in clone 17 cells. Surprisingly, up to this concentration clone 1 had almost no difference in viability when compared to the HT22 cells.

## **5.7 Implications for a role in diseases**

In addition to the protection observed in HT22CR cells, mGPR39 was found to be upregulated in various tumor cell lines (Bayer Pharmaceuticals, personal communication), and in the retina during development (Figure 4.28D). Using PCR and FACS-Analysis, the presence of mGPR39 in the retinal pigment epithelium was proven (Figure 4.34). As RPE cells contain the pigments required for vision, they can fluoresce under certain wavelengths. This was also the case in our hands, as freshly prepared mouse RPE cells without any antibodies or dyes fluoresced to a certain extent. Addition of a GPR39-specific antibody increased the fluorescence, albeit slightly.

As mGPR39 protected HT22 cells against oxidative stress, it was postulated that it could have a similar function in RPE, as a defense mechanism against age-related macular degeneration (AMD). Moreover, its upregulation in various tumor cell lines indicates an important role in cancer. Future investigations concerning the role of mGPR39 in these areas could be of importance for the identification of new pathways and drugs.

## 6 Summary

The aim of this study was to demonstrate a protection against oxidative glutamate toxicity by G-protein coupled receptors, and to characterize the mechanism of protection mediated by the mouse orphan GPCR mGPR39. Oxidative glutamate toxicity in the neuronal cell line HT22 is a paradigm of programmed cell death due to glutamate-mediated depletion of glutathione, an important antioxidant in the brain, and subsequent oxidative stress. As oxidative stress was implicated in neurological diseases like Alzheimer's dementia and Parkinson's disease, a detailed characterization of the antioxidant defence of neuronal cells might broaden the understanding of their pathophysiology.

The data presented in this thesis show that the susceptibility of HT22 cells to glutamate-induced cell death is inversely correlated with cell density and directly correlated with serum concentration. Additionally, medium conditioned by confluent HT22 or HT22CR cells protected low-density cultures, even under high concentrations of glutamate. Under serum-free conditions, the glutamate susceptibility was low, increasing serum concentration prominently exacerbated cell death, indicating serum-derived death promoting factors, which modulate the susceptibility to oxidative glutamate toxicity.

To investigate whether G-protein coupled receptors are involved in the propagation of this modulation, cellular pathways activated through GPCRs were compared between sensitive and resistant cells. An activation of the cAMP pathway was observed, most probably due to G<sub>s</sub> activation and was confirmed by CRE induced EGFP activation. This difference in the cellular pathways led us to investigate protection and apoptosis related GPCRs. The highest upregulation was observed in vasointestinal peptide (VIP) receptor, VPAC<sub>2</sub>. Stimulating the cells with VIP, increased the observed protective effects against glutamate in the cells, and resulted in Bcl-2 activation, similar to the activation observed in HT22CR cells. Further investigations led us to identify VPAC<sub>2</sub> as a GPCR to take a role in protection against oxidative stress, which we then used as a positive control in glutamate-induced oxidative toxicity.

Following the identification of a GPCR taking a role in glutamate-induced oxidative stress, 82 known mouse orphan GPCRs were investigated. Three different receptors were found to be repetitively upregulated in glutamate resistant cells. Only one of the receptors, mGPR39, yielded a protection. This receptor was tested using different oxidative stress inducers and observing a protection, it was investigated through development. The clear signals observed in the gastrointestinal tract and epithelial tissues as well as the retina

throughout the development led to the generation of stable cell lines overexpressing mGPR39. These cells were tested for their surface expression of mGPR39 using HA- and GPR39-specific antibodies and the least and most protection conferring ones were selected for further analyses. Both of these new cell lines protected against the oxidative stress inducers used in this study, indicating a protection by the orphan receptor mGPR39.

Expression analyses and personal communications indicated a role for mGPR39 in various diseases like age-related macular degeneration (AMD) and cancer, though the exact roles and mechanisms have yet to be elucidated.

7Taken together, this work provides further insight into the mechanisms of protection against glutamate-induced oxidative stress, in particular into the mechanisms mediated by G-protein coupled receptors. Furthermore, an orphan receptor from mouse was found to be a likely candidate for protection against diverse kinds of stresses.

## 7 Literature

- Abremski, K., R. Hoess, et al. (1983). "Studies on the properties of P1 site-specific recombination: evidence for topologically unlinked products following recombination." *Cell* **32**(4): 1301-11.
- Ambati, J., B. K. Ambati, et al. (2003). "Age-related macular degeneration: etiology, pathogenesis, and therapeutic strategies." *Surv Ophthalmol* **48**(3): 257-93.
- Annis, M. G., N. Zamzami, et al. (2001). "Endoplasmic reticulum localized Bcl-2 prevents apoptosis when redistribution of cytochrome c is a late event." *Oncogene* **20**(16): 1939-52.
- Aw, T. Y. (1999). "Molecular and cellular responses to oxidative stress and changes in oxidation-reduction imbalance in the intestine." *Am J Clin Nutr* **70**(4): 557-65.
- Azad, S. C., M. Eder, et al. (2003). "Activation of the cannabinoid receptor type 1 decreases glutamatergic and GABAergic synaptic transmission in the lateral amygdala of the mouse." *Learn Mem* **10**(2): 116-28.
- Baehr, W., S. M. Wu, et al. (2003). "The retinoid cycle and retina disease." *Vision Res* **43**(28): 2957-8.
- Bashir, Z. I., Z. A. Bortolotto, et al. (1993). "Induction of LTP in the hippocampus needs synaptic activation of glutamate metabotropic receptors." *Nature* **363**(6427): 347-50.
- Basma, A. N., E. J. Morris, et al. (1995). "L-dopa cytotoxicity to PC12 cells in culture is via its autoxidation." *J Neurochem* **64**(2): 825-32.
- Beatty, S., H. Koh, et al. (2000). "The role of oxidative stress in the pathogenesis of age-related macular degeneration." *Surv Ophthalmol* **45**(2): 115-34.
- Behl, C., J. Davis, et al. (1992). "Vitamin E protects nerve cells from amyloid beta protein toxicity." *Biochem Biophys Res Commun* **186**(2): 944-50.
- Behl, C., J. B. Davis, et al. (1994). "Hydrogen peroxide mediates amyloid beta protein toxicity." *Cell* **77**(6): 817-27.
- Blaak, H., P. H. Boers, et al. (2005). "CCR5, GPR15, and CXCR6 are major coreceptors of human immunodeficiency virus type 2 variants isolated from individuals with and without plasma viremia." *J Virol* **79**(3): 1686-700.
- Blazquez, C., I. Galve-Roperh, et al. (2000). "De novo-synthesized ceramide signals apoptosis in astrocytes via extracellular signal-regulated kinase." *Faseb J* **14**(14): 2315-22.
- Bockaert, J., S. Claeyssen, et al. (2002). "G protein-coupled receptors: dominant players in cell-cell communication." *Int Rev Cytol* **212**: 63-132.
- Bogoyevitch, M. A., A. Clerk, et al. (1995). "Activation of the mitogen-activated protein kinase cascade by pertussis toxin-sensitive and -insensitive pathways in cultured ventricular cardiomyocytes." *Biochem J* **309** (Pt 2): 437-43.
- Bond, A., M. J. O'Neill, et al. (1998). "Neuroprotective effects of a systemically active group II metabotropic glutamate receptor agonist LY354740 in a gerbil model of global ischaemia." *Neuroreport* **9**(6): 1191-3.
- Boulton, M. and P. Dayhaw-Barker (2001). "The role of the retinal pigment epithelium: topographical variation and ageing changes." *Eye* **15**(Pt 3): 384-9.
- Braak, H. and E. Braak (1991). "Demonstration of amyloid deposits and neurofibrillary changes in whole brain sections." *Brain Pathol* **1**(3): 213-6.
- Brockhaus, F. and B. Brune (1999). "Overexpression of CuZn superoxide dismutase protects RAW 264.7 macrophages against nitric oxide cytotoxicity." *Biochem J* **338** (Pt 2): 295-303.

- Brown, D. R. (2000). "Neuronal release of vasoactive intestinal peptide is important to astrocytic protection of neurons from glutamate toxicity." Mol Cell Neurosci **15**(5): 465-75.
- Bruno, V., G. Battaglia, et al. (1995). "Activation of class II or III metabotropic glutamate receptors protects cultured cortical neurons against excitotoxic degeneration." Eur J Neurosci **7**(9): 1906-13.
- Bruno, V., A. Copani, et al. (1995). "Activation of metabotropic glutamate receptors coupled to inositol phospholipid hydrolysis amplifies NMDA-induced neuronal degeneration in cultured cortical cells." Neuropharmacology **34**(8): 1089-98.
- Bryckaert, M., X. Guillonnet, et al. (1999). "Both FGF1 and bcl-x synthesis are necessary for the reduction of apoptosis in retinal pigmented epithelial cells by FGF2: role of the extracellular signal-regulated kinase 2." Oncogene **18**(52): 7584-93.
- Campbell, V. A. (2001). "Tetrahydrocannabinol-induced apoptosis of cultured cortical neurones is associated with cytochrome c release and caspase-3 activation." Neuropharmacology **40**(5): 702-9.
- Canals, S., M. J. Casarejos, et al. (2001). "Glutathione depletion switches nitric oxide neurotrophic effects to cell death in midbrain cultures: implications for Parkinson's disease." J Neurochem **79**(6): 1183-95.
- Canals, S., M. J. Casarejos, et al. (2001). "Neurotrophic and neurotoxic effects of nitric oxide on fetal midbrain cultures." J Neurochem **76**(1): 56-68.
- Capellier, G., V. Maupoil, et al. (1999). "Oxygen toxicity and tolerance." Minerva Anesthesiol **65**(6): 388-92.
- Chen, C. J., S. L. Liao, et al. (2000). "Gliotoxic action of glutamate on cultured astrocytes." J Neurochem **75**(4): 1557-65.
- Choi, D. W. (1988). "Glutamate neurotoxicity and diseases of the nervous system." Neuron **1**(8): 623-34.
- Civelli, O. (2005). "GPCR deorphanizations: the novel, the known and the unexpected transmitters." Trends Pharmacol Sci **26**(1): 15-9.
- Colombaioni, L. and M. Garcia-Gil (2004). "Sphingolipid metabolites in neural signalling and function." Brain Res Brain Res Rev **46**(3): 328-55.
- Cook, J. A., H. I. Pass, et al. (1989). "Use of monochlorobimane for glutathione measurements in hamster and human tumor cell lines." Int J Radiat Oncol Biol Phys **16**(5): 1321-4.
- Couvineau, A., C. Rouyer-Fessard, et al. (1994). "Human intestinal VIP receptor: cloning and functional expression of two cDNA encoding proteins with different N-terminal domains." Biochem Biophys Res Commun **200**(2): 769-76.
- Coyle, J. T. and P. Puttfarcken (1993). "Oxidative stress, glutamate, and neurodegenerative disorders." Science **262**(5134): 689-95.
- Crespo, P., N. Xu, et al. (1994). "Ras-dependent activation of MAP kinase pathway mediated by G-protein beta gamma subunits." Nature **369**(6479): 418-20.
- Crichton, R. R. and M. Charloreaux-Wauters (1987). "Iron transport and storage." Eur J Biochem **164**(3): 485-506.
- Dale, L. B., A. V. Babwah, et al. (2002). "Mechanisms of metabotropic glutamate receptor desensitization: role in the patterning of effector enzyme activation." Neurochem Int **41**(5): 319-26.
- Dargusch, R. and D. Schubert (2002). "Specificity of resistance to oxidative stress." J Neurochem **81**(6): 1394-400.
- Davies, K. J. (1995). "Oxidative stress: the paradox of aerobic life." Biochem Soc Symp **61**: 1-31.
- Davis, C. B., I. Dikic, et al. (1997). "Signal transduction due to HIV-1 envelope interactions with chemokine receptors CXCR4 or CCR5." J Exp Med **186**(10): 1793-8.

- Davis, J. B. and P. Maher (1994). "Protein kinase C activation inhibits glutamate-induced cytotoxicity in a neuronal cell line." Brain Res **652**(1): 169-73.
- Delgado, M. and D. Ganea (2001). "Inhibition of endotoxin-induced macrophage chemokine production by vasoactive intestinal peptide and pituitary adenylate cyclase-activating polypeptide in vitro and in vivo." J Immunol **167**(2): 966-75.
- Delori, F. C., D. G. Goger, et al. (2001). "Age-related accumulation and spatial distribution of lipofuscin in RPE of normal subjects." Invest Ophthalmol Vis Sci **42**(8): 1855-66.
- Deng, H. K., D. Unutmaz, et al. (1997). "Expression cloning of new receptors used by simian and human immunodeficiency viruses." Nature **388**(6639): 296-300.
- Desire, L., Y. Courtois, et al. (2000). "Endogenous and exogenous fibroblast growth factor 2 support survival of chick retinal neurons by control of neuronal neuronal bcl-x(L) and bcl-2 expression through a fibroblast berowth factor receptor 1- and ERK-dependent pathway." J Neurochem **75**(1): 151-63.
- Deslauriers, B., C. Ponce, et al. (1999). "N-glycosylation requirements for the AT1a Angiotensin II receptor delivery to the plasma membrane." Biochem. J. **339**(0264-6021): 397-405.
- Devesa, A., J. E. O'Connor, et al. (1993). "Glutathione metabolism in primary astrocyte cultures: flow cytometric evidence of heterogeneous distribution of GSH content." Brain Res **618**(2): 181-9.
- Duvernay, M. T., C. M. Filipeanu, et al. (2005). "The regulatory mechanisms of export trafficking of G protein-coupled receptors." Cell Signal **17**(12): 1457-65.
- Ellerby, L. M., H. M. Ellerby, et al. (1996). "Shift of the cellular oxidation-reduction potential in neural cells expressing Bcl-2." J Neurochem **67**(3): 1259-67.
- Farzan, M., H. Choe, et al. (1997). "Two orphan seven-transmembrane segment receptors which are expressed in CD4-positive cells support simian immunodeficiency virus infection." J Exp Med **186**(3): 405-11.
- Feeney-Burns, L., E. S. Hilderbrand, et al. (1984). "Aging human RPE: morphometric analysis of macular, equatorial, and peripheral cells." Invest Ophthalmol Vis Sci **25**(2): 195-200.
- Freeland, K., L. M. Boxer, et al. (2001). "The cyclic AMP response element in the Bcl-2 promoter confers inducibility by hypoxia in neuronal cells." Brain Res Mol Brain Res **92**(1-2): 98-106.
- Fridovich, I. (1978). "The biology of oxygen radicals." Science **201**(4359): 875-80.
- Fridovich, I. (1989). "Superoxide dismutases. An adaptation to a paramagnetic gas." J Biol Chem **264**(14): 7761-4.
- Fridovich, I. (1998). "Oxygen toxicity: a radical explanation." J Exp Biol **201**(Pt 8): 1203-9.
- Fridovich, I. (1999). "Fundamental aspects of reactive oxygen species, or what's the matter with oxygen?" Ann N Y Acad Sci **893**: 13-8.
- Froissard, P., H. Monrocoq, et al. (1997). "Role of glutathione metabolism in the glutamate-induced programmed cell death of neuronal-like PC12 cells." Eur J Pharmacol **326**(1): 93-9.
- Fullerton, H. J., J. S. Ditelberg, et al. (1998). "Copper/zinc superoxide dismutase transgenic brain accumulates hydrogen peroxide after perinatal hypoxia ischemia." Ann Neurol **44**(3): 357-64.
- Garcia, D. E., B. Li, et al. (1998). "G-protein beta-subunit specificity in the fast membrane-delimited inhibition of Ca<sup>2+</sup> channels." J Neurosci **18**(22): 9163-70.
- Gavel, Y. and G. von Heijne (1990). "Sequence differences between glycosylated and non-glycosylated Asn-X-Thr/Ser acceptor sites: implications for protein engineering." Protein Eng **3**(5): 433-42.

- Glenner, G. G. and C. W. Wong (1984). "Alzheimer's disease: initial report of the purification and characterization of a novel cerebrovascular amyloid protein." Biochem Biophys Res Commun **120**(3): 885-90.
- Goodman, O. B., Jr., J. G. Krupnick, et al. (1996). "Beta-arrestin acts as a clathrin adaptor in endocytosis of the beta2-adrenergic receptor." Nature **383**(6599): 447-50.
- Goodman, Y. and M. P. Mattson (1996). "Ceramide protects hippocampal neurons against excitotoxic and oxidative insults, and amyloid beta-peptide toxicity." J Neurochem **66**(2): 869-72.
- Graham, D. G. (1978). "Oxidative pathways for catecholamines in the genesis of neuromelanin and cytotoxic quinones." Mol Pharmacol **14**(4): 633-43.
- Gressens, P., J. M. Hill, et al. (1993). "Growth factor function of vasoactive intestinal peptide in whole cultured mouse embryos." Nature **362**(6416): 155-8.
- Gutierrez-Canas, I., N. Rodriguez-Henche, et al. (2003). "VIP and PACAP are autocrine factors that protect the androgen-independent prostate cancer cell line PC-3 from apoptosis induced by serum withdrawal." Br J Pharmacol **139**(5): 1050-8.
- Gutkind, J. S. (1998). "Cell growth control by G protein-coupled receptors: from signal transduction to signal integration." Oncogene **17**(11 Reviews): 1331-42.
- Gutkind, J. S. (1998). "The pathways connecting G protein-coupled receptors to the nucleus through divergent mitogen-activated protein kinase cascades." J Biol Chem **273**(4): 1839-42.
- Hageman, G. S., P. J. Luthert, et al. (2001). "An integrated hypothesis that considers drusen as biomarkers of immune-mediated processes at the RPE-Bruch's membrane interface in aging and age-related macular degeneration." Prog Retin Eye Res **20**(6): 705-32.
- Halliwell, B. (1992). "Reactive oxygen species and the central nervous system." J Neurochem **59**(5): 1609-23.
- Halliwell, B. and O. I. Aruoma (1991). "DNA damage by oxygen-derived species. Its mechanism and measurement in mammalian systems." FEBS Lett **281**(1-2): 9-19.
- Halliwell, B. and J. M. Gutteridge (1990). "Role of free radicals and catalytic metal ions in human disease: an overview." Methods Enzymol **186**: 1-85.
- Hamann, S. (2002). "Molecular mechanisms of water transport in the eye." Int Rev Cytol **215**: 395-431.
- Hanyaloglu, A. C., M. Vrecl, et al. (2001). "Casein Kinase II Sites in the Intracellular C-terminal Domain of the Thyrotropin-releasing Hormone Receptor and Chimeric Gonadotropin-releasing Hormone Receptors Contribute to beta -Arrestin-dependent Internalization." J. Biol. Chem. **276**(21): 18066-18074.
- Harding, H. P., Y. Zhang, et al. (1999). "Protein translation and folding are coupled by an endoplasmic-reticulum-resident kinase." Nature **397**(6716): 271-4.
- Hastings, T. G. (1995). "Enzymatic oxidation of dopamine: the role of prostaglandin H synthase." J Neurochem **64**(2): 919-24.
- Hayes, J. D. and L. I. McLellan (1999). "Glutathione and glutathione-dependent enzymes represent a co-ordinately regulated defence against oxidative stress." Free Radic Res **31**(4): 273-300.
- Heiber, M., A. Marchese, et al. (1996). "A novel human gene encoding a G-protein-coupled receptor (GPR15) is located on chromosome 3." Genomics **32**(3): 462-5.
- Hermeij, G., A. Methner, et al. (1999). "Identification of a novel seven-transmembrane receptor with homology to glycoprotein receptors and its expression in the adult and developing mouse." Biochem Biophys Res Commun **254**(1): 273-9.
- Holst, B., N. D. Holliday, et al. (2004). "Common structural basis for constitutive activity of the ghrelin receptor family." J Biol Chem **279**(51): 53806-17.

- Holst, B. and T. W. Schwartz (2003). "Molecular Mechanism of Agonism and Inverse Agonism in the Melanocortin Receptors: Zn<sup>2+</sup> as a Structural and Functional Probe." Ann NY Acad Sci **994**(1): 1-11.
- Hornykiewicz, O. and S. J. Kish (1987). "Biochemical pathophysiology of Parkinson's disease." Adv Neurol **45**: 19-34.
- Howard, A. D., G. McAllister, et al. (2001). "Orphan G-protein-coupled receptors and natural ligand discovery." Trends Pharmacol Sci **22**(3): 132-40.
- Hui, H., A. Nourparvar, et al. (2003). "Glucagon-like peptide-1 inhibits apoptosis of insulin-secreting cells via a cyclic 5'-adenosine monophosphate-dependent protein kinase A- and a phosphatidylinositol 3-kinase-dependent pathway." Endocrinology **144**(4): 1444-55.
- Ikeda, J., L. Ma, et al. (1994). "Involvement of nitric oxide and free radical (O<sub>2</sub><sup>-</sup>) in neuronal injury induced by deprivation of oxygen and glucose in vitro." Acta Neurochir Suppl (Wien) **60**: 94-7.
- Ilizarov, A. M., H. C. Koo, et al. (2001). "Overexpression of manganese superoxide dismutase protects lung epithelial cells against oxidant injury." Am J Respir Cell Mol Biol **24**(4): 436-41.
- Irie, F. and Y. Hirabayashi (1998). "Application of exogenous ceramide to cultured rat spinal motoneurons promotes survival or death by regulation of apoptosis depending on its concentrations." J Neurosci Res **54**(4): 475-85.
- Ishige, K., Q. Chen, et al. (2001). "The activation of dopamine D4 receptors inhibits oxidative stress-induced nerve cell death." J Neurosci **21**(16): 6069-76.
- Ishihara, T., R. Shigemoto, et al. (1992). "Functional expression and tissue distribution of a novel receptor for vasoactive intestinal polypeptide." Neuron **8**(4): 811-9.
- Jolkkonen, J., K. Puurunen, et al. (1999). "Neuroprotection by the alpha2-adrenoceptor agonist, dexmedetomidine, in rat focal cerebral ischemia." Eur J Pharmacol **372**(1): 31-6.
- Jones, D. C., P. G. Gunasekar, et al. (2000). "Dopamine-induced apoptosis is mediated by oxidative stress and is enhanced by cyanide in differentiated PC12 cells." J Neurochem **74**(6): 2296-304.
- Joost, P. and A. Methner (2002). "Phylogenetic analysis of 277 human G-protein-coupled receptors as a tool for the prediction of orphan receptor ligands." Genome Biol **3**(11): RESEARCH0063.
- Kamencic, H., A. Lyon, et al. (2000). "Monochlorobimane fluorometric method to measure tissue glutathione." Anal Biochem **286**(1): 35-7.
- Kane, D. J., T. A. Sarafian, et al. (1993). "Bcl-2 inhibition of neural death: decreased generation of reactive oxygen species." Science **262**(5137): 1274-7.
- Kim, S. G., Z. G. Gao, et al. (2003). "P2Y6 nucleotide receptor activates PKC to protect 1321N1 astrocytoma cells against tumor necrosis factor-induced apoptosis." Cell Mol Neurobiol **23**(3): 401-18.
- Kim, S. G., K. A. Soltysiak, et al. (2003). "Tumor necrosis factor alpha-induced apoptosis in astrocytes is prevented by the activation of P2Y6, but not P2Y4 nucleotide receptors." Biochem Pharmacol **65**(6): 923-31.
- Kimura, M., Y. Mizukami, et al. (2001). "Orphan G protein-coupled receptor, GPR41, induces apoptosis via a p53/Bax pathway during ischemic hypoxia and reoxygenation." J Biol Chem **276**(28): 26453-60.
- Koch, W. J., B. E. Hawes, et al. (1994). "Direct evidence that Gi-coupled receptor stimulation of mitogen-activated protein kinase is mediated by G beta gamma activation of p21ras." Proc Natl Acad Sci U S A **91**(26): 12706-10.
- Koh, J. Y., B. J. Gwag, et al. (1995). "Potentiated necrosis of cultured cortical neurons by neurotrophins." Science **268**(5210): 573-5.

- Kojima, M., Hosoda, H., et al. (1999). "Ghrelin is a growth-hormone-releasing acylated peptide from stomach." *Nature* **402**(6762): 656-60.
- Kowall, N. W., A. C. McKee, et al. (1992). "In vivo neurotoxicity of beta-amyloid [beta(1-40)] and the beta(25-35) fragment." *Neurobiol Aging* **13**(5): 537-42.
- Kriegstein, K., J. Strelau, et al. (2002). "TGF-beta and the regulation of neuron survival and death." *J Physiol Paris* **96**(1-2): 25-30.
- Krupnick, J. G. and J. L. Benovic (1998). "The role of receptor kinases and arrestins in G protein-coupled receptor regulation." *Annu Rev Pharmacol Toxicol* **38**: 289-319.
- Laburthe, M., M. Rousset, et al. (1978). "Vasoactive intestinal peptide: a potent stimulator of adenosine 3':5'-cyclic monophosphate accumulation in gut carcinoma cell lines in culture." *Proc Natl Acad Sci U S A* **75**(6): 2772-5.
- Lanctot, P. M., P. C. Leclerc, et al. (2005). "Importance of N-glycosylation positioning for cell-surface expression, targeting, affinity and quality control of the human AT1 receptor." *Biochem J* **390**(Pt 1): 367-76.
- Lander, E. S., L. M. Linton, et al. (2001). "Initial sequencing and analysis of the human genome." *Nature* **409**(6822): 860-921.
- Lee, B., G. Q. Butcher, et al. (2005). "Activity-Dependent Neuroprotection and cAMP Response Element-Binding Protein (CREB): Kinase Coupling, Stimulus Intensity, and Temporal Regulation of CREB Phosphorylation at Serine 133." *J. Neurosci.* **25**(5): 1137-1148.
- Lewerenz, J., J. Letz, et al. (2003). "Activation of stimulatory heterotrimeric G proteins increases glutathione and protects neuronal cells against oxidative stress." *J Neurochem* **87**(2): 522-31.
- Li, Y., P. Maher, et al. (1997). "Requirement for cGMP in nerve cell death caused by glutathione depletion." *J Cell Biol* **139**(5): 1317-24.
- Li, Y., P. Maher, et al. (1997). "A role for 12-lipoxygenase in nerve cell death caused by glutathione depletion." *Neuron* **19**(2): 453-63.
- Lu, F. G. and C. S. Wong (2004). "Radiation-induced apoptosis of oligodendrocytes and its association with increased ceramide and down-regulated protein kinase B/Akt activity." *Int J Radiat Biol* **80**(1): 39-51.
- Luo, X., W. Zeng, et al. (1999). "Alternate coupling of receptors to Gs and Gi in pancreatic and submandibular gland cells." *J Biol Chem* **274**(25): 17684-90.
- Lutz, E. M., W. J. Sheward, et al. (1993). "The VIP2 receptor: molecular characterisation of a cDNA encoding a novel receptor for vasoactive intestinal peptide." *FEBS Lett* **334**(1): 3-8.
- Maher, P. (2001). "How protein kinase C activation protects nerve cells from oxidative stress-induced cell death." *J Neurosci* **21**(9): 2929-38.
- Maher, P. and J. B. Davis (1996). "The role of monoamine metabolism in oxidative glutamate toxicity." *J Neurosci* **16**(20): 6394-401.
- Maker, H. S., C. Weiss, et al. (1981). "Coupling of dopamine oxidation (monoamine oxidase activity) to glutathione oxidation via the generation of hydrogen peroxide in rat brain homogenates." *J Neurochem* **36**(2): 589-93.
- Manzoni, O. J., M. G. Weisskopf, et al. (1994). "MCPG antagonizes metabotropic glutamate receptors but not long-term potentiation in the hippocampus." *Eur J Neurosci* **6**(6): 1050-4.
- Marmor, M. F. (1999). "Mechanisms of fluid accumulation in retinal edema." *Doc Ophthalmol* **97**(3-4): 239-49.
- Marsicano, G., S. Goodenough, et al. (2003). "CB1 cannabinoid receptors and on-demand defense against excitotoxicity." *Science* **302**(5642): 84-8.

- Marsicano, G., B. Moosmann, et al. (2002). "Neuroprotective properties of cannabinoids against oxidative stress: role of the cannabinoid receptor CB1." *J Neurochem* **80**(3): 448-56.
- Mates, J. M. and F. M. Sanchez-Jimenez (2000). "Role of reactive oxygen species in apoptosis: implications for cancer therapy." *Int J Biochem Cell Biol* **32**(2): 157-70.
- Maudsley, S., B. Martin, et al. (2005). "The origins of diversity and specificity in G protein-coupled receptor signaling." *J Pharmacol Exp Ther* **314**(2): 485-94.
- McKee, K. K., C. P. Tan, et al. (1997). "Cloning and characterization of two human G protein-coupled receptor genes (GPR38 and GPR39) related to the growth hormone secretagogue and neurotensin receptors." *Genomics* **46**(3): 426-34.
- Metaye, T., H. Gibelin, et al. (2005). "Pathophysiological roles of G-protein-coupled receptor kinases." *Cell Signal* **17**(8): 917-28.
- Methner, A., G. Hermey, et al. (1997). "A novel G protein-coupled receptor with homology to neuropeptide and chemoattractant receptors expressed during bone development." *Biochem Biophys Res Commun* **233**(2): 336-42.
- Metzger, D. and R. Feil (1999). "Engineering the mouse genome by site-specific recombination." *Curr Opin Biotechnol* **10**(5): 470-6.
- Midorikawa, K. and S. Kawanishi (2001). "Superoxide dismutases enhance H<sub>2</sub>O<sub>2</sub>-induced DNA damage and alter its site specificity." *FEBS Lett* **495**(3): 187-90.
- Milligan, G. (1987). "Foetal-calf serum stimulates a pertussis-toxin-sensitive high-affinity GTPase activity in rat glioma C6 BU1 cells." *Biochem J* **245**(2): 501-5.
- Mori, K. (2000). "Tripartite management of unfolded proteins in the endoplasmic reticulum." *Cell* **101**(5): 451-4.
- Murphy, T. H., M. Miyamoto, et al. (1989). "Glutamate toxicity in a neuronal cell line involves inhibition of cystine transport leading to oxidative stress." *Neuron* **2**(6): 1547-58.
- Murphy, T. H., R. L. Schnaar, et al. (1990). "Immature cortical neurons are uniquely sensitive to glutamate toxicity by inhibition of cystine uptake." *Faseb J* **4**(6): 1624-33.
- Neves, S. R., P. T. Ram, et al. (2002). "G protein pathways." *Science* **296**(5573): 1636-9.
- Ng, D. T., E. D. Spear, et al. (2000). "The unfolded protein response regulates multiple aspects of secretory and membrane protein biogenesis and endoplasmic reticulum quality control." *J Cell Biol* **150**(1): 77-88.
- Noguchi, K., S. Ishii, et al. (2003). "Identification of p2y9/GPR23 as a novel G protein-coupled receptor for lysophosphatidic acid, structurally distant from the Edg family." *J Biol Chem* **278**(28): 25600-6.
- O'Neill, M. J., C. A. Hicks, et al. (1998). "Dopamine D2 receptor agonists protect against ischaemia-induced hippocampal neurodegeneration in global cerebral ischaemia." *Eur J Pharmacol* **352**(1): 37-46.
- Offen, D., Y. Sherki, et al. (2000). "Vasoactive intestinal peptide (VIP) prevents neurotoxicity in neuronal cultures: relevance to neuroprotection in Parkinson's disease." *Brain Res* **854**(1-2): 257-62.
- Oka, A., M. J. Bellow, et al. (1993). "Vulnerability of oligodendroglia to glutamate: pharmacology, mechanisms, and prevention." *J Neurosci* **13**(4): 1441-53.
- Olanow, C. W. and W. G. Tatton (1999). "Etiology and pathogenesis of Parkinson's disease." *Annu Rev Neurosci* **22**: 123-44.
- Papadia, S., P. Stevenson, et al. (2005). "Nuclear Ca<sup>2+</sup> and the cAMP Response Element-Binding Protein Family Mediate a Late Phase of Activity-Dependent Neuroprotection." *J. Neurosci.* **25**(17): 4279-4287.
- Papadopoulos, M. C., I. L. Koumenis, et al. (1997). "Vulnerability to glucose deprivation injury correlates with glutathione levels in astrocytes." *Brain Res* **748**(1-2): 151-6.

- Parnot, C., S. Miserey-Lenkei, et al. (2002). "Lessons from constitutively active mutants of G protein-coupled receptors." Trends in Endocrinology and Metabolism **13**(8): 336.
- Pippig, S., S. Andexinger, et al. (1993). "Overexpression of beta-arrestin and beta-adrenergic receptor kinase augment desensitization of beta 2-adrenergic receptors." J Biol Chem **268**(5): 3201-8.
- Pizzi, M., F. Boroni, et al. (1999). "Neuroprotective effect of thyrotropin-releasing hormone against excitatory amino acid-induced cell death in hippocampal slices." Eur J Pharmacol **370**(2): 133-7.
- Pugazhenthil, S., A. Nesterova, et al. (2003). "Oxidative stress-mediated down-regulation of bcl-2 promoter in hippocampal neurons." J Neurochem **84**(5): 982-96.
- Pugazhenthil, S., A. Nesterova, et al. (2000). "Akt/Protein Kinase B Up-regulates Bcl-2 Expression through cAMP-response Element-binding Protein." J. Biol. Chem. **275**(15): 10761-10766.
- Radhika, V. and N. Dhanasekaran (2001). "Transforming G proteins." Oncogene **20**(13): 1607-14.
- Raff, M. C., B. A. Barres, et al. (1993). "Programmed cell death and the control of cell survival: lessons from the nervous system." Science **262**(5134): 695-700.
- Ratan, R. R., T. H. Murphy, et al. (1994). "Oxidative stress induces apoptosis in embryonic cortical neurons." J Neurochem **62**(1): 376-9.
- Rayan, G. M., S. I. Said, et al. (1991). "Vasoactive intestinal peptide and nerve regeneration." J Hand Surg [Br] **16**(5): 515-8.
- Reichelt, W., J. Stabel-Burow, et al. (1997). "The glutathione level of retinal Muller glial cells is dependent on the high-affinity sodium-dependent uptake of glutamate." Neuroscience **77**(4): 1213-24.
- Resh, M. D. (2004). "Membrane targeting of lipid modified signal transduction proteins." Subcell Biochem **37**: 217-32.
- Rice, G. C., E. A. Bump, et al. (1986). "Quantitative analysis of cellular glutathione by flow cytometry utilizing monochlorobimane: some applications to radiation and drug resistance in vitro and in vivo." Cancer Res **46**(12 Pt 1): 6105-10.
- Riedel, G. and K. G. Reymann (1996). "Metabotropic glutamate receptors in hippocampal long-term potentiation and learning and memory." Acta Physiol Scand **157**(1): 1-19.
- Roeder, T., D. Gorich, et al. (2004). "A green-fluorescent-protein-based assay for the characterization of G-protein-coupled receptors." Anal Biochem **332**(1): 38-45.
- Ruilope, L. M., E. A. Rosei, et al. (2005). "Angiotensin receptor blockers: therapeutic targets and cardiovascular protection." Blood Press **14**(4): 196-209.
- Saeki, K., A. Yuo, et al. (1997). "Cell density-dependent apoptosis in HL-60 cells, which is mediated by an unknown soluble factor, is inhibited by transforming growth factor beta1 and overexpression of Bcl-2." J Biol Chem **272**(32): 20003-10.
- Sagara, Y., R. Dargusch, et al. (1996). "Increased antioxidant enzyme activity in amyloid beta protein-resistant cells." J Neurosci **16**(2): 497-505.
- Sagara, Y. and D. Schubert (1998). "The activation of metabotropic glutamate receptors protects nerve cells from oxidative stress." J Neurosci **18**(17): 6662-71.
- Salinas, M., R. Lopez-Valdaliso, et al. (2000). "Inhibition of PKB/Akt1 by C2-ceramide involves activation of ceramide-activated protein phosphatase in PC12 cells." Mol Cell Neurosci **15**(2): 156-69.
- Schlessinger, J. and A. Ullrich (1992). "Growth factor signaling by receptor tyrosine kinases." Neuron **9**(3): 383-91.
- Schubert, D., C. Behl, et al. (1995). "Amyloid peptides are toxic via a common oxidative mechanism." Proc Natl Acad Sci U S A **92**(6): 1989-93.
- Schubert, D., H. Kimura, et al. (1992). "Growth factors and vitamin E modify neuronal glutamate toxicity." Proc Natl Acad Sci U S A **89**(17): 8264-7.

- Schubert, D. and D. Piasecki (2001). "Oxidative glutamate toxicity can be a component of the excitotoxicity cascade." J Neurosci **21**(19): 7455-62.
- Sener, G., S. Arbak, et al. (2005). "Estrogen protects the liver and intestines against sepsis-induced injury in rats." J Surg Res **128**(1): 70-8.
- Shaulian, E. and M. Karin (2002). "AP-1 as a regulator of cell life and death." Nat Cell Biol **4**(5): E131-6.
- Shaw, S., M. Bencherif, et al. (2002). "Janus Kinase 2, an Early Target of alpha 7 Nicotinic Acetylcholine Receptor-mediated Neuroprotection against Abeta -(1-42) Amyloid." J. Biol. Chem. **277**(47): 44920-44924.
- Shaw, S., M. Bencherif, et al. (2003). "Angiotensin II Blocks Nicotine-Mediated Neuroprotection against {beta}-Amyloid (1-42) via Activation of the Tyrosine Phosphatase SHP-1." J. Neurosci. **23**(35): 11224-11228.
- Shreeve, S. M., S. P. Sreedharan, et al. (2000). "VIP activates G(s) and G(i3) in rat alveolar macrophages and G(s) in HEK293 cells transfected with the human VPAC(1) receptor." Biochem Biophys Res Commun **272**(3): 922-8.
- Si, F., G. M. Ross, et al. (1998). "Glutathione protects PC12 cells from ascorbate- and dopamine-induced apoptosis." Exp Brain Res **123**(3): 263-8.
- Singer, T. P. and R. R. Ramsay (1995). "Flauoprotein structure and mechanism 2. Monoamine oxidases: old friends hold many surprises." Faseb J **9**(8): 605-10.
- Slater, E. C. (1977). "Mechanism of oxidative phosphorylation." Annu Rev Biochem **46**: 1015-26.
- Spencer, J. P., P. Jenner, et al. (1998). "Conjugates of catecholamines with cysteine and GSH in Parkinson's disease: possible mechanisms of formation involving reactive oxygen species." J Neurochem **71**(5): 2112-22.
- Spencer, J. P., M. Whiteman, et al. (2002). "5-s-Cysteinyl-conjugates of catecholamines induce cell damage, extensive DNA base modification and increases in caspase-3 activity in neurons." J Neurochem **81**(1): 122-9.
- Spillantini, M. G., M. L. Schmidt, et al. (1997). "Alpha-synuclein in Lewy bodies." Nature **388**(6645): 839-40.
- Sreedharan, S. P., D. R. Patel, et al. (1993). "Cloning and functional expression of a human neuroendocrine vasoactive intestinal peptide receptor." Biochem Biophys Res Commun **193**(2): 546-53.
- St George-Hyslop, P. (1995). "Genetic determinants of Alzheimer disease." Prog Clin Biol Res **393**: 139-45.
- Steingart, R. A., B. Solomon, et al. (2000). "VIP and peptides related to activity-dependent neurotrophic factor protect PC12 cells against oxidative stress." J Mol Neurosci **15**(3): 137-45.
- Strauss, O. (2005). "The retinal pigment epithelium in visual function." Physiol Rev **85**(3): 845-81.
- Strawn, W. B. (2002). "[Pathophysiological and clinical implications of AT(1) and AT(2) angiotensin II receptors in metabolic disorders: hypercholesterolaemia and diabetes]." Drugs **62 Spec No 1**: 31-41.
- Takei, N., Y. Skoglosa, et al. (1998). "Neurotrophic and neuroprotective effects of pituitary adenylate cyclase-activating polypeptide (PACAP) on mesencephalic dopaminergic neurons." J Neurosci Res **54**(5): 698-706.
- Tan, S., Y. Sagara, et al. (1998). "The regulation of reactive oxygen species production during programmed cell death." J Cell Biol **141**(6): 1423-32.
- Tan, S., D. Schubert, et al. (2001). "Oxytosis: A novel form of programmed cell death." Curr Top Med Chem **1**(6): 497-506.
- Tan, S., N. Somia, et al. (2001). "Regulation of antioxidant metabolism by translation initiation factor 2alpha." J Cell Biol **152**(5): 997-1006.

- Tan, S., M. Wood, et al. (1998). "Oxidative stress induces a form of programmed cell death with characteristics of both apoptosis and necrosis in neuronal cells." J Neurochem **71**(1): 95-105.
- Tanzi, R. E., D. M. Kovacs, et al. (1996). "The gene defects responsible for familial Alzheimer's disease." Neurobiol Dis **3**(3): 159-68.
- Thomsen, C., H. Klitgaard, et al. (1994). "(S)-4-carboxy-3-hydroxyphenylglycine, an antagonist of metabotropic glutamate receptor (mGluR) 1a and an agonist of mGluR2, protects against audiogenic seizures in DBA/2 mice." J Neurochem **62**(6): 2492-5.
- Thomson, A., D. Hemphill, et al. (1998). "Oxidative stress and antioxidants in intestinal disease." Dig Dis **16**(3): 152-8.
- Tordai, A., L. F. Brass, et al. (1995). "Tunicamycin inhibits the expression of functional thrombin receptors on human T-lymphoblastoid cells." Biochem Biophys Res Commun **206**(3): 857-62.
- Towler, D. A., J. I. Gordon, et al. (1988). "The biology and enzymology of eukaryotic protein acylation." Annu Rev Biochem **57**: 69-99.
- Turrens, J. F. and A. Boveris (1980). "Generation of superoxide anion by the NADH dehydrogenase of bovine heart mitochondria." Biochem J **191**(2): 421-7.
- Urano, F., A. Bertolotti, et al. (2000). "IRE1 and efferent signaling from the endoplasmic reticulum." J Cell Sci **113 Pt 21**: 3697-702.
- Vaudry, D., B. J. Gonzalez, et al. (2000). "Pituitary Adenylate Cyclase-Activating Polypeptide and Its Receptors: From Structure to Functions." Pharmacol Rev **52**(2): 269-324.
- Venter, J. C., M. D. Adams, et al. (2001). "The sequence of the human genome." Science **291**(5507): 1304-51.
- Verheij, M., R. Bose, et al. (1996). "Requirement for ceramide-initiated SAPK/JNK signalling in stress-induced apoptosis." Nature **380**(6569): 75-9.
- Wada, M., C. M. Gelfman, et al. (2001). "Density-dependent expression of FGF-2 in response to oxidative stress in RPE cells in vitro." Curr Eye Res **23**(3): 226-31.
- Walton, M., E. Sirimanne, et al. (1996). "The role of the cyclic AMP-responsive element binding protein (CREB) in hypoxic-ischemic brain damage and repair." Brain Res Mol Brain Res **43**(1-2): 21-9.
- Waschek, J. A. (1995). "Vasoactive intestinal peptide: an important trophic factor and developmental regulator?" Dev Neurosci **17**(1): 1-7.
- Washo-Stultz, D., C. Crowley, et al. (2000). "Increased susceptibility of cells to inducible apoptosis during growth from early to late log phase: an important caveat for in vitro apoptosis research." Toxicol Lett **116**(3): 199-207.
- Wei, M. C., W. X. Zong, et al. (2001). "Proapoptotic BAX and BAK: a requisite gateway to mitochondrial dysfunction and death." Science **292**(5517): 727-30.
- Wenzel, S., C. Muller, et al. (2005). "p38 MAP-kinase in cultured adult rat ventricular cardiomyocytes: expression and involvement in hypertrophic signalling." Eur J Heart Fail **7**(4): 453-60.
- Weyler, W., Y. P. Hsu, et al. (1990). "Biochemistry and genetics of monoamine oxidase." Pharmacol Ther **47**(3): 391-417.
- Wheeler, M. D., M. Nakagami, et al. (2001). "Overexpression of manganese superoxide dismutase prevents alcohol-induced liver injury in the rat." J Biol Chem **276**(39): 36664-72.
- Wilson, S. and D. Bergsma (2000). "Orphan G-protein coupled receptors: novel drug targets for the pharmaceutical industry." Drug Des Discov **17**(2): 105-14.
- Wise, A., S. C. Jupe, et al. (2004). "The identification of ligands at orphan G-protein coupled receptors." Annu Rev Pharmacol Toxicol **44**: 43-66.

- Xia, Z., M. Dickens, et al. (1995). "Opposing effects of ERK and JNK-p38 MAP kinases on apoptosis." Science **270**(5240): 1326-31.
- Xu, J., S. Y. Kao, et al. (2002). "Dopamine-dependent neurotoxicity of alpha-synuclein: a mechanism for selective neurodegeneration in Parkinson disease." Nat Med **8**(6): 600-6.
- Yankner, B. A., L. R. Dawes, et al. (1989). "Neurotoxicity of a fragment of the amyloid precursor associated with Alzheimer's disease." Science **245**(4916): 417-20.
- Yasui, M. and K. Kawasaki (1995). "CCKB receptor activation protects CA1 neurons from ischemia-induced dysfunction in stroke-prone spontaneously hypertensive rats hippocampal slices." Neurosci Lett **191**(1-2): 99-102.
- Zhang, J. V., P. G. Ren, et al. (2005). "Obestatin, a peptide encoded by the ghrelin gene, opposes ghrelin's effects on food intake." Science **310**(5750): 996-9.
- Zhou, Y., Q. Wang, et al. (2005). "Signal transduction pathways involved in oxidative stress-induced intestinal epithelial cell apoptosis." Pediatr Res **58**(6): 1192-7.
- Zhu, H., G. L. Bannenberg, et al. (1994). "Oxidation pathways for the intracellular probe 2',7'-dichlorofluorescein." Arch Toxicol **68**(9): 582-7.

## 8 Abbreviations

7-AAD	7-amino-actinomycin D
A $\beta$	amyloid $\beta$ protein
APP	amyloid $\beta$ precursor protein
ALDH	aldehyde dehydrogenase
ATP	adenosine triphosphate
BSA	bovine serum albumin
cAK	cAMP-activated kinase
cAMP	adenosine-3',5'-cyclic monophosphate
cGMP	guanosine -3',5'-cyclic monophosphate
CMF	5-chloromethylfluorescein
Cpm	counts per minute
dATP	2'-deoxyadenosine 5'-triphosphate
dCTP	2'-deoxycytidine 5'-triphosphate
dGTP	2'-deoxyguanosine 5'-triphosphate
dTTP	2'-deoxythymidine 5'-triphosphate
DCFDA	dihydrodichlorofluorescein diacetate
DMEM	Dulbecco's modified minimal essential medium
DMSO	dimethyl sulfoxide
DTT	DL-Dithiothreitol
<i>E. coli</i>	Escherichia coli
EDTA	Ethylendiaminetetraacetic acid
ERK	extracellular signal-regulated kinase
EtBr	ethidium bromide
GDP $\beta$ S	guanosine 5'-O-2-thiophosphate
$\gamma$ -GCS	$\gamma$ -glutamylcysteine synthetase

GPCR	G protein-coupled receptor
G3PDH	glyceraldehyde-3-phosphate dehydrogenase
GPx	glutathione peroxidase
GSH	reduced glutathione
GSSG	oxidised glutathione
HEPES	N-(2-hydroxyethyl)-piperazine-N'-(2-ethanesulfonic acid)
HO·	hydroxyl radical
H <sub>2</sub> O <sub>2</sub>	hydrogen peroxide
HT22CR	chronically resistant HT22 cells
IgG	immunoglobulin G
JNK	c-Jun NH2-terminal kinase
MAP2	microtubule-associated protein 2
MOPS	3-(morpholino)-propanesulfonic acid
MTT	methylthiazolotetrazolium
MDA	malondialdehyde
NADPH	β-nicotinamide adenine dinucleotide phosphate, reduced form
NO	nitric oxide
O <sub>2</sub>	oxygen
O <sub>2</sub> <sup>·-</sup>	superoxide radical
ONOO <sup>-</sup>	peroxynitrite
PBS	phosphate-buffered saline
PCR	polymerase chain reaction
3PDGH	3-phosphoglycerate dehydrogenase
PI3K	phosphoinositide-3 kinase
PKC	protein kinase C
PLC	phospholipase C
PMA	phorbol 12-myristate 13-acetate
PSL	photostimulated luminescence
rcu	randomly chosen units
ROS	reactive oxygen species
SOD	superoxide dismutase
SSC	sodium/ sodium citrate
SDS	sodium dodecyl phosphate
TAE	Tris-acetate EDTA buffer

Tris	Tris-(hydroxymethyl)aminomethane
UTR	untranslated region